A three-dimensional finite element model for the rolling contact problem in the capstan drive of a video recorder

van Doormaal, J.C.A.M.

Award date:
1991

A Three-dimensional Finite Element Model for the Rolling Contact Problem in the Capstan Drive of a Video Recorder

WFW-report 91.026

J.C.A.M. van Doormaal

Eindhoven, April 1991

A Three-dimensional Finite Element Model for the Rolling Contact Problem in the Capstan Drive of a Video Recorder

J.C.A.M. van Doormaal

Eindhoven, April 1991

Coaches: Prof. dr. ir. F.P.T. Baayens
Ir. P.A.A. van Hoogstraten

WFW-report 91.026

Abstract

In this report, a three-dimensional model for the rolling contact problem in a capstan drive in a video recorder is presented. The model is based on two elements, that have been implemented in the finite element package SEPRAN. In these elements a Lagrangian approach has been used for the description of the deformations.

The first element is a brick element with nine nodes. It models the isotropic, elastic, incompressible neo-Hookean rubber material.

The second element is a quadrilateral boundary element with four nodes. It models the contact conditions between a rigid shaft and another body. The contact conditions consist of a geometrical constraint and an adapted constitutive equation for Coulomb friction.

Both elements have been checked for some problems. Several results are satisfactory. The neo-Hookean element is suitable for moderate deformations as occurring in for instance rubber rollers and tires. The contact element is suitable to describe frictionless contact problems. For contact problems with friction the model provides only satisfactory results when the friction force and the freedom of movement of the rubber body are limited. As a consequence of these limits the model is not yet suitable to describe the rolling contact problem between capstan and pinch roller.

Preface

This report treats the research, I have done for my graduation. This research has been carried out at the Philips Research Laboratory in Eindhoven in the group Sastra.

Here, I would like to thank all members of the group for their support. Thanks to the good atmosphere in the group, the time I have passed at the Natlab has been great. Never in my life I ate so many pieces of cake as during my work at the Natlab. Fortunately, I have no natural tendency for growing fat. Whatever future will bring for me, I will never forget this period of my live.

Particularly, I would like to thank my coaches Frank Baaijens and Peter van Hoogstraten for their supervision. Often, I troubled them with my questions, but they were always willing to answer them in spite of pressure of their own work.

Finally, I would like to thank my parents. They made it possible for me to study. They never lost faith in my capabilities. I know, they take pride in their daughter, now that she almost has finished her studies.

Ans van Doormaal

Contents

List of symbols

$\underset{\sim}{a}$	column with derivatives of the displacement shape functions
$\underline{A}$	matrix with gradients of the displacement shape functions
$\underline{B}$	a tangent matrix
$\vec{b}$	boundary force
$\underset{\sim}{b}$	column with boundary forces in the element nodes
$\vec{b}_{cap}$	boundary force on the capstan roller
$\vec{b}_p$	boundary force on the pinch roller coating
$\vec{b}_t$	tangential boundary force
c	material constant
$\vec{d}$	direction of the relative displacement
$\underset{\sim}{\hat{d}}$	column with x-, y- and z-component of vector $\hat{\vec{d}}$
$\mathbf{D}_{\Delta x}$	deformation rate tensor for the displacement
$\mathbf{D}_w$	deformation rate tensor for shape function $\vec{w}$
$\underline{D}_{\Delta x}$	matrix representation of the deformation rate tensor $\mathbf{D}_{\Delta x}$
$\underline{D}_w$	matrix representation of tensor $\mathbf{D}_w$
$\underline{D}$	material tangent matrix
$\mathbf{F}$	deformation tensor
$\underline{F}$	matrix representation of the deformation tensor
$\underset{\sim}{f}$	right hand side containing non-linear terms and boundary forces
g	impenetrability constraint
$\mathbf{G}$	shorter notation for a complex tensor
$\underline{G}$	matrix representation of tensor $\mathbf{G}$
$\underline{H}$	matrix with pressure shape functions
$\mathbf{I}$	unit tensor
$\underline{I}$	matrix representation of the unit tensor
J	volume change factor
$\hat{k}$	non-linear right hand side factor
$\underset{\sim}{k}$	right hand side containing a non-linear term
$\mathbf{K}$	shorter notation for a complex tensor
$\underline{K}$	matrix representation of tensor $\mathbf{K}$
$\mathbf{L}_{\Delta x}$	displacement gradient tensor
$\mathbf{L}_w$	shape function gradient tensor
$\underline{L}_{\Delta x}$	matrix representation of the displacement gradient tensor

$\underline{L_w}$	matrix representation of tensor $\mathbf{L}_w$
$\underline{L}$	continuity matrix
$\underline{M}$	pressure mass matrix
$\vec{n}$	unit outward vector, perpendicular to the contact zone
$\underset{\sim}{\hat{n}}$	column with the x-, y- and z-component of $\hat{\vec{n}}$
$\underline{N}$	matrix composed of the components of $\hat{\vec{n}}$
nb	number of nodes for the boundary element
np	number of nodes for the pressure
nx	number of nodes for the position
p	pressure like quantity
$\underset{\sim}{\hat{p}}$	column with estimations for the pressure at element nodes
$p^{n,i}$	estimation for the pressure like quantity after n time steps and i iterations
$\underline{P}$	matrix with displacement shape functions
$\vec{q}$	external volume forces
$\underline{Q}$	matrix with derivatives of the displacement shape functions and with the pressure shape functions
r	weighting function for the pressure
$\underset{\sim}{r}$	column with weighting functions for the pressure
R_c	radius of the capstan
$\vec{r}$	tangential direction
$\underset{\sim}{\hat{r}}$	column with the x, y- and z-component of $\hat{\vec{r}}$
$\underline{R}$	matrix composed of components of $\underset{\sim}{\hat{r}}$
$\vec{s}$	displacement of the capstan
$\underline{S}$	diffusion matrix
t	time
$\underline{T}$	initial stress matrix
$\vec{u}$	displacement vector of a contact point of the pinch roller coating
$\vec{u}_c$	displacement vector of a contact point of the capstan
u_{dif}	length of vector $\hat{\vec{u}}_c - \hat{\vec{u}}$
$\vec{u}_{rel}$	relative displacement
$\vec{v}$	velocity
$\vec{v}_{rel}$	relative velocity
$\vec{w}$	weighting function for the position
$\underset{\sim}{w}$	column with weighting functions for the position at element nodes
$\vec{x}$	position of a material point

$\hat{\vec{x}}^{n,i}$	estimation for the position after n time steps and i iterations
$\vec{x}_c$	projection of $\vec{x}$ on the axis of the capstan
x_{dif}	length of vector $\hat{\vec{x}}_c - \hat{\vec{x}}$
$\vec{\alpha}$	support vector of the axis of the capstan
$\vec{\beta}$	direction vector of the axis of the capstan
Γ	boundary
Γ_c	contact boundary
Γ_{cap}	boundary of the capstan
Γ_{ccap}	candidate contact boundary of the capstan
Γ_{cp}	candidate contact boundary of the pinch roller coating
Γ_p	boundary of the pinch roller coating
$\Delta\underset{\sim}{p}$	column with variations of the pressure at element nodes
Δt	time step
$\Delta\underset{\sim}{x}$	column with variations of the position at element nodes
ϵ_1	penalty parameter for the incompressibility constraint
ϵ_2	penalty parameter for the impenetrability constraint
ϵ_3	regularization parameter for the Coulomb friction
ϵ_4	regularization parameter for the Coulomb friction
λ	parameter for the points on the axis of the capstan
μ	friction coefficient
ρ	density
ρ_0	density at time t_0
$\boldsymbol{\sigma}$	Cauchy stress tensor
$\vec{\sigma}_{coulomb}$	coulomb friction
σ_n	contact pressure
$\vec{\sigma}_{ncap}$	normal boundary force on the capstan
$\vec{\sigma}_{np}$	normal boundary force on the pinch roller
$\vec{\sigma}_{tcap}$	tangential boundary force on the capstan
$\vec{\sigma}_{tp}$	tangential boundary force on the pinch roller
$\boldsymbol{\tau}$	stress tensor
$\underline{\hat{\tau}}$	matrix representation of stress tensor $\hat{\boldsymbol{\tau}}$
$\underset{\sim}{\hat{\tau}}$	column with stress components
φ_i	shape function for the position belonging to node i
$\underline{\varphi}$	matrix with interpolation functions for the position

ϕ	regularization function for the friction
χ_i	shape function of the boundary element belonging to node i
$\underline{\chi}$	matrix with shape functions χ_i
ψ_i	shape function for the pressure belonging to node i
$\underset{\sim}{\psi}$	column with interpolation functions for the pressure
$\bar{\omega}$	mean rotation velocity of the capstan
Ω	volume
$\mathbf{\Omega}_{\Delta x}$	spin tensor for the displacement
$\mathbf{\Omega}_w$	spin tensor for shape function $\vec{w}$
$\underline{\Omega}_{\Delta x}$	matrix representation of the spin tensor $\mathbf{\Omega}_{\Delta x}$
$\underline{\Omega}_w$	matrix representation of the spin tensor $\mathbf{\Omega}_w$
Ω_p	bounded open domain of the pinch roller coating
$\bar{\Omega}_p$	domain of the pinch roller coating
Ω_{cap}	bounded open domain of the capstan
$\bar{\Omega}_{cap}$	domain of the capstan
$\underset{\sim}{\nabla}$	column with gradients
$\vec{\nabla}$	gradient operator
$\vec{\nabla}_0$	gradient operator with respect to the reference configuration
$\dot{()}$	material time derivative
$()^c$	conjugate tensor
$()^{-1}$	inverse tensor
$()^T$	transponed of a matrix
$()_{,j}$	j-derivative
$()_i$	value of a quantity or vector in node i
$\Delta()$	variation of a quantity, vector or tensor
$\hat{()}$	estimation of a quantity, vector or tensor
det()	determinant of a tensor
tr()	trade of a tensor
$()^x$	x-component of a vector
$()^y$	y-component of a vector
$()^z$	z-component of a vector
$()^e$	a quantity or vector with respect to the element

Chapter 1

Introduction

1.1 General introduction

In data systems, magnetic recording is often applied as a carrier of information, thanks to its high density of information, its convenience of use, its low costs and its reusability. An example of magnetic recording is video recording.

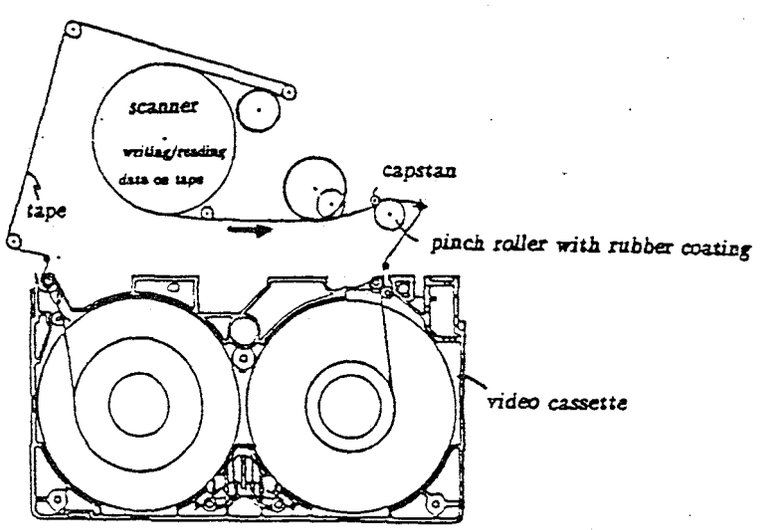

Figure 1.1: *Tape transport mechanism in a standard Philips VHS video recorder*

The fidelity of video recording depends among others on the mechanics of the system. That is why at the Philips Research Laboratory Eindhoven a research project has been started on the behaviour of the mechanics in a video recorder. In the group "Continuum Mechanics, Systems & Control and Tribology", the behaviour of the capstan drive is examined. This research is carried out in co-operation with the

Eindhoven University of Technology.

In almost every video recorder the tape is driven by a combination of a metal shaft, the so-called capstan, and a metal cylinder with a rubber coating, the so-called pinch roller (see figure 1.1 and figure 1.2). The capstan is driven by a DC-motor. The pinch roller is pressed against the capstan by an elastic spring. The tape between both rollers is transported due to the frictional forces in the contact zones.

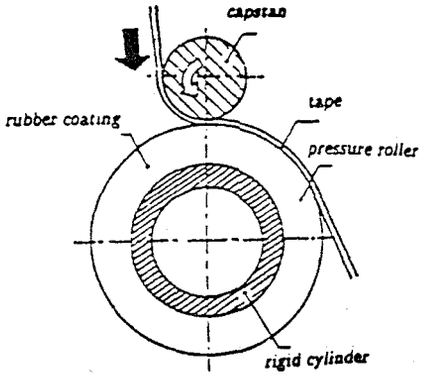

Figure 1.2: *Capstan drive*

Some research has already been carried out on a method for calculating the stresses and deformations in the tape and pinch roller coating with a two-dimensional model, [1] and [2]. However, there is a strong need for a three-dimensional model. The path of the tape in a recorder is of a three-dimensional nature.

In this report, a three-dimensional model will be presented for the rolling contact problem between capstan and pinch roller. Because of its complexity, the problem is reduced to contact between two bodies. The tape has been left out of consideration, but can be added as a third contacting body later on.

1.2 Problem definition

A model of the capstan drive has been shown in figure 1.2. The capstan is being driven at a certain angular speed. The purpose of the drive is to transfer this velocity to the tape as well as possible. In this conveyance of velocity, the deformations of the pinch roller are of great importance.

As already has been remarked in the previous section, the tape is left out of consideration. Since the tape is very thin (about 18 μm or thinner) in comparison with the diameter of the pinch roller (about 12.5 mm for a standard Philips VHS video recorder), it is not of importance for the deformation of the rubber coating.

The metal capstan and the metal cylinder of the pinch roller are much stiffer than the rubber pinch roller coating. Therefore, they are supposed to be rigid.

The material of the rubber coating is assumed to behave elastic, isotropic and incompressible. A simple and suitable constitutive relation for such behaviour is the neo-Hookean constitutive equation. It contains only one material parameter. The suitability of the neo-Hookean material model has been shown by experiments on the rubber material of the coating.

1.3 Strategy

A Lagrangian approach is used to calculate deformations and stresses in the body. This means, that the reference system and mesh are attached to the body.

Based on the balance of mass, momentum and angular momentum and the neo-Hookean constitutive equation an algebraic system of equations is obtained for the material behaviour of the rubber coating, with the position $\vec{x}$ of a material point and a pressure-like quantity p in the body as unknowns. The system of equations is obtained by using the weighted residual method, a linearization and a discretization of the body. For the discretization a trilinear hexahedral element is used. This is a three-dimensional brick element with eight nodes for the position at the vertices of the element and one for the pressure-like quantity at the centre of the element. The element applies linear interpolation functions for the position and a constant interpolation function for the pressure-like quantity.

The neo-Hookean element has been implemented in SEPRAN (see [7]). The computational burden has been reduced considerably by use of the penalty function method.

A quadrilateral bilinear boundary element has also been implemented in SEPRAN. This boundary element describes the contact conditions between capstan and pinch roller coating. The system of equations for this boundary element is based on the geometrical constraint in the contact region and an adapted constitutive equation for Coulomb friction. The only unknown in the system of equations is the position $\vec{x}$, for which the boundary element contains four nodal points.

Both elements are checked for some test cases. Contact problems with and without friction are simulated. The results of these simulations are compared with numerical results, obtained with the finite element package MARC (see [8]).

Finally, some conclusions are given.

Chapter 2

Material behaviour

2.1 Introduction

In this chapter mathematical relations to describe the behaviour of a neo-Hookean rubber material will be derived, based on the laws of conservation and the constitutive equation for a neo-Hookean rubber material. The derived relations form the basis for a numerical algorithm to compute the quantities of interest.

2.2 System of equations

Primary variables are the position $\vec{x}$ of the material points, the Cauchy stress tensor $\boldsymbol{\sigma}$ and the density ρ. If these variables are known, the configuration of the rubber body can be described completely.

The state variables must satisfy the balance of mass, momentum and angular momentum. These laws are given here in a local form (see [3]):

$$\rho J = \rho_0 \tag{2.1}$$

$$\vec{\nabla} \cdot \boldsymbol{\sigma}^c + \rho \vec{q} = \rho \dot{\vec{v}} \tag{2.2}$$

$$\boldsymbol{\sigma} = \boldsymbol{\sigma}^c \tag{2.3}$$

where ρ_0 is *the density at time* t_0,

J is *the volume change factor*,

$\vec{q}$ denotes *external volume forces*,

$\vec{v}$ is *the velocity*,

$\vec{\nabla}$ is *the gradient operator*,

$\dot{(\,)}$ denotes *a material time derivative,*

$()^c$ denotes *a conjugate tensor.*

The rubber body is considered to be incompressible and it is assumed that there are no external volume forces and inertia forces. This simplifies the system of equations:

$$J = \det(\mathbf{F}) = 1 \tag{2.4}$$

$$\vec{\nabla} \cdot \boldsymbol{\sigma}^c = \vec{0} \tag{2.5}$$

$$\boldsymbol{\sigma} = \boldsymbol{\sigma}^c \tag{2.6}$$

where $\mathbf{F} = (\vec{\nabla}_0 \vec{x})^c$ is *the deformation tensor,*

$\vec{\nabla}_0$ is *the gradient operator with respect to the reference configuration.*

The material behaviour is described with a so-called constitutive equation. One way to model a neo-Hookean rubber material is with the following constitutive relation (see [9]):

$$\boldsymbol{\sigma} = -p\mathbf{I} + \boldsymbol{\tau} \quad ; \quad \boldsymbol{\tau} = 2c(\mathbf{F} \cdot \mathbf{F}^c - \mathbf{I}) \tag{2.7}$$

where $\boldsymbol{\tau}$ is *a stress tensor,*

$\mathbf{I}$ is *the unit tensor,*

c is *a material constant,*

p is *a pressure-like quantity.*

The constitutive equation introduces one extra unknown, the pressure-like quantity p. This pressure-like quantity p depends on the hydrostatic pressure and on the left Cauchy Green strain tensor ($\mathbf{B} = \mathbf{F} \cdot \mathbf{F}^c$).

Together with the other unknowns, the position vector (three components) and the stress tensor (nine components), there are thirteen unknowns in a three-dimensional problem. Consequently, thirteen equations are needed to obtain a solvable system. The number of derived equations has to be equal to the number of unknowns. Equation (2.4) represents one equation. Both equation (2.5) and equation (2.6) offer three equations. And finally, the constitutive relation (2.7) provides six equations. Totally, there are thirteen equations. This is exactly the number of equations, needed for a solvable system. So, a combination of equations (2.4), (2.5), (2.6) and (2.7) results in a solvable system of equations with the position vector and the pressure-like quantity as unknowns.

2.3 Discretization and linearization

A weighted residual method is applied to the system of equations. The equations are multiplied by a weighting function and integrated over the volume. Application on equations (2.4) and (2.5) yields

$$\int_\Omega \vec{w} \cdot (\vec{\nabla} \cdot \boldsymbol{\sigma}^c) d\Omega = 0 \qquad \forall \quad \vec{w} \tag{2.8}$$

$$\int_\Omega r \, (\det(\mathbf{F}) - 1) d\Omega = 0 \qquad \forall \quad r \tag{2.9}$$

Before derivation of the weak form of these equations, the set of trial solutions and the set of weighting functions have to be defined. The set of trial solutions $\vec{x}$ is defined as

$$\mathcal{X} = \{\vec{x} | \vec{x} \in [C^1]^n, \vec{u}|_{\Gamma_x} = \vec{u}_0\}$$

The set of weighting functions $\vec{w}$ is defined likewise by

$$\mathcal{W} = \{\vec{w} | \vec{w} \in [C^1]^n, \vec{w}|_{\Gamma_x} = \vec{0}\}$$

The set of trial solutions p is defined as

$$\mathcal{P} = \{p | p \in C^0, p|_{\Gamma_p} = p_0\}$$

The set of weighting functions r is defined likewise by

$$\mathcal{R} = \{r | r \in C^0, r|_{\Gamma_p} = 0\}$$

where: $[\quad]^n$ means *that every component must satisfy the condition,*
$\vec{u}|_{\Gamma_x}$ is $\vec{u}$ *on that part of the boundary where* $\vec{u}$ *is prescribed,*
$p|_{\Gamma_p}$ is p *on that part of the boundary where* p *is prescribed,*
$\vec{u}_0$ is *the prescribed position vector,*
p_0 is *the prescribed pressure-like quantity,*
and C^k is *the class of functions that are at least* k *times differentiable.*

For non-linear problems it is difficult to indicate the conditions with respect to continuity and differentiability.
With these definitions the equations (2.8) and (2.9) can be converted into the next system:

$$\int_\Omega (\vec{\nabla}\vec{w})^c : \boldsymbol{\sigma} \, d\Omega = \int_\Gamma \vec{w} \cdot \boldsymbol{\sigma} \cdot \vec{n} \, d\Gamma \qquad \forall \quad \vec{w} \in \mathcal{W} \tag{2.10}$$

$$\int_\Omega r \, (\det(\mathbf{F}) - 1) d\Omega = 0 \qquad \forall \quad r \in \mathcal{R} \tag{2.11}$$

using: 1. the symmetry of the stress tensor

$$\boldsymbol{\sigma} = \boldsymbol{\sigma}^c$$

2. partial integration according to

$$\vec{\nabla} \cdot (\boldsymbol{\sigma} \cdot \vec{w}) = \vec{w} \cdot (\vec{\nabla} \cdot \boldsymbol{\sigma}) + (\vec{\nabla}\vec{w})^c : \boldsymbol{\sigma}$$

3. transformation of a volume integral into a boundary integral according to the divergence theorem

$$\int_\Omega \vec{\nabla} \cdot (\boldsymbol{\sigma} \cdot \vec{w}) d\Omega = \int_\Gamma \vec{n} \cdot (\boldsymbol{\sigma} \cdot \vec{w}) d\Gamma$$

Equation (2.10) is called a weak formulation. The restriction of being continuously differentiable is imposed on the weighting function $\vec{w}$ instead of the stress tensor $\boldsymbol{\sigma}$.

Substitution of the constitutive equation (2.7) in (2.10) yields

$$\int_\Omega (\vec{\nabla}\vec{w})^c : (-p\mathbf{I} + \boldsymbol{\tau}) d\Omega = \int_\Gamma \vec{w} \cdot \vec{b}\, d\Gamma \qquad \forall \quad \vec{w} \in \mathcal{W} \tag{2.12}$$

$$\int_\Omega r\,(\det(\mathbf{F}) - 1) d\Omega = 0 \qquad \forall \quad r \in \mathcal{R} \tag{2.13}$$

where $\vec{b}$ is *the boundary force.*

The derived system of equations is nonlinear. In order to solve the system with a finite element method, it has to be linearized. The way, this will be done, is by using estimations for the unknowns $\vec{x}$, p and $\boldsymbol{\sigma}$, indicated by $\hat{\vec{x}}$, $\hat{p}$ and $\hat{\boldsymbol{\sigma}}$. The difference between the exact solution and the estimate is given by $\Delta\vec{x}$, Δp and $\Delta\boldsymbol{\sigma}$:

$$\vec{x} = \hat{\vec{x}} + \Delta\vec{x} \tag{2.14}$$

$$p = \hat{p} + \Delta p \tag{2.15}$$

$$\boldsymbol{\sigma} = \hat{\boldsymbol{\sigma}} + \Delta\boldsymbol{\sigma} \tag{2.16}$$

Supposing the estimations are accurate, then the differences are relatively small compared to the estimates and it is allowed to neglect terms of order Δ^2 and higher. Substitution of equations (2.14), (2.15) and (2.16) in (2.12) and (2.13) then yields (see appendix A)

$$\int_\Omega \mathbf{L}_w : (-\hat{p}\mathbf{I} - \Delta p\mathbf{I} + \hat{p}\,\mathbf{L}_{\Delta x}) d\Omega +$$

$$\int_\Omega \mathbf{L}_w : (\hat{\boldsymbol{\tau}} + 4c\,\mathbf{D}_{\Delta x} + \hat{\boldsymbol{\tau}} \cdot \mathbf{L}_{\Delta x}{}^c) d\Omega = \int_\Gamma \vec{w} \cdot \vec{b}\, d\Gamma \qquad \forall \quad \vec{w} \in \mathcal{W} \tag{2.17}$$

$$\int_\Omega r\,(\hat{\vec{\nabla}} \cdot \Delta\vec{x}) d\Omega = \int_\Omega r\,(\frac{1}{\det(\hat{\mathbf{F}})} - 1) d\Omega \qquad \forall \quad r \in \mathcal{R} \tag{2.18}$$

where

$$\mathbf{L}_w = (\hat{\vec{\nabla}}\vec{w})^c$$
$$\mathbf{L}_{\Delta x} = (\hat{\vec{\nabla}}\Delta\vec{x})^c$$
$$\mathbf{D}_{\Delta x} = \frac{1}{2}(\mathbf{L}_{\Delta x} + \mathbf{L}_{\Delta x}{}^c)$$

With respect to the system of equations (2.17) and (2.18) some remarks have to be made:

1. In order to derive a symmetrical matrix, in the incompressibility constraint the original weighting function r has been replaced by a weighting function $\frac{r}{\det \hat{\mathbf{F}}}$. The resulting equation (2.18) is consistent. This can be seen by substitution of the real solution ($\Delta\vec{x} = \vec{0}$). This substitution gives the original equation.

2. The real configuration of the body is unknown. There is only an estimation for this configuration. To solve the problem in a decent way, the volume of the body should be written as the sum of an estimation and a variation. This has not been done. The integration has been carried out over the estimated volume. Since the problem will be solved iteratively, this will have no consequence for the solution, only for the convergence.

Equations (2.17) and (2.18) can be discretized geometrically by a finite element method. This means that the volume Ω will be divided into a finite number of pieces, the so-called elements. In each element, there are a finite number of discrete points, the so-called nodes, in which the unknown positions and pressures are computed. For other points of the element the unknowns can be derived by interpolation between the nodes.

The weighting functions are also computed in the nodes and interpolated between the nodes. They are chosen according to the Galerkin method, which means that they are interpolated in the same way as the corresponding unknowns. So, in the procedure of discretization, the unknown variables and the weighting functions are approximated by a linear combination of the values in the nodes.

$$\begin{aligned}
\vec{x}(x,y,z) &= \sum_{i=1}^{nx} \vec{x}_i \varphi_i \\
p(x,y,z) &= \sum_{i=1}^{np} p_i \psi_i \\
\vec{w}(x,y,z) &= \sum_{i=1}^{nx} \vec{w}_i \varphi_i \\
r(x,y,z) &= \sum_{i=1}^{np} r_i \psi_i
\end{aligned}$$

where nx denotes *the number of nodes for the position*,
np denotes *the number of pressure nodes*,
φ_i is *the shape function for the position belonging to node i*,
ψ_i is *the shape function for the pressure belonging to node i*,
$\vec{w}_i$ is *the value of the weighting function* $\vec{w}$ *in node i*,
r_i is *the value of the weighting function r in node i.*

In this report, a three-dimensional body will be discretized by a trilinear hexahedral element, containing eight nodes for the position and one for the pressure. This hexahedral element with its interpolation functions will be treated in the next section.

In appendix B it is shown how discretization of equations (2.17) and (2.18) with use of the approximations for the position and the pressure results in the following system of equations and the following contributions for each element to the global stiffness matrix and right hand side vector:

$$\begin{aligned} & \underset{\sim}{w}^T \int_\Omega (-\underline{Q}\,\underset{\sim}{\hat{p}} + \underline{A}^T \underset{\sim}{\hat{\tau}})\,d\Omega \\ + \underset{\sim}{w}^T \int_\Omega & [-\underline{Q}\,\underset{\sim}{\Delta p} + \underline{A}^T (\underset{\sim}{\psi}^T \underset{\sim}{\hat{p}}\,\underline{B} + 4c\,\underline{D} + \underline{T})\underline{A}\,\underset{\sim}{\Delta x}]\,d\Omega \\ & = \underset{\sim}{w}^T \int_\Gamma \underline{P}\,\underset{\sim}{b}\,d\Gamma \qquad \forall\ \underset{\sim}{w} \end{aligned} \tag{2.19}$$

$$\underset{\sim}{r}^T \int_\Omega \underline{Q}^T \underset{\sim}{\Delta x}\,d\Omega = \underset{\sim}{r}^T \int_\Omega \underset{\sim}{\psi}\,\hat{k}\,d\Omega \qquad \forall\ \underset{\sim}{r} \tag{2.20}$$

$$\begin{aligned} \hat{k}^e &= \frac{1}{\det(\hat{\mathbf{F}})} - 1 \\ (\underset{\sim}{\Delta x}^e)^T &= \begin{bmatrix} \Delta x_1 & \Delta y_1 & \Delta z_1 & .... & \Delta x_8 & \Delta y_8 & \Delta z_8 \end{bmatrix} \\ (\underset{\sim}{\Delta p}^e)^T &= \begin{bmatrix} \Delta p_1 \end{bmatrix} \\ (\underset{\sim}{\hat{p}}^e)^T &= \begin{bmatrix} \hat{p}_1 \end{bmatrix} \\ (\underset{\sim}{w}^e)^T &= \begin{bmatrix} w_1{}^x & w_1{}^y & w_1{}^z & .... & w_8{}^x & w_8{}^y & w_8{}^z \end{bmatrix} \\ (\underset{\sim}{r}^e)^T &= \begin{bmatrix} r_1 \end{bmatrix} \\ (\underset{\sim}{\psi}^e)^T &= \begin{bmatrix} \psi_1 \end{bmatrix} \end{aligned}$$

$$
\begin{aligned}
(\underset{\sim}{b}^{e})^{T} &= \begin{bmatrix} b_1{}^x & b_1{}^y & b_1{}^z & .... & b_8{}^x & b_8{}^y & b_8{}^z \end{bmatrix} \\
(\underset{\sim}{\hat{\tau}}^{e})^{T} &= \begin{bmatrix} \hat{\tau}_{xx} & \hat{\tau}_{xy} & \hat{\tau}_{yy} & \hat{\tau}_{zz} & \hat{\tau}_{yz} & \hat{\tau}_{xz} & 0 & 0 & 0 \end{bmatrix}
\end{aligned}
$$

$$
\underline{B}^{e} = \begin{bmatrix}
1 & 0 & 0 & 0 & 0 & 0 & 0 & 0 & 0 \\
0 & \frac{1}{2} & 0 & 0 & 0 & 0 & 0 & 0 & 0 \\
0 & 0 & 1 & 0 & 0 & 0 & 0 & 0 & 0 \\
0 & 0 & 0 & 1 & 0 & 0 & 0 & 0 & 0 \\
0 & 0 & 0 & 0 & \frac{1}{2} & 0 & 0 & 0 & 0 \\
0 & 0 & 0 & 0 & 0 & \frac{1}{2} & 0 & 0 & 0 \\
0 & 0 & 0 & 0 & 0 & 0 & -\frac{1}{2} & 0 & 0 \\
0 & 0 & 0 & 0 & 0 & 0 & 0 & -\frac{1}{2} & 0 \\
0 & 0 & 0 & 0 & 0 & 0 & 0 & 0 & -\frac{1}{2}
\end{bmatrix}
$$

$$
\underline{D}^{e} = \begin{bmatrix}
1 & 0 & 0 & 0 & 0 & 0 & 0 & 0 & 0 \\
0 & \frac{1}{2} & 0 & 0 & 0 & 0 & 0 & 0 & 0 \\
0 & 0 & 1 & 0 & 0 & 0 & 0 & 0 & 0 \\
0 & 0 & 0 & 1 & 0 & 0 & 0 & 0 & 0 \\
0 & 0 & 0 & 0 & \frac{1}{2} & 0 & 0 & 0 & 0 \\
0 & 0 & 0 & 0 & 0 & \frac{1}{2} & 0 & 0 & 0 \\
0 & 0 & 0 & 0 & 0 & 0 & 0 & 0 & 0 \\
0 & 0 & 0 & 0 & 0 & 0 & 0 & 0 & 0 \\
0 & 0 & 0 & 0 & 0 & 0 & 0 & 0 & 0
\end{bmatrix}
$$

$$
\underline{T}^{e} = \begin{bmatrix}
\hat{\tau}_{xx} & \frac{\hat{\tau}_{xy}}{2} & 0 & 0 & 0 & \frac{\hat{\tau}_{xz}}{2} & \frac{\hat{\tau}_{xy}}{2} & 0 & -\frac{\hat{\tau}_{xz}}{2} \\
 & \frac{\hat{\tau}_{xx}+\hat{\tau}_{yy}}{4} & \frac{\hat{\tau}_{xy}}{2} & 0 & \frac{\hat{\tau}_{xz}}{4} & \frac{\hat{\tau}_{yz}}{4} & \frac{\hat{\tau}_{yy}-\hat{\tau}_{xx}}{4} & \frac{\hat{\tau}_{xz}}{4} & -\frac{\hat{\tau}_{yz}}{4} \\
 & & \hat{\tau}_{yy} & 0 & \frac{\hat{\tau}_{yz}}{2} & 0 & -\frac{\hat{\tau}_{xy}}{2} & \frac{\hat{\tau}_{yz}}{2} & 0 \\
 & & & \hat{\tau}_{zz} & \frac{\hat{\tau}_{yz}}{2} & \frac{\hat{\tau}_{xz}}{2} & 0 & -\frac{\hat{\tau}_{yz}}{2} & \frac{\hat{\tau}_{xz}}{2} \\
 & & & & \frac{\hat{\tau}_{yy}+\hat{\tau}_{zz}}{4} & \frac{\hat{\tau}_{xy}}{4} & -\frac{\hat{\tau}_{xz}}{4} & \frac{\hat{\tau}_{zz}-\hat{\tau}_{yy}}{4} & \frac{\hat{\tau}_{xy}}{4} \\
 & & & & & \frac{\hat{\tau}_{xx}+\hat{\tau}_{zz}}{4} & \frac{\hat{\tau}_{yz}}{4} & -\frac{\hat{\tau}_{xy}}{4} & \frac{\hat{\tau}_{xx}-\hat{\tau}_{zz}}{4} \\
 & symm & & & & & \frac{\hat{\tau}_{xx}+\hat{\tau}_{yy}}{4} & -\frac{\hat{\tau}_{xz}}{4} & -\frac{\hat{\tau}_{yz}}{4} \\
 & & & & & & & \frac{\hat{\tau}_{yy}+\hat{\tau}_{zz}}{4} & -\frac{\hat{\tau}_{xy}}{4} \\
 & & & & & & & & \frac{\hat{\tau}_{xx}+\hat{\tau}_{zz}}{4}
\end{bmatrix}
$$

$$
\underline{A}^{e} = \begin{bmatrix}
\frac{\partial}{\partial x} & 0 & 0 \\
\frac{\partial}{\partial y} & \frac{\partial}{\partial x} & 0 \\
0 & \frac{\partial}{\partial y} & 0 \\
0 & 0 & \frac{\partial}{\partial z} \\
0 & \frac{\partial}{\partial z} & \frac{\partial}{\partial y} \\
\frac{\partial}{\partial z} & 0 & \frac{\partial}{\partial x} \\
\frac{\partial}{\partial y} & -\frac{\partial}{\partial x} & 0 \\
0 & \frac{\partial}{\partial z} & -\frac{\partial}{\partial y} \\
-\frac{\partial}{\partial z} & 0 & \frac{\partial}{\partial x}
\end{bmatrix}
\begin{bmatrix}
\varphi_1 & 0 & 0 & ..... & \varphi_8 & 0 & 0 \\
0 & \varphi_1 & 0 & & 0 & \varphi_8 & 0 \\
0 & 0 & \varphi_1 & & 0 & 0 & \varphi_8
\end{bmatrix}
$$

$$\underline{Q}^e = \begin{bmatrix} \frac{\partial}{\partial x}(\varphi_1) \\ \frac{\partial}{\partial y}(\varphi_1) \\ \frac{\partial}{\partial z}(\varphi_1) \\ \cdot \\ \cdot \\ \frac{\partial}{\partial x}(\varphi_8) \\ \frac{\partial}{\partial y}(\varphi_8) \\ \frac{\partial}{\partial z}(\varphi_8) \end{bmatrix} \begin{bmatrix} \psi_1 \end{bmatrix}$$

$$\underline{P}^e = \begin{bmatrix} \varphi_1 & 0 & 0 \\ 0 & \varphi_1 & 0 \\ 0 & 0 & \varphi_1 \\ \cdot & & \\ \cdot & & \\ \varphi_8 & 0 & 0 \\ 0 & \varphi_8 & 0 \\ 0 & 0 & \varphi_8 \end{bmatrix} \begin{bmatrix} \varphi_1 & 0 & 0 & ..... & \varphi_8 & 0 & 0 \\ 0 & \varphi_1 & 0 & & 0 & \varphi_8 & 0 \\ 0 & 0 & \varphi_1 & & 0 & 0 & \varphi_8 \end{bmatrix}$$

An assembly process is required to obtain the global matrix and right hand side vector.

Transferring the estimated terms in equations (2.19) and (2.20) to the right hand side yields

$$\begin{aligned} &\underset{\sim}{w}^T \int_\Omega [-\underline{Q}\Delta\underset{\sim}{p} + \underline{A}^T(\underset{\sim}{\psi}^T \hat{\underset{\sim}{p}}\, \underline{B} + 4c\,\underline{D} + \underline{T})\underline{A}\Delta\underset{\sim}{x}]d\Omega \\ &= \underset{\sim}{w}^T \int_\Omega (\underline{Q}\,\hat{\underset{\sim}{p}} - \underline{A}^T\hat{\underset{\sim}{\tau}})d\Omega + \underset{\sim}{w}^T \int_\Gamma \underline{P}\underset{\sim}{b}\, d\Gamma \qquad \forall\ \underset{\sim}{w} \end{aligned} \tag{2.21}$$

$$\underset{\sim}{r}^T \int_\Omega \underline{Q}^T \Delta\underset{\sim}{x}\, d\Omega = \underset{\sim}{r}^T \int_\Omega \underset{\sim}{\psi}\, \hat{k}\, d\Omega \qquad \forall\ \underset{\sim}{r} \tag{2.22}$$

The derived system of equations (2.21) and (2.22) must hold for all admissible weighting functions $\underset{\sim}{w}$ and $\underset{\sim}{r}$. Therefore, the system can be generalized by the following matrix formulation:

$$\begin{bmatrix} \underline{S} & -\underline{L}^T \\ -\underline{L} & \underline{0} \end{bmatrix} \begin{bmatrix} \Delta\underset{\sim}{x} \\ \Delta\underset{\sim}{p} \end{bmatrix} = \begin{bmatrix} \underset{\sim}{f} \\ \underset{\sim}{k} \end{bmatrix} \tag{2.23}$$

where:

$$\begin{aligned} \underline{S} &= \int_\Omega \underline{A}^T(\underset{\sim}{\psi}^T \hat{\underset{\sim}{p}}\, \underline{B} + 4c\,\underline{D} + \underline{T})\underline{A}\, d\Omega \\ \underline{L} &= \int_\Omega \underline{Q}^T\, d\Omega \end{aligned}$$

$$\underset{\sim}{f} = \int_\Omega (\underline{Q}\,\underset{\sim}{\hat{p}} - \underline{A}^T \underset{\sim}{\hat{\tau}})\,d\Omega + \int_\Gamma \underline{P}\,\underset{\sim}{b}\,d\Gamma$$
$$\underset{\sim}{k} = -\int_\Omega \underset{\sim}{\psi}\,\hat{k}\,d\Omega$$

2.4 Trilinear hexahedral element

The domain of a straight edged hexahedral element is completely defined by the location of its eight nodal points $\vec{x}_i^e$, i=1,..,8. The local node ordering is given in figure 2.1.

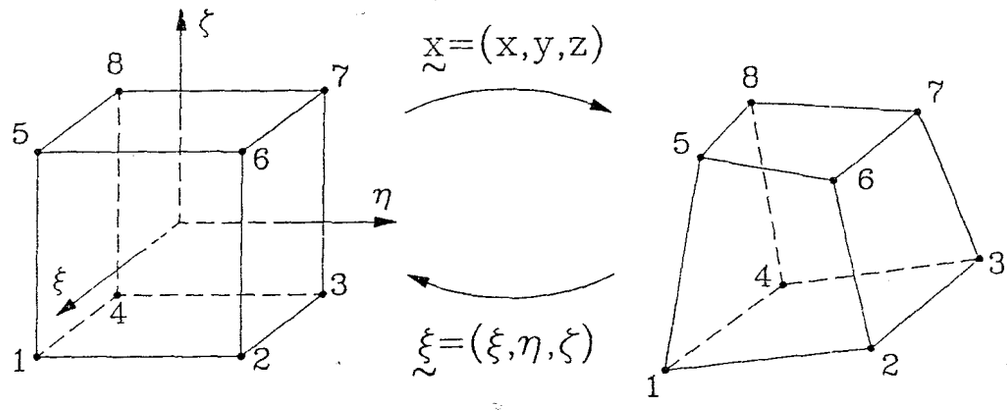

Figure 2.1: *Parent domain and local node ordering*

It is impossible to define shape functions for an arbitrary hexahedral element. That is why a parent domain is used, for which it is relatively simple to define shape functions. The parent domain is defined in another space, the so-called $\underset{\sim}{\xi}$-space. This $\underset{\sim}{\xi}$-space is an orthonormal space, with ξ, η and ζ as independent coordinates. The parent domain is a cube with edges of length two in $\underset{\sim}{\xi}$-space, given in figure 2.1. The centre of the bi-unit-cube is located in the origin of the coordinate system.

The shape functions, belonging to the bi-unit-cube can be used to approximate the position $\vec{x}^e$ of an arbitrary point in the element, because the domain Ω^e of the arbitrary hexahedral element is the image of the bi-unit-cube under trilinear mapping (see appendix C). So, the approximation of the position vector $\vec{x}$ is given by

$$\vec{x}(\underset{\sim}{\xi}) = \sum_{i=1}^{8} \varphi_i(\underset{\sim}{\xi})\,\vec{x}_i^e \tag{2.24}$$

where the shape functions for a bi-unit-cube with center in point $(\xi,\eta,\zeta) = (0,0,0)$

are given by

$$\varphi_i(\xi,\eta,\zeta) = \frac{1}{8}(1+\xi_i\,\xi)(1+\eta_i\,\eta)(1+\zeta_i\,\zeta) \tag{2.25}$$

where ξ_i is *the ξ-coordinate of node i in $\underset{\sim}{\xi}$-space,*
η_i is *the η-coordinate of node i in $\underset{\sim}{\xi}$-space,*
ζ_i is *the ζ-coordinate of node i in $\underset{\sim}{\xi}$-space.*

How these shap7e functions are determined is treated in appendix C.

The shape functions (2.25) are a function of the coordinates in $\underset{\sim}{\xi}$-space. However, in the discretized system of equations (2.23) appear the x-, y- and z-derivatives of the shape functions. How these derivatives can be determined is presented in appendix C. The result is given here.

$$\begin{bmatrix} \varphi_{i,x} \\ \varphi_{i,y} \\ \varphi_{i,z} \end{bmatrix} = \begin{bmatrix} x_{,\xi} & x_{,\eta} & x_{,\zeta} \\ y_{,\xi} & y_{,\eta} & y_{,\zeta} \\ z_{,\xi} & z_{,\eta} & z_{,\zeta} \end{bmatrix}^{-T} \begin{bmatrix} \varphi_{i,\xi} \\ \varphi_{i,\eta} \\ \varphi_{i,\zeta} \end{bmatrix} \tag{2.26}$$

where $\varphi_{i,j}$ is *the j-derivative of φ_i,*
$x_{,j}$ is *the j-derivative of x,*
$y_{,j}$ is *the j-derivative of y,*
$z_{,j}$ is *the j-derivative of z,*
$()^T$ denotes *the transponed of a matrix.*

2.5 Penalty function method

In the previous sections the system of equations, describing the behaviour of a rubber body, has been linearized and discretized in order to solve it with the computer. The discretized system of equations is given by equation (2.23):

$$\begin{bmatrix} \underline{S} & -\underline{L}^T \\ -\underline{L} & \underline{0} \end{bmatrix} \begin{bmatrix} \Delta\underset{\sim}{x} \\ \Delta\underset{\sim}{p} \end{bmatrix} = \begin{bmatrix} \underset{\sim}{f} \\ \underset{\sim}{k} \end{bmatrix} \tag{2.27}$$

Because of the null matrix in the lower right part the total system matrix is not positive definite. Partial pivoting can be necessary to solve the system. Partial pivoting is the interchanging of rows in the system matrix. Since the implementation will be performed within the finite element package SEPRAN and SEPRAN does not

perform partial pivoting, the penalty function method is an efficient alternative. In stead of the incompressibility constraint (2.18) the penalty formulation is imposed:

$$\int_\Omega r \hat{\vec{\nabla}} \cdot \Delta\vec{x}\, d\Omega + \int_\Omega r\, \epsilon_1\, \Delta p\, d\Omega = \int_\Omega r\, \hat{k}\, d\Omega \tag{2.28}$$

or, in discretized form (see appendix B):

$$\underline{L}\,\underset{\sim}{\Delta x} + \epsilon_1\, \underline{M}\,\underset{\sim}{\Delta p} = -\underset{\sim}{k} \tag{2.29}$$

where ϵ_1 is *the penalty parameter,*

$\underline{M}$ is *the pressure mass matrix.*

$$\underline{M} = \int_\Omega \underline{H}\, d\Omega = \int_\Omega \underset{\sim}{\psi}\, \underset{\sim}{\psi}^T\, d\Omega$$

In each element, there is one node for the pressure-like quantity. So, the elemental mass matrix $\underline{M}^e$ is a scalar.

With use of the penalty formulation the total system of equations looks as follows:

$$\begin{bmatrix} \underline{S} & -\underline{L}^T \\ -\underline{L} & -\epsilon_1\, \underline{M} \end{bmatrix} \begin{bmatrix} \underset{\sim}{\Delta x} \\ \underset{\sim}{\Delta p} \end{bmatrix} = \begin{bmatrix} \underset{\sim}{f} \\ \underset{\sim}{k} \end{bmatrix} \tag{2.30}$$

Since the pressure-like quantity is interpolated discontinuously, the number of unknowns can be reduced by eliminating the pressure $\underset{\sim}{\Delta p}$ per element. Discontinuous interpolation means that there is no overlap of the elemental matrices in the global matrix. Elimination of $\underset{\sim}{\Delta p}$ results in

$$(\underline{S} + \frac{1}{\epsilon_1}\, \underline{L}^T\, \underline{M}^{-1}\, \underline{L})\underset{\sim}{\Delta x} = \underset{\sim}{f} - \frac{1}{\epsilon_1}\, \underline{L}^T\, \underline{M}^{-1}\, \underset{\sim}{k} \tag{2.31}$$

After solving (2.31) for $\underset{\sim}{\Delta x}$, $\underset{\sim}{\Delta p}$ can be found according to

$$\underset{\sim}{\Delta p} = -\frac{1}{\epsilon_1}\, \underline{M}^{-1}\, (\underline{L}\,\underset{\sim}{\Delta x} + \underset{\sim}{k}) \tag{2.32}$$

The calculation of the inverse of the pressure mass matrix $\underline{M}$ is very simple because of its diagonal structure. This diagonal structure is a consequence of the discontinuous interpolation of the pressure-like quantity.

The penalty function method has two advantages compared to a direct method. The first one is that the system matrix is symmetric and positive definite. No partial pivoting is needed to solve the system. Partial pivoting costs a lot of computation time and memory space. The second advantage is the possibility to reduce the number of unknowns, which also reduces the computation times considerably.

When applying a penalty function method, special attention should be payed to the choice of the penalty function parameter. In the penalty formulation an extra term has been added to the incompressibility constraint $\underset{\sim}{L}\Delta\underset{\sim}{x} = -\underset{\sim}{k}$. In order to approximate the solution of the incompressibility constraint the extra term must be small. Usually, this requirement is satisfied by choosing a small value for the penalty parameter ϵ_1. However, when the penalty parameter has been chosen too small, an ill conditioned system will induce and the solution will deteriorate becausé of the ill conditioning and accumulation of round-off errors.

In the problem here considered, the extra term is the product of the penalty parameter ϵ_1 and the variation of the pressure-like quantity Δp. This variation Δp tends to zero in a converging iterative solution proces. Then the extra term also tends to zero, regardless of the value of the penalty parameter. Consequently, in this problem the penalty parameter does not influence the final solution, which indeed has been ascertained. This is a very unusual phenomenon for the penalty parameter method.

The system of equations (2.31) and (2.32) has been developed for one representative element. This element has been implemented in the finite element package SEPRAN [7]. SEPRAN creates the matrices and right hand sides for all elements and assembles them. This results in one large matrix and one large right hand side column. After this assembly SEPRAN also solves the resulting matrix equation. The structure of the program, in which the assembly process and the solving of the system of equations occurs, is discussed in appendix F.

Chapter 3

Contact

3.1 Introduction

Due to friction in the contact zones of the capstan drive the tape is driven. In this chapter, the contact phenomena for the combination of capstan, pinch roller and tape will be analyzed.

In this research, the problem will be reduced to contact between two bodies, the capstan and the pinch roller coating. Later on, the tape can be added as a third contacting body.

In the contact region extra conditions have to be fulfilled. Firstly, a material point of one body can't occupy the same position as a material point of the other body. Because of this impenetrability, a geometrical constraint has to be taken into account.

Secondly, each body is loaded by contact forces in the contact zone. At contact points the law of action and reaction applies.

In this chapter, the impenetrability constraint and the contact stresses for the contact between capstan and pinch roller coating will be described mathematically.

3.2 Impenetrability constraint

Before describing the contact conditions, some assumptions have to be made. Firstly, it is assumed that the capstan is rigid with respect to the pinch roller coating. This assumption is tenable, because the metal capstan is much stiffer than the rubber pinch roller coating.

Another important aspect is the interaction between the bodies. Adhesion is

not allowed. The friction between the two bodies can be described with the aid of a constitutive equation. For the moment however, only frictionless contact is considered.

Furthermore, the position and the movement of the capstan are supposed to be known. Material points of the pinch roller may not penetrate the capstan.

In this section the system of equations for the impenetrability will be determined. Afterwards, this system of equations will be treated such that it can be solved computationally.

3.2.1 System of equations

First, a few notations have to be defined. The pinch roller coating is a three-dimensional body that occupies a bounded open domain $\Omega_p(t)$ with boundary $\Gamma_p(t)$ at the current state t. $\bar{\Omega}_p(t)$ denotes the closure of $\Omega_p(t)$, i.e. $\bar{\Omega}_p(t) = \Omega_p(t) \cup \Gamma_p(t)$. Similar notations will be used for the domain, the bounded open domain and the boundary of the capstan. These are indicated by $\bar{\Omega}_{cap}(t)$, $\Omega_{cap}(t)$ and $\Gamma_{cap}(t)$ respectively.

The candidate contact area of the pinch roller coating is indicated by $\Gamma_{cp}(t)$, whereas the candidate contact area of the capstan is indicated by $\Gamma_{ccap}(t)$. The real contact area $\Gamma_c(t)$ is a part of $\Gamma_{cp}(t)$ ($\Gamma_c(t) \subset \Gamma_{cp}(t)$), but also a part of $\Gamma_{ccap}(t)$ ($\Gamma_c(t) \subset \Gamma_{ccap}(t)$).

Now, at each state t a scalar quantity $g = g(\vec{x}, \Gamma_{ccap}(t))$ has to be defined for all $\vec{x} \in \Gamma_{cp}(t)$, such that (see [10])

$$
\begin{aligned}
g(\vec{x}, \Gamma_{ccap}(t)) &< 0 \qquad \text{if} \quad \vec{x} \notin \bar{\Omega}_{cap}(t) \\
g(\vec{x}, \Gamma_{ccap}(t)) &= 0 \qquad \text{if} \quad \vec{x} \in \Gamma_{ccap}(t) \\
g(\vec{x}, \Gamma_{ccap}(t)) &> 0 \qquad \text{if} \quad \vec{x} \in \Omega_{cap}(t)
\end{aligned}
$$

It can be seen that no penetration occurs if and only if

$$
g(\vec{x}, \Gamma_{ccap}(t)) \leq 0 \qquad \forall \quad \vec{x} \in \Gamma_{cp}(t) \tag{3.1}
$$

In this section such a functional g will be formulated for the contact between the pinch roller coating and the capstan.

The capstan is a cylinder with radius R_c. The distance between a material point on the curved boundary of a cylinder and the axis of the cylinder is equal to the radius. If the cylinder is rigid and if another body comes in contact with the curved boundary of the cylinder and no penetration is allowed, the distance from a material

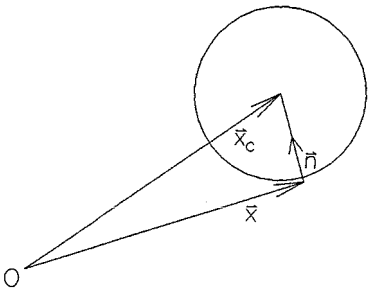

Figure 3.1: *Definition of the normal vector* $\vec{n}$

point on the candidate contact boundary of this body to the axis of the cylinder has to be equal to at least the radius of the cylinder.

So, the distance between a material point on the candidate contact boundary of the pinch roller coating and the axis of the capstan has to be equal to or greater than R_c. This can be formulated mathematically by the following equation:

$$|\vec{x} - \vec{x}_c| \geq R_c \qquad \forall \quad \vec{x} \in \Gamma_{cp}(t) \tag{3.2}$$

where $\vec{x}_c$ is *the orthogonal projection of vector* $\vec{x}$ *on the axis of the capstan.*

If the set of points $\vec{x}_a$ on the axis of the capstan is described by

$$\vec{x}_a = \vec{\alpha} + \lambda\,\vec{\beta} \qquad (\lambda \in I\!R) \tag{3.3}$$

then vector $\vec{x}_c$ is given as a function of vector $\vec{x}$ by the following relation.

$$\vec{x}_c = \frac{\vec{\beta}\vec{\beta}}{|\vec{\beta}|^2} \cdot \vec{x} + (\mathbf{I} - \frac{\vec{\beta}\vec{\beta}}{|\vec{\beta}|^2}) \cdot \vec{\alpha} \tag{3.4}$$

with $\vec{\alpha}$ is *the support vector of the axis of the capstan,*
$\vec{\beta}$ is *the direction vector of the axis of the capstan.*

The derivation of this relation is discussed in detail in appendix E.

Now, a unit vector $\vec{n}$ will be defined:

$$\vec{n} \stackrel{\text{def}}{=} \frac{\vec{x}_c - \vec{x}}{|\vec{x}_c - \vec{x}|} \tag{3.5}$$

This unit vector points from $\vec{x}$ to $\vec{x}_c$ on the axis of the capstan. This can also be seen in figure 3.1.

With this definition, the inequality constraint (3.2) can be rewritten as

$$-(\vec{x} - \vec{x}_c) \cdot \vec{n} \geq R_c \qquad \forall \quad \vec{x} \in \Gamma_{cp}(t)$$

Or:

$$(\vec{x} - \vec{x}_c) \cdot \vec{n} + R_c \leq 0 \qquad \forall \quad \vec{x} \in \Gamma_{cp}(t) \tag{3.6}$$

This is the functional g looked for.

Another contact condition is that at current contact points the law of action and reaction applies, i.e.

$$\vec{b}_p + \vec{b}_{cap} = \vec{0} \qquad \text{on} \quad \Gamma_c(t)$$

The normal vectors are opposite at current contact points. So, splitting the contact forces in a normal and a tangential component yields

$$\vec{\sigma}_{np} + \vec{\sigma}_{ncap} = \vec{0} \qquad \text{on} \quad \Gamma_c(t) \tag{3.7}$$

$$\vec{\sigma}_{tp} + \vec{\sigma}_{tcap} = \vec{0} \qquad \text{on} \quad \Gamma_c(t) \tag{3.8}$$

Initially, the contact is supposed to be frictionless. Then the shear stress can be left out of consideration. Later, the shear stress will be determined with the help of a constitutive equation.

Since the normal contact stresses are equal, a contact pressure σ_n is introduced.

$$\sigma_n = \sigma_{np} = \sigma_{ncap}$$

Adhesion between the contact bodies is not allowed. This means that the contact pressure σ_n is less than or equal to zero.

$$\sigma_n \leq 0 \qquad \text{on} \quad \Gamma_c(t)$$

It is allowed to impose this condition for the contact pressure not only on points of the real contact area, but also on other points of the candidate contact area. In these points the contact pressure equals to zero. So, the contact pressure has to satisfy the following constraint.

$$\sigma_n \leq 0 \qquad \text{on} \quad \Gamma_{cp}(t) \tag{3.9}$$

For convenience, here a summary of all contact conditions is presented.

$$\begin{cases} \sigma_n & \leq & 0 \\ g & \leq & 0 \end{cases} \tag{3.10}$$

$$\begin{cases} \text{if} \quad g = 0 \quad \text{then} \quad \sigma_n \leq 0 \\ \text{if} \quad g < 0 \quad \text{then} \quad \sigma_n = 0 \end{cases} \tag{3.11}$$

From equation (3.11) it follows that

$$\sigma_n \, g = 0 \qquad \text{on} \quad \Gamma_{cp}(t) \tag{3.12}$$

3.2.2 Penalty function method

The impenetrability constraint $g \leq 0$ is weakened by replacing it by $g_\epsilon = g + \epsilon_2 \, \sigma_n \leq 0$, with $\epsilon_2 > 0$. The penalty parameter ϵ_2 is chosen small, such that $\epsilon_2 \sigma_n$ is small compared to g in order to guarantee a good approximation of the constraint $g \leq 0$. But the penalty parameter must also be chosen large enough to avoid an ill conditioned problem. An optimal value for the penalty parameter ϵ_2 can be found by numerical experiments with several values for the parameter.

Replacing functional g in the contact conditions by $g + \epsilon_2 \, \sigma_n$ yields

$$\begin{cases} \sigma_n & \leq & 0 \\ g_\epsilon & \leq & 0 \end{cases} \tag{3.13}$$

$$\begin{cases} \text{if} \quad g_\epsilon = 0 \quad \text{then} \quad \sigma_n \leq 0 \\ \text{if} \quad g_\epsilon < 0 \quad \text{then} \quad \sigma_n = 0 \end{cases} \Longrightarrow \sigma_n \, g_\epsilon = 0 \tag{3.14}$$

Physically the penalty formulation can be interpreted as a contact problem with capstan with a somewhat smaller radius.

From the penalty formulation (3.14) it follows that, if $\sigma_n < 0$, then $g_\epsilon = 0$, which yields $\sigma_n = -\frac{1}{\epsilon_2} g$. And it follows that if $\sigma_n = 0$, then $g \leq 0$ is valid. Hence,

$$\sigma_n = -\frac{1}{\epsilon_2} g^+ \tag{3.15}$$

where $g^+ = max\{0, g\}$.

With equation (3.15) a relation has been found for the normal component of the boundary force in the contact region. Relations for boundary forces have to be substituted in the right hand side of the weak formulation of the balance of momentum (2.12):

$$\int_\Gamma \vec{w} \cdot \vec{b} \, d\Gamma = \int_\Gamma \vec{w} \cdot (\vec{b}_n + \vec{b}_t) \, d\Gamma$$

where $\vec{b}_n$ is *the normal boundary force*
$\vec{b}_t$ is *the tangential boundary force*

The boundary Γ_p is splitted in two parts, the candidate contact boundary, Γ_{cp} and the rest of the boundary $\Gamma_p \backslash \Gamma_{cp}$. Here, attention is only paid to boundary forces in the candidate contact zone. However, boundary forces on other parts of the boundary have to be treated in the same way.

On the candidate contact surface, the following forces are prescribed for a frictionless problem.

$$\vec{b}_t = 0 \qquad \text{on} \quad \Gamma_{cp} \tag{3.16}$$

$$\vec{b}_n = \sigma_n \vec{n} \qquad \text{on} \quad \Gamma_{cp} \tag{3.17}$$

Substitution of the prescribed boundary forces (3.16) and (3.17) and of equation (3.15) in equation (3.2.2) yields

$$\int_{\Gamma_{cp}} \vec{w} \cdot \vec{b}\, d\Gamma = -\int_{\Gamma_{cp}} \vec{w} \cdot \frac{1}{\epsilon_2} g^+ \vec{n}\, d\Gamma \tag{3.18}$$

3.2.3 Linearization and discretization

The impenetrability constraint is a nonlinear equation. In order to be able to solve it with the finite element method, it has to be linearized in the same way as the equations for the material behaviour. So, vector $\vec{x}$ is written as

$$\vec{x} = \hat{\vec{x}} + \Delta\vec{x} \tag{3.19}$$

Using this expression for $\vec{x}$, a linearization has been carried out for the contribution of the boundary force to the system of equations in appendix A. The result is given here:

$$\int_{\Gamma_{cp}} \vec{w} \cdot \vec{b}\, d\Gamma = -\int_{\Gamma_{cp}} \frac{1}{\epsilon_2} \vec{w} \cdot (\hat{g}^+ \hat{\vec{n}} + (\hat{\vec{n}}\hat{\vec{n}})^+ \cdot \Delta\vec{x} - \hat{g}^+ \frac{\hat{\vec{r}}\hat{\vec{r}}}{|\hat{\vec{x}}_c - \hat{\vec{x}}|} \cdot \Delta\vec{x}) d\Gamma + \mathcal{O}(\Delta^2) \tag{3.20}$$

with:

$$\begin{aligned}
\hat{g} &= (\hat{\vec{x}} - \hat{\vec{x}}_c) \cdot \hat{\vec{n}} + R_c \\
\hat{\vec{n}} &= \frac{(\hat{\vec{x}}_c - \hat{\vec{x}})}{|\hat{\vec{x}}_c - \hat{\vec{x}}|} \\
\hat{\vec{x}}_c &= \frac{\vec{\beta}\vec{\beta}}{|\vec{\beta}|^2} \cdot \hat{\vec{x}} + (\mathbf{I} - \frac{\vec{\beta}\vec{\beta}}{|\vec{\beta}|^2}) \cdot \vec{\alpha}
\end{aligned}$$

$$\hat{\vec{r}} = \frac{\hat{\vec{n}} * \vec{\beta}}{|\vec{\beta}|}$$

$(\ )^+$ means *that the mathematical quantity is only taken into account if* $g > 0$

The vector $\hat{\vec{r}}$ is the estimate for the tangential vector $\vec{r}$, which is defined by

$$\vec{r} = \frac{\vec{n} * \vec{\beta}}{|\vec{\beta}|}$$

The contribution for the impenetrability constraint (3.20) will be discretized geometrically by the finite element method. It is sufficient to discretize the candidate contact surface.

The element used for the discretization is a bilinear quadrilateral boundary element with four nodes for the position. This element will be treated in the next section.

In the discretization process, the unknown variable $\Delta\vec{x}$ and the weighting function $\vec{w}$ are approximated by a linear combination of their values in the nodes of the element.

$$\Delta\vec{x} = \sum_{i=1}^{4} \chi_i \, \Delta\vec{x}_i \tag{3.21}$$

$$\vec{w} = \sum_{i=1}^{4} \chi_i \, \vec{w}_i \tag{3.22}$$

where χ_i is *the shape function belonging to node i,*

$\vec{w}_i$ is *the value of weighting function* $\vec{w}$ *in node i.*

The result of the discretization is given by

$$\int_{\Gamma_{cp}} \vec{w} \cdot \vec{b} \, d\Gamma =$$

$$-\int_{\Gamma_{cp}} \frac{1}{\epsilon_2} \hat{g}^+ \underset{\sim}{w}^T \underline{\chi}^T \underset{\sim}{\hat{n}} \, d\Gamma - \int_{\Gamma_{cp}} \frac{1}{\epsilon_2} \underset{\sim}{w}^T \underline{\chi}^T [\underline{N}^+ - \frac{\hat{g}^+}{x_{dif}} \underline{R}] \underline{\chi} \, \underset{\sim}{\Delta x} \, d\Gamma + \mathcal{O}(\Delta^2) \tag{3.23}$$

with:

$$\underset{\sim}{w}^T = \begin{bmatrix} w_1{}^x & w_1{}^y & w_1{}^z & .... & w_4{}^x & w_4{}^y & w_4{}^z \end{bmatrix}$$

$$\underset{\sim}{\Delta x}^T = \begin{bmatrix} \Delta x_1 & \Delta y_1 & \Delta z_1 & .... & \Delta x_4 & \Delta y_4 & \Delta z_4 \end{bmatrix}$$

$$\underset{\sim}{\hat{n}}^T = \begin{bmatrix} \hat{n}^x & \hat{n}^y & \hat{n}^z \end{bmatrix}$$

$$\underline{\chi} = \begin{bmatrix} \chi_1 & 0 & 0 & .... & \chi_4 & 0 & 0 \\ 0 & \chi_1 & 0 & & 0 & \chi_4 & 0 \\ 0 & 0 & \chi_1 & & 0 & 0 & \chi_4 \end{bmatrix}$$

$$
\begin{aligned}
\underline{N} &= \begin{bmatrix} \hat{n}^x \hat{n}^x & \hat{n}^x \hat{n}^y & \hat{n}^x \hat{n}^z \\ \hat{n}^y \hat{n}^x & \hat{n}^y \hat{n}^y & \hat{n}^y \hat{n}^z \\ \hat{n}^z \hat{n}^x & \hat{n}^z \hat{n}^y & \hat{n}^z \hat{n}^z \end{bmatrix} \\
\underline{R} &= \begin{bmatrix} \hat{r}^x \hat{r}^x & \hat{r}^x \hat{r}^y & \hat{r}^x \hat{r}^z \\ \hat{r}^y \hat{r}^x & \hat{r}^y \hat{r}^y & \hat{r}^y \hat{r}^z \\ \hat{r}^z \hat{r}^x & \hat{r}^z \hat{r}^y & \hat{r}^z \hat{r}^z \end{bmatrix} \\
x_{dif} &= \sqrt{(\hat{x}_c - \hat{x})^2 + (\hat{y}_c - \hat{y})^2 + (\hat{z}_c - \hat{z})^2}
\end{aligned}
$$

The derivation of this result is given in appendix B.

Substitution of the discretized formulation (3.23) in the discretized equation for the balance of momentum (2.21) results in a new system of equations. Terms with unknowns are brought to the left hand side:

$$
\begin{aligned}
&\underset{\sim}{w}^T \int_\Omega [-\underline{Q}\Delta\underset{\sim}{p} + \underline{A}^T(\underset{\sim}{\psi}^T \hat{\underset{\sim}{p}}\, \underline{B} + 4c\,\underline{D} + \underline{T})\underline{A}\Delta\underset{\sim}{x}]d\Omega \\
&\qquad + \underset{\sim}{w}^T \int_{\Gamma_{cp}} \frac{1}{\epsilon_2} \underline{\chi}^T [\underline{N}^+ - \frac{\hat{g}^+}{x_{dif}} \underline{R}]\, \underline{\chi}\, \Delta\underset{\sim}{x}\, d\Gamma \\
&= \underset{\sim}{w}^T \int_\Omega (\underline{Q}\, \hat{\underset{\sim}{p}} - \underline{A}^T \hat{\underset{\sim}{\tau}})d\Omega + \underset{\sim}{w}^T \int_{\Gamma_p \setminus \Gamma_{cp}} \underline{P}\underset{\sim}{b}\, d\Gamma \\
&\qquad - \underset{\sim}{w}^T \int_{\Gamma_{cp}} \frac{1}{\epsilon_2} \hat{g}^+ \underline{\chi}^T \hat{\underset{\sim}{n}}\, d\Gamma \qquad \forall\ \underset{\sim}{w}
\end{aligned} \tag{3.24}
$$

$$
\underset{\sim}{r}^T \int_\Omega \underline{Q}^T \Delta\underset{\sim}{x}\, d\Omega = \underset{\sim}{r}^T \int_\Omega \underset{\sim}{\psi}\, \hat{k}\, d\Omega \qquad \forall\ \underset{\sim}{r} \tag{3.25}
$$

Since this system of equations must hold for all admissible weighting functions $\underset{\sim}{w}$ and $\underset{\sim}{r}$, the system can be generalized. After application of the penalty function method, this system is given by

$$
\begin{bmatrix} \underline{S} & -\underline{L}^T \\ -\underline{L} & -\epsilon_1 \underline{M} \end{bmatrix} \begin{bmatrix} \Delta\underset{\sim}{x} \\ \Delta\underset{\sim}{p} \end{bmatrix} = \begin{bmatrix} \underset{\sim}{f} \\ \underset{\sim}{k} \end{bmatrix} \tag{3.26}
$$

where:

$$
\begin{aligned}
\underline{S} &= \int_\Omega \underline{A}^T(\underset{\sim}{\psi}^T \hat{\underset{\sim}{p}}\, \underline{B} + 4c\,\underline{D} + \underline{T})\underline{A}d\Omega + \int_{\Gamma_{cp}} \frac{1}{\epsilon_2} \underline{\chi}^T [\underline{N}^+ - \frac{\hat{g}^+}{x_{dif}} \underline{R}]\, \underline{\chi}\, d\Gamma \\
\underline{L} &= \int_\Omega \underline{Q}^T\, d\Omega \\
\underset{\sim}{f} &= \int_\Omega (\underline{Q}\, \hat{\underset{\sim}{p}} - \underline{A}^T \hat{\underset{\sim}{\tau}})d\Omega + \int_{\Gamma_p \setminus \Gamma_{cp}} \underline{P}\underset{\sim}{b}\, d\Gamma - \int_{\Gamma_{cp}} \frac{1}{\epsilon_2} \hat{g}^+ \underline{\chi}^T \hat{\underset{\sim}{n}}\, d\Gamma \\
\underset{\sim}{k} &= -\int_\Omega \underset{\sim}{\psi}\, \hat{k}\, d\Omega
\end{aligned}
$$

Solving this system is analogue to solving the system of equations without contact.

3.2.4 Bilinear quadrilateral boundary element

A bilinear quadrilateral boundary element has four nodes. The domain of the element is completely defined by the locations of its four nodes. The domain is the geometrical area inside the four nodal points. The nodal points are labelled in ascending order corresponding to the counterclockwise direction (see figure 3.2).

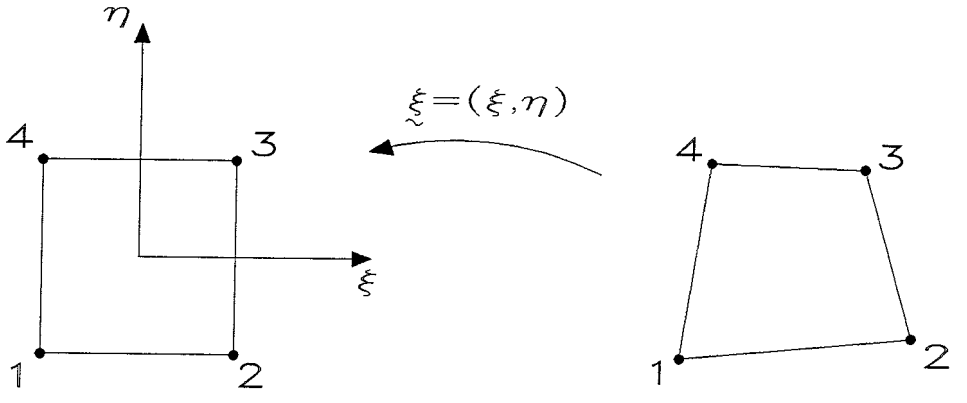

Figure 3.2: *Parent domain and local node ordering of the boundary element*

In order to define the shape functions for an arbitrary bilinear quadrilateral boundary element a parent domain is used. Such a parent domain has also been used for the trilinear hexahedral element, that has been applied to discretize the rubber body. The parent domain is defined in a $\mathbb{R}^2$-plane. In this plane, ξ and η are the independent coordinates. The parent domain of the bilinear quadrilateral boundary element is a bi-unit square, as depicted in figure 3.2.

The coordinates of a point (ξ, η) in the bi-unit square are related to the coordinates of a point (x, y, z) in the real boundary element by the following mapping.

$$\vec{x}(\xi,\eta) = \sum_{i=1}^{4} \chi_i(\xi,\eta)\vec{x}_i^e \tag{3.27}$$

where $\vec{x}_i^e$ is *the position of nodal point i of the element,*

χ_i is *the shape function belonging to node i.*

The shape function χ_i is a function of the natural coordinates ξ and η and is given by the following relation, which has been derived in appendix D.

$$\chi_i(\xi,\eta) = \frac{1}{4}(1+\xi_i\xi)(1+\eta_i\eta) \tag{3.28}$$

3.3 Friction

An essential aspect of the interaction between capstan, tape and pinch roller is the friction in the contact regions. Due to frictional forces in these contact zones, the tape is transported.

In this section, a constitutive relation for the friction will be added to the system of equations.

3.3.1 Coulomb law

In engineering, a commonly used model for dry friction is the Coulomb friction. According to the Coulomb law, the frictional force is proportional to the normal contact force, if relative velocity between the contacting bodies occurs. The direction of the friction force is opposite to the direction of the relative velocity of both bodies (see figure 3.3). If the relative velocity is equal to zero, then stick occurs and the frictional force is unknown.

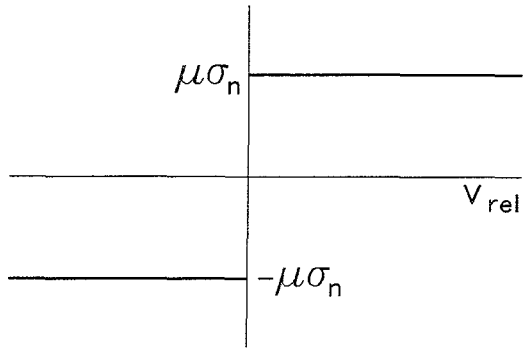

Figure 3.3: *Coulomb friction*

For slip ($\vec{v}_{rel} = 0$), the Coulomb friction $\vec{\sigma}_{coulomb}$ can be presented mathematically by the following equation.

$$\vec{\sigma}_{coulomb} = -\mu\,\sigma_n \frac{\vec{v}_{rel}}{|\vec{v}_{rel}|} = -\mu\,\sigma_n \frac{\vec{u}_{rel}/\Delta t}{|\vec{u}_{rel}|/\Delta t} = -\mu\,\sigma_n \frac{\vec{u}_{rel}}{|\vec{u}_{rel}|} \tag{3.29}$$

where μ is *the friction coefficient,*
$\vec{u}_{rel}$ is *the relative displacement.*

Constitutive equation (3.29) only describes slip. This constitutive relation will be substituted in the system of equations as a prescribed boundary force, in the next

section. Later on, the constitutive relation will be adapted, so that stick is also described.

3.3.2 Coulomb friction (slip)

In case of slip, the shear forces in the candidate contact zone must satisfy the constitutive equation for Coulomb friction.

$$\vec{b}_t = -\mu\,\sigma_n \frac{\vec{u}_c - \vec{u}}{|\vec{u}_c - \vec{u}|} \qquad \text{on} \qquad \Gamma_{cp} \tag{3.30}$$

where $\vec{u}$ is *the displacement of a contact point* $\vec{x}$ *of the pinch roller coating,*
$\vec{u}_c$ is *the displacement of the contact point of the capstan.*

The constitutive relation for the shear forces has to be substituted in equation (3.2.2).

$$\int_\Gamma \vec{w}\cdot\vec{b}\,d\Gamma = \int_{\Gamma_{cp}} \vec{w}\cdot(\vec{b}_n + \vec{b}_t)\,d\Gamma + \int_{\Gamma_p\setminus\Gamma_{cp}} \vec{w}\cdot\vec{b}\,d\Gamma \tag{3.31}$$

With respect to frictionless contact problems, there is one extra term unequal to zero:

$$\int_{\Gamma_{cp}} \vec{w}\cdot\vec{b}_t\,d\Gamma = -\int_{\Gamma_{cp}} \vec{w}\cdot\mu\,\sigma_n \frac{\vec{u}_c - \vec{u}}{|\vec{u}_c - \vec{u}|}\,d\Gamma \tag{3.32}$$

In this section, this term will be worked out and afterwards it will be added to the system of equations for a frictionless contact problem.

The movement of the capstan is assumed to be a combination of a translation and a rotation around its axis. So, the displacement of a contact point of the capstan in a time step Δt is given by

$$\vec{u}_c = \vec{s} + \bar{\omega}\,\Delta t\,R_c\,\vec{r} \tag{3.33}$$

where $\vec{s}$ is *the displacement of the capstan,*
$\bar{\omega}$ is *the mean rotation velocity of the capstan during the time step,*
$\vec{r}$ is *the tangential vector.*

The rotation direction $\vec{r}$ is defined as follows:

$$\vec{r} = \frac{\vec{n} * \vec{\beta}}{|\vec{\beta}|} \tag{3.34}$$

This definition implies, that the direction of vector $\vec{\beta}$ determines the direction of rotation as well.

Substitution of equation (3.15) in (3.32) yields

$$\int_{\Gamma_{cp}} \vec{w} \cdot \vec{b}_t \, d\Gamma = \int_{\Gamma_{cp}} \frac{\mu}{\epsilon_2} g^+ \vec{w} \cdot \frac{\vec{u}_c - \vec{u}}{|\vec{u}_c - \vec{u}|} \, d\Gamma \tag{3.35}$$

Linearization of the friction force has been carried out in appendix A. The result is given here.

$$\int_{\Gamma_{cp}} \vec{w} \cdot \vec{b}_t \, d\Gamma = \int_{\Gamma_{cp}} \frac{\mu}{\epsilon_2} \hat{g}^+ \vec{w} \cdot \hat{\vec{d}} \, d\Gamma + \int_{\Gamma_{cp}} \frac{\mu}{\epsilon_2} \vec{w} \cdot ((\hat{\vec{d}}\hat{\vec{n}})^+ + \hat{g}^+ \mathbf{K} \cdot \mathbf{G}) \cdot \Delta\vec{x} \, d\Gamma + \mathcal{O}(\Delta^2) \tag{3.36}$$

where:

$$\begin{aligned}
\hat{\vec{d}} &= \frac{\hat{\vec{u}}_c - \hat{\vec{u}}}{|\hat{\vec{u}}_c - \hat{\vec{u}}|} \\
\hat{\vec{r}} &= \frac{\hat{\vec{n}} * \vec{\beta}}{|\vec{\beta}|} \\
\mathbf{K} &= \frac{\mathbf{I} - \hat{\vec{d}}\hat{\vec{d}}}{|\hat{\vec{u}}_c - \hat{\vec{u}}|} \\
\mathbf{G} &= \bar{\omega} \Delta t \, R_c \frac{\hat{\vec{n}}\hat{\vec{r}}}{|\hat{\vec{x}}_c - \hat{\vec{x}}|} - \mathbf{I}
\end{aligned}$$

It is sufficient to discretize only the candidate contact surface. For the discretization a bilinear quadrilateral boundary element is used. After discretization of equation (3.36) with this element the following result will be obtained (see appendix B).

$$\begin{aligned}
\int_{\Gamma_{cp}} \vec{w} \cdot \vec{b}_t \, d\Gamma &= \int_{\Gamma_{cp}} \frac{\mu}{\epsilon_2} \hat{g}^+ \underset{\sim}{w}^T \underline{\chi}^T \underset{\sim}{\hat{d}} \, d\Gamma \\
&+ \int_{\Gamma_{cp}} \frac{\mu}{\epsilon_2} \underset{\sim}{w}^T \underline{\chi}^T ((\underset{\sim}{\hat{d}} \underset{\sim}{\hat{n}}^T)^+ + \hat{g}^+ \underline{K}\,\underline{G}) \underline{\chi} \, \Delta \underset{\sim}{x} \, d\Gamma + \mathcal{O}(\Delta^2)
\end{aligned} \tag{3.37}$$

where

$$\begin{aligned}
\underset{\sim}{\hat{d}}^T &= \begin{bmatrix} \hat{d}^x & \hat{d}^y & \hat{d}^z \end{bmatrix} \\
\underset{\sim}{\hat{r}}^T &= \begin{bmatrix} \hat{r}^x & \hat{r}^y & \hat{r}^z \end{bmatrix} \\
\underset{\sim}{w}^T &= \begin{bmatrix} {w_1}^x & {w_1}^y & {w_1}^z & .... & {w_4}^x & {w_4}^y & {w_4}^z \end{bmatrix} \\
\underline{K} &= \frac{\underline{I} - \underset{\sim}{\hat{d}}\,\underset{\sim}{\hat{d}}^T}{u_{dif}} \\
u_{dif} &= \sqrt{(\hat{u}_c^x - \hat{u}^x)^2 + (\hat{u}_c^y - \hat{u}^y)^2 + (\hat{u}_c^z - \hat{u}^z)^2} \\
\underline{G} &= \bar{\omega} \Delta t \, R_c \frac{\underset{\sim}{\hat{n}}\,\underset{\sim}{\hat{r}}^T}{x_{dif}} - \underline{I} \\
x_{dif} &= \sqrt{(\hat{x}_c - \hat{x})^2 + (\hat{y}_c - \hat{y})^2 + (\hat{z}_c - \hat{z})^2}
\end{aligned}$$

Substitution of the discretized formulation (3.37) in the discretized equation for the balance of momentum (2.21) results in a new system of equations. Terms with unknowns are brought to the left hand side:

$$
\begin{aligned}
&\underset{\sim}{w}^T \int_\Omega [-\underline{Q}\Delta\underset{\sim}{p} + \underline{A}^T(\underset{\sim}{\psi}^T \hat{p}\, \underline{B} + 4c\,\underline{D} + \underline{T})\underline{A}\Delta\underset{\sim}{x}]d\Omega \\
&\qquad + \underset{\sim}{w}^T \int_{\Gamma_{cp}} \frac{1}{\epsilon_2}\underline{\chi}^T[\underline{N}^+ - \frac{\hat{g}^+}{x_{dif}}\underline{R}]\,\underline{\chi}\Delta\underset{\sim}{x}\; d\Gamma \\
&-\underset{\sim}{w}^T \int_{\Gamma_{cp}} \frac{\mu}{\epsilon_2}\underline{\chi}^T((\hat{\underset{\sim}{d}}\,\hat{\underset{\sim}{n}}^T)^+ + \hat{g}^+\,\underline{K}\,\underline{G})\,\underline{\chi}\Delta\underset{\sim}{x}\; d\Gamma \\
&= \underset{\sim}{w}^T \int_\Omega (\underline{Q}\,\hat{\underset{\sim}{p}} - \underline{A}^T\hat{\underset{\sim}{\tau}})d\Omega + \underset{\sim}{w}^T \int_{\Gamma_p\setminus\Gamma_{cp}} \underline{P}\underset{\sim}{b}\; d\Gamma \\
&-\underset{\sim}{w}^T \int_{\Gamma_{cp}} \frac{1}{\epsilon_2}\hat{g}^+\underline{\chi}^T\hat{\underset{\sim}{n}}\; d\Gamma + \underset{\sim}{w}^T \int_{\Gamma_{cp}} \frac{\mu}{\epsilon_2}\hat{g}^+\,\underline{\chi}^T\hat{\underset{\sim}{d}}\; d\Gamma \qquad \forall\ \underset{\sim}{w}
\end{aligned}
\tag{3.38}
$$

$$
\underset{\sim}{r}^T \int_\Omega \underline{Q}^T\Delta\underset{\sim}{x}\, d\Omega = \underset{\sim}{r}^T \int_\Omega \underset{\sim}{\psi}\,\hat{k}\, d\Omega \qquad \forall\ \underset{\sim}{r} \tag{3.39}
$$

Since this system of equations must hold for all admissible weighting functions $\underset{\sim}{w}$ and $\underset{\sim}{r}$, the system can be generalized. After application of the penalty function method, this system is given by

$$
\begin{bmatrix} \underline{S} & -\underline{L}^T \\ -\underline{L} & -\epsilon_1\,\underline{M} \end{bmatrix} \begin{bmatrix} \Delta\underset{\sim}{x} \\ \Delta\underset{\sim}{p} \end{bmatrix} = \begin{bmatrix} \underset{\sim}{f} \\ \underset{\sim}{k} \end{bmatrix} \tag{3.40}
$$

where:

$$
\begin{aligned}
\underline{S} &= \int_\Omega \underline{A}^T(\underset{\sim}{\psi}^T\hat{p}\,\underline{B} + 4c\,\underline{D} + \underline{T})\underline{A}d\Omega + \int_{\Gamma_{cp}} \frac{1}{\epsilon_2}\underline{\chi}^T[\underline{N}^+ - \frac{\hat{g}^+}{x_{dif}}\underline{R}]\,\underline{\chi}\, d\Gamma \\
&\quad - \int_{\Gamma_{cp}} \frac{\mu}{\epsilon_2}\underline{\chi}^T((\hat{\underset{\sim}{d}}\,\hat{\underset{\sim}{n}}^T)^+ + \hat{g}^+\,\underline{K}\,\underline{G})\,\underline{\chi}\, d\Gamma \\
\underline{L} &= \int_\Omega \underline{Q}^T\, d\Omega \\
\underset{\sim}{f} &= \int_\Omega (\underline{Q}\,\hat{\underset{\sim}{p}} - \underline{A}^T\hat{\underset{\sim}{\tau}})d\Omega + \int_{\Gamma_p\setminus\Gamma_{cp}} \underline{P}\underset{\sim}{b}\; d\Gamma - \int_{\Gamma_{cp}} \frac{1}{\epsilon_2}\hat{g}^+\underline{\chi}^T\hat{\underset{\sim}{n}}\; d\Gamma \\
&\quad + \int_{\Gamma_{cp}} \frac{\mu}{\epsilon_2}\hat{g}^+\underline{\chi}^T\hat{\underset{\sim}{d}}\; d\Gamma \\
\underset{\sim}{k} &= -\int_\Omega \underset{\sim}{\psi}\,\hat{k}\, d\Omega
\end{aligned}
$$

Solving this system is analogue to solving the system of equations without friction.

3.3.3 Coulomb friction (regularized)

It turns out that the system of equations, derived in the previous section, will not converge. The discontinuity of the Coulomb friction curve at the point where the

relative displacement equals to zero, causes numerical problems. A regularization procedure is applied to overcome this problem.

In this procedure, the Coulomb law will be approximated by the following relation (see also figure 3.4):

$$\hat{\vec{\sigma}}_{coulomb} = -\mu\,\sigma_n\,\phi(\vec{u}_{rel})\,\frac{\vec{u}_{rel}}{|\vec{u}_{rel}|} \tag{3.41}$$

Two possibilities for function ϕ are

$$\phi_1(\vec{u}_{rel}) = \tanh(\frac{|\vec{u}_{rel}|}{\epsilon_3\,\Delta t}) \tag{3.42}$$

$$\phi_2(\vec{u}_{rel}) = \frac{2}{\pi}\arctan(\frac{|\vec{u}_{rel}|}{\epsilon_4\,\Delta t}) \tag{3.43}$$

The parameters ϵ_3 and ϵ_4 regulate the amount of smoothing. These parameters can be interpreted as the relative velocity below which the friction force starts dropping considerably to zero.

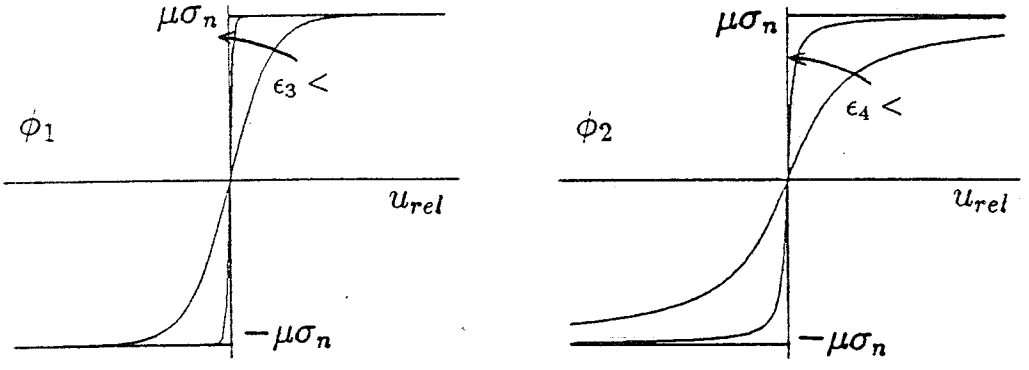

Figure 3.4: *Regularization of the Coulomb friction*

An additional advantage of the type of formulation of equation (3.41) is that it automatically handles both stick and slip. Logical steps of making distinction between sticking and sliding are not necessary.

The implementation of this friction model is analogous to the implementation of the Coulomb friction. Relation (3.41) will be substituted in the right hand side of the balance of momentum (2.12):

$$\int_{\Gamma_{cp}} \vec{w}\cdot\vec{b}_t\,d\Gamma = -\int_{\Gamma_{cp}} \mu\,\sigma_n\,\phi\,\vec{w}\cdot\frac{\vec{u}_c-\vec{u}}{|\vec{u}_c-\vec{u}|}\,d\Gamma \tag{3.44}$$

Linearization of this equation produces different results for both regularization functions ϕ. Therefore, they will be treated separately.

Regularized Coulomb friction 1

If the regularization function ϕ is given by equation (3.42), then linearization of equation (3.44) gives the following result (see appendix A).

$$\int_{\Gamma_{cp}} \vec{w} \cdot \vec{b}_t \, d\Gamma = \int_{\Gamma_{cp}} \frac{\mu}{\epsilon_2} \hat{g}^+ \hat{\phi}_1 \vec{w} \cdot \hat{\vec{d}} \, d\Gamma$$
$$+ \int_{\Gamma_{cp}} \frac{\mu}{\epsilon_2} \vec{w} \cdot \left[\hat{\phi}_1 (\hat{\vec{d}}\vec{\hat{n}})^+ + \left(\frac{\hat{g}^+}{\epsilon_3 \Delta t} \{1 - \tanh^2(\frac{|\hat{\vec{u}}_c - \hat{\vec{u}}|}{\epsilon_3 \Delta t})\} \hat{\vec{d}}\hat{\vec{d}} + \hat{g}^+ \hat{\phi}_1 \mathbf{K} \right) \cdot \mathbf{G} \right] \cdot \Delta \vec{x} \, d\Gamma$$
$$+ \mathcal{O}(\Delta^2) \tag{3.45}$$

where

$$\hat{\phi}_1 = \tanh(\frac{|\hat{\vec{u}}_c - \hat{\vec{u}}|}{\epsilon_3 \Delta t}) \tag{3.46}$$

This relation is discretized (see appendix B), yielding

$$\int_{\Gamma_{cp}} \vec{w} \cdot \vec{b}_t \, d\Gamma = \int_{\Gamma_{cp}} \frac{\mu}{\epsilon_2} \hat{g}^+ \hat{\phi}_1 \underset{\sim}{w}^T \underline{\chi}^T \hat{\underset{\sim}{d}} \, d\Gamma$$
$$+ \int_{\Gamma_{cp}} \frac{\mu}{\epsilon_2} \underset{\sim}{w}^T \underline{\chi}^T \left[\hat{\phi}_1 (\hat{\underset{\sim}{d}} \, \hat{\underset{\sim}{n}}^T)^+ + \left(\frac{\hat{g}^+}{\epsilon_3 \Delta t} \{1 - \tanh^2(\frac{u_{dif}}{\epsilon_3 \Delta t})\} \hat{\underset{\sim}{d}} \, \hat{\underset{\sim}{d}}^T + \hat{g}^+ \hat{\phi}_1 \underline{K} \right) \underline{G} \right] \underline{\chi} \Delta \underset{\sim}{x} \, d\Gamma$$
$$+ \mathcal{O}(\Delta^2) \tag{3.47}$$

This discretized formulation is substituted in the discretized equation for the balance of momentum (2.21). Application of the penalty function method yields the system of equations given by equation (3.40). However, the diffusion matrix $\underline{S}$ and right hand side $\underset{\sim}{f}$ are now represented by

$$\underline{S} = \int_\Omega \underline{A}^T (\underset{\sim}{\psi}^T \hat{\underset{\sim}{p}} \, \underline{B} + 4c \, \underline{D} + \underline{T}) \underline{A} d\Omega + \int_{\Gamma_{cp}} \frac{1}{\epsilon_2} \underline{\chi}^T [\underline{N}^+ - \frac{\hat{g}^+}{x_{dif}} \underline{R}] \underline{\chi} \, d\Gamma$$
$$- \int_{\Gamma_{cp}} \frac{\mu}{\epsilon_2} \underline{\chi}^T \left[\hat{\phi}_1 (\hat{\underset{\sim}{d}} \, \hat{\underset{\sim}{n}}^T)^+ + \left(\frac{\hat{g}^+}{\epsilon_3 \Delta t} \{1 - \tanh^2(\frac{u_{dif}}{\epsilon_3 \Delta t})\} \hat{\underset{\sim}{d}} \, \hat{\underset{\sim}{d}}^T + \hat{g}^+ \hat{\phi}_1 \underline{K} \right) \underline{G} \right] \underline{\chi} \, d\Gamma$$
$$\underset{\sim}{f} = \int_\Omega (\underline{Q} \hat{\underset{\sim}{p}} - \underline{A}^T \hat{\underset{\sim}{\tau}}) d\Omega + \int_{\Gamma_p \setminus \Gamma_{cp}} \underline{P} \underset{\sim}{b} \, d\Gamma - \int_{\Gamma_{cp}} \frac{1}{\epsilon_2} \hat{g}^+ \underline{\chi}^T \hat{\underset{\sim}{n}} \, d\Gamma$$
$$+ \int_{\Gamma_{cp}} \frac{\mu}{\epsilon_2} \hat{g}^+ \hat{\phi}_1 \underline{\chi}^T \hat{\underset{\sim}{d}} \, d\Gamma$$

Regularized Coulomb friction 2

The Coulomb friction can also be approximated using regularization function ϕ_2, as given in relation (3.43). Linearization of the friction then yields (see appendix A)

$$\int_{\Gamma_{cp}} \vec{w} \cdot \vec{b}_t \, d\Gamma = \int_{\Gamma_{cp}} \frac{\mu}{\epsilon_2} \hat{g}^+ \hat{\phi}_2 \vec{w} \cdot \hat{\vec{d}} \, d\Gamma$$

$$+\int_{\Gamma_{cp}} \frac{\mu}{\epsilon_2}\,\vec{w}\cdot\left[\hat{\phi}_2\,(\hat{\vec{d}}\hat{\vec{n}})^+ + \left(\frac{2\,\hat{g}^+\,\epsilon_4\,\Delta t}{\pi((\epsilon_4\Delta t)^2+|\hat{\vec{u}}_c-\hat{\vec{u}}|^2)}\,\hat{\vec{d}}\hat{\vec{d}} + \hat{g}^+\,\hat{\phi}_2\,\mathbf{K}\right)\cdot\mathbf{G}\right]\cdot\Delta\vec{x}\,d\Gamma$$
$$+\mathcal{O}(\Delta^2) \tag{3.48}$$

where

$$\hat{\phi}_2 = \frac{2}{\pi}\arctan\left(\frac{|\hat{\vec{u}}_c-\hat{\vec{u}}|}{\epsilon_4\Delta t}\right) \tag{3.49}$$

Discretization of this expression gives the following result (see appendix B).

$$\int_{\Gamma_{cp}} \vec{w}\cdot\vec{b}_t\,d\Gamma = \int_{\Gamma_{cp}} \frac{\mu}{\epsilon_2}\,\hat{g}^+\,\hat{\phi}_2\,\underset{\sim}{w}^T\underline{\chi}^T\underset{\sim}{\hat{d}}\;d\Gamma$$
$$+\int_{\Gamma_{cp}} \frac{\mu}{\epsilon_2}\,\underset{\sim}{w}^T\underline{\chi}^T\left[\hat{\phi}_2\,(\underset{\sim}{\hat{d}}\,\underset{\sim}{\hat{n}}^T)^+ + \left(\frac{2\,\hat{g}^+\,\epsilon_4\,\Delta t}{\pi((\epsilon_4\Delta t)^2+u_{dif}{}^2)}\,\underset{\sim}{\hat{d}}\,\underset{\sim}{\hat{d}}^T + \hat{g}^+\,\hat{\phi}_2\,\underline{K}\right)\underline{G}\right]\underline{\chi}\,\underset{\sim}{\Delta x}\;d\Gamma$$
$$+\mathcal{O}(\Delta^2) \tag{3.50}$$

The penalty function formulation of the generalized system of equations is again given by equation (3.40). However, the diffusion matrix $\underline{S}$ and the right hand side $\underset{\sim}{f}$ are now represented by

$$\begin{aligned}
\underline{S} &= \int_\Omega \underline{A}^T(\underset{\sim}{\psi}^T\underset{\sim}{\hat{p}}\,\underline{B}+4c\,\underline{D}+\underline{T})\underline{A}\,d\Omega + \int_{\Gamma_{cp}} \frac{1}{\epsilon_2}\underline{\chi}^T[\underline{N}^+ - \frac{\hat{g}^+}{x_{dif}}\underline{R}]\,\underline{\chi}\,d\Gamma \\
&- \int_{\Gamma_{cp}} \frac{\mu}{\epsilon_2}\underline{\chi}^T\left[\hat{\phi}_2\,(\underset{\sim}{\hat{d}}\,\underset{\sim}{\hat{n}}^T)^+ + \left(\frac{2\,\hat{g}^+\,\epsilon_4\,\Delta t}{\pi((\epsilon_4\Delta t)^2+u_{dif}{}^2)}\,\underset{\sim}{\hat{d}}\,\underset{\sim}{\hat{d}}^T + \hat{g}^+\,\hat{\phi}_2\,\underline{K}\right)\underline{G}\right]\underline{\chi}\,d\Gamma \\
\underset{\sim}{f} &= \int_\Omega (\underline{Q}\,\underset{\sim}{\hat{p}} - \underline{A}^T\underset{\sim}{\hat{t}})\,d\Omega + \int_{\Gamma_p\setminus\Gamma_{cp}} \underline{P}\,\underset{\sim}{b}\,d\Gamma - \int_{\Gamma_{cp}} \frac{1}{\epsilon_2}\hat{g}^+\,\underline{\chi}^T\underset{\sim}{\hat{n}}\;d\Gamma \\
&+ \int_{\Gamma_c} \frac{\mu}{\epsilon_2}\,\hat{g}^+\,\hat{\phi}_2\,\underline{\chi}^T\underset{\sim}{\hat{d}}\;d\Gamma
\end{aligned}$$

Chapter 4

Results

4.1 Introduction

In this chapter, some results, obtained with the neo-Hookean element and the contact element, will be presented. Two test problems are examined. Their results are compared with results obtained with the finite element package MARC [8], which were already available.

The first test is a frictionless contact problem. In this test case a rubber block is indented by a rigid shaft.

The second test is a rolling contact problem. A rubber block is indented by a rolling rigid shaft. In the contact zone, friction is prescribed.

Previous the neo-Hookean element has been checked for some test cases. These test cases and their results are described and discussed in "A Lagrangian approach to the three-dimensional finite element modelling of a neo-Hookean rubber material" [11]. There, it is concluded that the element is suitable to describe the behaviour of an isotropic, elastic and incompressible material for moderate deformations, as occurring in rubber rollers and tires.

4.2 Frictionless contact

A rigid shaft is pushed in a rubber block at three different angles. The data and the results of these tests are presented in appendix G. They are discussed here.

In the first simulation, the shaft is parallel with one of the edges of the rubber block. This test case is simulated in SEPRAN as well as in MARC. The results are compared.

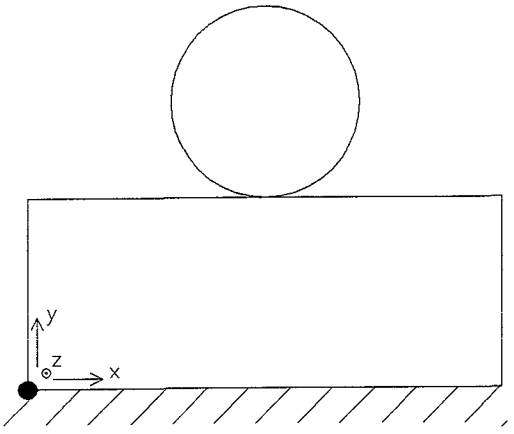

Figure 4.1: *Indentation of a rubber block by a rigid shaft*

Both simulations give nearly the same deformed geometry. With respect to the stresses, there are some more differences observable, chiefly quantitative.

The maximum differences for the Von Mises stress, for stress component σ_{yy} and stress component σ_{xz} are given in table 4.1. These differences are acceptable. The largest difference occurs for the Von Mises stress, since the Von Mises stress is determined from the separate stress components.

	SEPRAN		MARC		maximum
	min	max	min	max	difference
Von Mises	3.62E-2	2.48E+0	3.62E-2	3.04E+0	15%
σ_{yy}	-3.40E+0	4.83E-2	-3.61E+0	4.78E-2	6%
σ_{xz}	-4.03E-1	4.03E-1	-3.67E-1	3.67E-1	9%

Table 4.1: *Differences in stresses between SEPRAN and MARC*

The maxima and minima for the different stress components appear on the same locations in both simulations.

The lines of constant stresses, the so-called isobars, have the same form in both simulations, except for the Von Mises stress. In the Von Mises stress, obtained by MARC, the isobars have an unexpected form. They are not symmetrical with regard to plane $x = 3.5$, whereas the problem is symmetrical with regard to this plane. It is clear, that this result of MARC is wrong. The fault can be attributed to the discretization of the shaft, performed by MARC. As a consequence of this discretization, the contact condition changes. In SEPRAN, the shaft does not have to be discretized.

The other differences between MARC and SEPRAN can be explained by two differences. Probably, there arise differences between MARC and SEPRAN during

postprocessing. Another difference between MARC and SEPRAN is the solution method. In SEPRAN a penalty function method is applied, whereas in MARC a direct method is applied. Therefore, a good choice for the penalty parameters ϵ_1 for the neo-Hookean element and ϵ_2 for the contact element is very important. For that purpose, both penalty parameters have been varied. It appears, that for both penalty parameters a rather large domain is tolerable. The admissible domains are:

$$1E-13 < \epsilon_1 < 1E-1$$
$$1E-14 < \epsilon_2 < 1E-3$$

As expected by reason of the fact that the extra term of the penalty formulation converges to zero undependently of the penalty parameter ϵ_1, for penalty parameter ϵ_1 a large value is admissible. But if penalty parameter ϵ_2 is chosen larger than admissible, then the solution of the problem is not correct. If both penalty parameters are chosen smaller than admissible, the problem is so ill-conditioned, that no solution is obtained.

Two more test cases are simulated. In both these test cases, the shaft has been pressed in the rubber block at an angle with the z-axis. These test cases have been carried out in order to show that it is possible to push the capstan in a rubber block at any angle.

For the computation time, it does not matter at which angle the capstan indents the rubber block. However, in MARC the computation time increases a lot when the capstan is pushed in the rubber at an angle with the z-axis. This is a consequence of the increment splitting technique. That is why the simulation is not carried out with MARC. Yet, by comparison with test case 1 it is allowed to conclude that the simulations are rather good.

It can be concluded, that the boundary contact element describes the contact conditions well and that it has some advantages with regard to MARC. These advantages are:

- The computation time does not increase when the capstan is pressed in the rubber at an angle.
- The capstan is not discretized, which prevents an inaccurate handling of the contact conditions.

It must be noticed that the contact element is restricted to description of contact problems for rigid shafts.

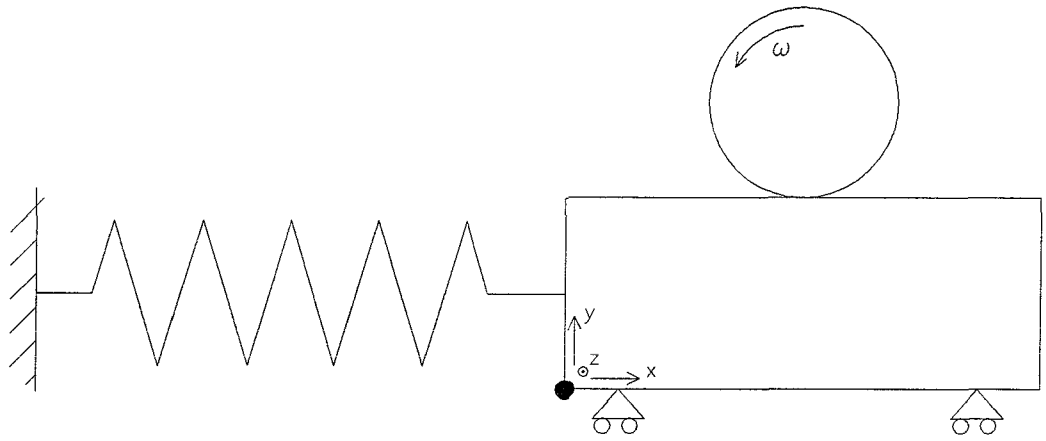

Figure 4.2: *Rolling contact problem*

4.3 Rolling contact

In this test case, a rubber block is indented by a rolling capstan. The rubber block is exposed to a friction force in the contact zone by this rolling capstan. At the bottom of the block a frictionless bearing is applied. One side of the block is joined to an elastic foundation with stiffness k per area (see figure 4.2). The data and results of the test are presented in appendix H. They are discussed here.

The friction force in the contact region has been modelled by both regularized Coulomb friction 1 and 2 (see section 3.3.3). It appears that both friction models give the same solution (test case 1 and 2). The regularization parameters ϵ_3 and ϵ_4 in these friction models are varied. They do not influence the results of this simulation (test case 3). In the field of slip, there is no difference between both friction models or between friction models with different regularization parameters.

After two time steps the position of equilibrium has been reached. In the following time step the position of the body does not change. This can lead to convergention problems in this time step. But since the final configuration has already been found, it is unnecessary to concern about these convergention problems.

The simulation has also been carried out with the finite element package MARC. These results are also presented in appendix H. Comparison of the results of both simulations shows mainly differences in the displacements. In MARC, the displacements are smaller. A possible explanation is that the elastic foundation is modelled differently in both simulations.

Another difference between both simulations is that in MARC the rubber body more or less vibrates around its position of equilibrium, without converging to this position of equilibrium. A possible explanation for this vibration is the discretization of the shaft. Simulations with a smaller mesh can possibly clearify this vibration.

In test case 4 the stiffness k of the elastic foundation has been reduced. As can be

seen in appendix H the rigid body displacement of the rubber block is larger. As a consequence of the reduced stiffness the resistance against displacement of the rubber block has been diminished. There are no significant changes in the stresses.

Reduction of the stiffness k can lead to numerical problems. Because of the small resistance against displacement, the friction imposes too large a displacement on the contact points. This displacement is so large, that it exceeds the tangential displacement of the capstan and contact is lost. As a consequence, the friction force is zero in the following iteration, and the point is forced back. In this way, points are alternatively in contact and not in contact. No solution will be found.

This numerical problem can be solved by the choice of the penalty parameter ϵ_2. However, it has to be taken into account that too large a penalty parameter results in bad contact conditions. Therefore, the deformed geometry must be checked on the boundary conditions.

In test case 4, the penalty parameter ϵ_2 had to be increased in order to obtain a solvable system. Checking the indentation of the rubber block shows that the contact conditions are not satisfied.

In test case 5, the friction between the capstan and rubber body is increased. The same problem as in test case 4 occurs. In order to obtain a solvable system penalty parameter ϵ_2 has to be increased too much. The contact conditions are not satisfied.

From the various test cases the following conclusions can be drawn:

- If the friction force is small and the freedom of movement of the rubber body is limited, the deformations of and the stresses in the body are computed satisfactorily.

- The model is not suitable for problems with large friction coefficients.

Chapter 5

Conclusions and recommendations

The neo-Hookean element and the contact element are tested for a frictionless contact problem. A rubber block has been indented by an rigid shaft. The results of this test are compared with results obtained with the finite element package MARC. Both numerical simulations show a good correspondence. The results obtained with use of the user-written elements are satisfactory.

In both elements, the penalty function method has been applied. In the frictionless contact problem the influence of the penalty parameters has been examined. It appears that for both penalty parameters a large domain is admissible. Penalty parameter ϵ_1 does not even influence the solution, because in the system of equations it has been multiplied with a quantity, that converges to zero.

In a second test a rolling capstan indents a rubber block. In the contact zone, friction must be prescribed. In general, friction is a very tiresome phenomenon in numerical models. In this test case, the friction causes numerical problems too. Only for limited friction forces and limited freedom of movement, the system of equations has been solved satisfactorily. The solution shows many correspondences with the results in the finite element package MARC.

For problems with large friction forces or a compliant foundation, the numerical problems can be overcome by the choice of the penalty parameter. However, this leads to unsatisfactory results for the contact conditions.

It can be concluded that the penalty function method in its present implementation is not suitable to describe contact conditions with large friction forces. Since the friction force and the freedom of movement are both large in the contact problem between capstan and pinch roller in a video recorder, the model is not yet suitable to describe this problem.

Since the model has specifically been created for contact between a rigid shaft and another body, it has some advantages with respect to finite element methods with a general approach of contact problems. These advantages are a substantial gain in computation time and an undiscretized capstan which prevents an inaccurate handling of the contact conditions. Of course, the applications of the model are restricted.

For future investigations in this research project it is advisable to pay attention to the following aspects:

- The description of the contact conditions should be improved. In stead of application of the penalty function method, another method could be applied, for instance a Lagrangian multiplier method.
- The influence of the element mesh should be examined.
- Also, the influence of the time step should be investigated.
- More attention should be paid to the appearance of stick or slip and to the division of these phenomena in the contact zone.
- The neo-Hookean and contact element should be checked for a real model of the capstan, first with two and later with three contact bodies.

Bibliography

[1] J. Durieu, M. Petit.
A 2D finite element solution of the steady rolling contact problem in the capstan/tape/roller mechanism of magnetic recorders.
Technical note N146, Philips Research Laboratories, Brussels, 1981.

[2] P. M. A. Slaats.
An Eulerian Approach to the finite deformations of rubber. Targeted on the modelling of a capstan drive in a video recorder.
Technical note N257, Philips Research Laboratories, Eindhoven, october 1989.

[3] F. E. Veldpaus.
Inleiding continuumsmechanica.
Collegedictaat 4612, Eindhoven University of Technology, 1984.

[4] T. J. R. Hughes.
The finite element method. Linear static and dynamic finite element analysis.
Prentice-Hall, New Jersey, 1987.

[5] C. Cuvelier, A. Segal and A. A. van Steenhoven.
Finite Element Methods and Navier-Stokes Equations.
D. Reidel Publishing Company, Dordrecht, Netherlands, 1986.

[6] T. J. R. Hughes and W. K. Liu.
Nonlinear finite element analysis of shells: Part 1. Three-dimensional shells.
Computer Methods in Applied Mechanics and Engineering, vol. 26, p. 331-362, 1981

[7] SEPRAN Manuals.
User's Manual, Programmers Guide and Standard Problems.
Ingenieursbureau SEPRA, Leidschendam, 1984.

[8] MARC Manuals.
Volume A, B, C and D, version K4.
MARC Analysis Research Corporation, January 1990.

[9] P. A. A. van Hoogstraten, P. M. A. Slaats and F. P. T. Baaijens.
A Eulerian approach to the finite element modelling of neo-Hookean rubber material.
Nationaal Mechanica Congres, Rolduc, april 1990.

[10] F. P. T. Baaijens.
On a numerical method to solve contact problems.
Eindhoven, january 1987.

[11] J. C. A. M. van Doormaal.
A Lagrangian approach to the three-dimensional finite element modelling of neo-Hookean rubber material.
Eindhoven, january 1991.

Appendices to

A Three-dimensional Finite Element Model for the Rolling Contact Problem in the Capstan Drive of a Video Recorder

WFW-report 91.026

J.C.A.M. van Doormaal

Eindhoven, April 1991

Appendix A

Linearization

In this appendix all non-linear equations will be linearized. These are the weighted residual equations for the balance of momentum and for the incompressibility constraint, the impenetrability constraint and the friction force. For that purpose the unknowns will be written as a sum of an estimate and a variation:

$$\vec{x} = \hat{\vec{x}} + \Delta\vec{x} \tag{A.1}$$

$$p = \hat{p} + \Delta p \tag{A.2}$$

After substitution terms of order Δ^2 or higher are neglected.

A.1 Balance of momentum and incompressibility constraint

First, the equations for the balance of momentum and for the incompressibility constraint will be linearized, given by

$$\int_\Omega (\vec{\nabla}\vec{w})^c : (-p\mathbf{I} + \boldsymbol{\tau})\, d\Omega = \int_\Gamma \vec{w}\cdot\vec{b}\, d\Gamma \quad ; \quad \boldsymbol{\tau} = 2c(\mathbf{F}\cdot\mathbf{F}^c - \mathbf{I}) \tag{A.3}$$

$$\int_\Omega r\,(\det(\mathbf{F}) - 1)\, d\Omega = 0 \tag{A.4}$$

Substitution of (A.1) in the deformation tensor yields

$$\begin{aligned}
\mathbf{F} &= (\vec{\nabla}_0\vec{x})^c \\
&= (\vec{\nabla}_0\hat{\vec{x}})^c + (\vec{\nabla}_0\Delta\vec{x})^c \\
&= \hat{\mathbf{F}} + \Delta\mathbf{F} \\
\hat{\mathbf{F}} &= (\vec{\nabla}_0\hat{\vec{x}})^c \\
\Delta\mathbf{F} &= (\vec{\nabla}_0\Delta\vec{x})^c
\end{aligned}$$

For the linearization of the inverse of the deformation tensor a Taylor series is used:

$$\begin{aligned}
\mathbf{F}^{-1} &= (\hat{\mathbf{F}} + \Delta\mathbf{F})^{-1} \\
&= (\mathbf{I} + \hat{\mathbf{F}}^{-1} \cdot \Delta\mathbf{F})^{-1} \cdot \hat{\mathbf{F}}^{-1} \\
&= (\mathbf{I} - \hat{\mathbf{F}}^{-1} \cdot \Delta\mathbf{F}) \cdot \hat{\mathbf{F}}^{-1} + \mathcal{O}(\Delta^2) \\
&= \hat{\mathbf{F}}^{-1} - \hat{\mathbf{F}}^{-1} \cdot \Delta\mathbf{F} \cdot \hat{\mathbf{F}}^{-1} + \mathcal{O}(\Delta^2) \\
&= \hat{\mathbf{F}}^{-1} + \Delta\mathbf{F}^{-1} \\
\Delta\mathbf{F}^{-1} &= -\hat{\mathbf{F}}^{-1} \cdot \Delta\mathbf{F} \cdot \hat{\mathbf{F}}^{-1} + \mathcal{O}(\Delta^2)
\end{aligned}$$

Linearization of the stress tensor $\boldsymbol{\tau}$:

$$\begin{aligned}
\boldsymbol{\tau} &= 2c(\mathbf{F} \cdot \mathbf{F}^c - \mathbf{I}) \\
&= 2c(\hat{\mathbf{F}} \cdot \hat{\mathbf{F}}^c + \hat{\mathbf{F}} \cdot \Delta\mathbf{F}^c + \Delta\mathbf{F} \cdot \hat{\mathbf{F}}^c + \Delta\mathbf{F} \cdot \Delta\mathbf{F}^c - \mathbf{I}) \\
&= \hat{\boldsymbol{\tau}} + \Delta\boldsymbol{\tau} \\
\hat{\boldsymbol{\tau}} &= 2c(\hat{\mathbf{F}} \cdot \hat{\mathbf{F}}^c - \mathbf{I}) \\
\Delta\boldsymbol{\tau} &= 2c(\hat{\mathbf{F}} \cdot \Delta\mathbf{F}^c + \Delta\mathbf{F} \cdot \hat{\mathbf{F}}^c + \Delta\mathbf{F} \cdot \Delta\mathbf{F}^c) \\
&= 2c[\hat{\mathbf{F}} \cdot \Delta\mathbf{F}^c + \Delta\mathbf{F} \cdot \hat{\mathbf{F}}^c] + \mathcal{O}(\Delta^2) \\
&= 2c[(\vec{\nabla}_0 \Delta\vec{x})^c \cdot \hat{\mathbf{F}}^c + \hat{\mathbf{F}} \cdot (\vec{\nabla}_0 \Delta\vec{x})] + \mathcal{O}(\Delta^2) \\
&= 2c[(\hat{\mathbf{F}}^{-c} \cdot \vec{\nabla}_0 \Delta\vec{x})^c \cdot \hat{\mathbf{F}} \cdot \hat{\mathbf{F}}^c + \hat{\mathbf{F}} \cdot \hat{\mathbf{F}}^c \cdot (\hat{\mathbf{F}}^{-c} \cdot \vec{\nabla}_0 \Delta\vec{x})] + \mathcal{O}(\Delta^2)
\end{aligned}$$

Using $\hat{\vec{\nabla}} = \hat{\mathbf{F}}^{-c} \cdot \vec{\nabla}_0$

$$\Delta\boldsymbol{\tau} = 2c[(\hat{\vec{\nabla}}\Delta\vec{x})^c \cdot \hat{\mathbf{F}} \cdot \hat{\mathbf{F}}^c + \hat{\mathbf{F}} \cdot \hat{\mathbf{F}}^c \cdot (\hat{\vec{\nabla}}\Delta\vec{x})] + \mathcal{O}(\Delta^2) \tag{A.5}$$

Using $\hat{\mathbf{F}} \cdot \hat{\mathbf{F}}^c = \frac{\hat{\boldsymbol{\tau}}}{2c} + \mathbf{I}$

$$\Delta\boldsymbol{\tau} \approx 2c[(\hat{\vec{\nabla}}\Delta\vec{x})^c + (\hat{\vec{\nabla}}\Delta\vec{x})] + (\hat{\vec{\nabla}}\Delta\vec{x})^c \cdot \hat{\boldsymbol{\tau}} + \hat{\boldsymbol{\tau}} \cdot (\hat{\vec{\nabla}}\Delta\vec{x}) \tag{A.6}$$

Linearization of the determinant of the deformation tensor:

$$\begin{aligned}
\det(\mathbf{F}) &= \det(\hat{\mathbf{F}} + \Delta\mathbf{F}) \\
&= \det(\hat{\mathbf{F}} + (\vec{\nabla}_0 \Delta\vec{x})^c) \\
&= \det(\hat{\mathbf{F}} \cdot (\mathbf{I} + \hat{\mathbf{F}}^{-1} \cdot (\vec{\nabla}_0 \Delta\vec{x})^c)) \\
&= \det(\hat{\mathbf{F}}) \det(\mathbf{I} + \hat{\mathbf{F}}^{-1} \cdot (\vec{\nabla}_0 \Delta\vec{x})^c) \\
&= \det(\hat{\mathbf{F}}) (1 + \mathrm{tr}(\hat{\mathbf{F}}^{-1} \cdot (\vec{\nabla}_0 \Delta\vec{x})^c) + \mathcal{O}(\Delta^2)
\end{aligned}$$

Using $(\vec{\nabla}_0 \Delta\vec{x})^c = (\hat{\vec{\nabla}}\Delta\vec{x})^c \cdot \hat{\mathbf{F}}$

$$\det(\mathbf{F}) = \det(\hat{\mathbf{F}}) (1 + \mathrm{tr}(\hat{\mathbf{F}}^{-1} \cdot (\hat{\vec{\nabla}}\Delta\vec{x})^c \cdot \hat{\mathbf{F}})) + \mathcal{O}(\Delta^2) \tag{A.7}$$

using $\mathrm{tr}(\mathbf{A}\cdot\mathbf{B}) = \mathrm{tr}(\mathbf{B}\cdot\mathbf{A})$

$$\begin{aligned}
\det(\mathbf{F}) &= \det(\hat{\mathbf{F}})\,(1+\mathrm{tr}(\hat{\mathbf{F}}\cdot\hat{\mathbf{F}}^{-1}\cdot(\hat{\vec{\nabla}}\Delta\vec{x})^c)+\mathcal{O}(\Delta^2)\\
&= \det(\hat{\mathbf{F}})\,(1+\mathrm{tr}(\hat{\vec{\nabla}}\Delta\vec{x})^c)+\mathcal{O}(\Delta^2)\\
&= \det(\hat{\mathbf{F}})\,(1+\hat{\vec{\nabla}}\cdot\Delta\vec{x})+\mathcal{O}(\Delta^2)
\end{aligned}$$

Using the linearizations above, the equations (A.3) and (A.4) can be linearized:

$$\begin{aligned}
(\vec{\nabla}\vec{w})^c : -p\mathbf{I} &= -p\,(\vec{\nabla}\cdot\vec{w})\\
&= -(\hat{p}+\Delta p)\,((\mathbf{F}^{-c}\cdot\vec{\nabla}_0)\cdot\vec{w})\\
&= -(\hat{p}+\Delta p)\,[[(\mathbf{I}-\hat{\mathbf{F}}^{-c}\cdot\Delta\mathbf{F}^c)\cdot\hat{\mathbf{F}}^{-c}\cdot\vec{\nabla}_0]\cdot\vec{w}]+\mathcal{O}(\Delta^2)\\
&= -\hat{p}\,[(\mathbf{I}-\hat{\mathbf{F}}^{-c}\cdot\Delta\mathbf{F}^c)\cdot\hat{\vec{\nabla}}]\cdot\vec{w}-\Delta p\,[\hat{\vec{\nabla}}\cdot\vec{w}]+\mathcal{O}(\Delta^2)\\
&= -\hat{p}\,(\hat{\vec{\nabla}}\cdot\vec{w})-\Delta p\,(\hat{\vec{\nabla}}\cdot\vec{w})+\hat{p}\,(\hat{\mathbf{F}}^{-c}\cdot\Delta\mathbf{F}^c\cdot\hat{\vec{\nabla}})\cdot\vec{w}+\mathcal{O}(\Delta^2)\\
(\vec{\nabla}\vec{w})^c : \boldsymbol{\tau} &= (\mathbf{F}^{-c}\cdot\vec{\nabla}_0\vec{w})^c : (\hat{\boldsymbol{\tau}}+\Delta\boldsymbol{\tau})\\
&= (\vec{\nabla}_0\vec{w})^c\cdot\mathbf{F}^{-1} : (\hat{\boldsymbol{\tau}}+\Delta\boldsymbol{\tau})\\
&= (\vec{\nabla}_0\vec{w})^c : [(\mathbf{I}-\hat{\mathbf{F}}^{-1}\cdot\Delta\mathbf{F})\cdot\hat{\mathbf{F}}^{-1}\cdot(\hat{\boldsymbol{\tau}}+\Delta\boldsymbol{\tau})]+\mathcal{O}(\Delta^2)\\
&= (\vec{\nabla}_0\vec{w})^c : [\hat{\mathbf{F}}^{-1}\cdot(\mathbf{I}-\Delta\mathbf{F}\cdot\hat{\mathbf{F}}^{-1})\cdot(\hat{\boldsymbol{\tau}}+\Delta\boldsymbol{\tau})]+\mathcal{O}(\Delta^2)\\
&= (\vec{\nabla}_0\vec{w})^c\cdot\hat{\mathbf{F}}^{-1} : (\mathbf{I}-\Delta\mathbf{F}\cdot\hat{\mathbf{F}}^{-1})\cdot(\hat{\boldsymbol{\tau}}+\Delta\boldsymbol{\tau})+\mathcal{O}(\Delta^2)\\
&= (\hat{\mathbf{F}}^{-c}\cdot\vec{\nabla}_0\vec{w})^c : (\mathbf{I}-\Delta\mathbf{F}\cdot\hat{\mathbf{F}}^{-1})\cdot(\hat{\boldsymbol{\tau}}+\Delta\boldsymbol{\tau})+\mathcal{O}(\Delta^2)\\
&= (\hat{\vec{\nabla}}\vec{w})^c : (\hat{\boldsymbol{\tau}}-\Delta\mathbf{F}\cdot\hat{\mathbf{F}}^{-1}\cdot\hat{\boldsymbol{\tau}}+\Delta\boldsymbol{\tau})+\mathcal{O}(\Delta^2)\\
&= (\hat{\vec{\nabla}}\vec{w})^c : [\hat{\boldsymbol{\tau}}-\Delta\mathbf{F}\cdot\hat{\mathbf{F}}^{-1}\cdot\hat{\boldsymbol{\tau}}+2c((\hat{\vec{\nabla}}\Delta\vec{x})^c+(\hat{\vec{\nabla}}\Delta\vec{x}))\\
&\quad +(\hat{\vec{\nabla}}\Delta\vec{x})^c\cdot\hat{\boldsymbol{\tau}}+\hat{\boldsymbol{\tau}}\cdot(\hat{\vec{\nabla}}\Delta\vec{x})]+\mathcal{O}(\Delta^2)\\
\det(\mathbf{F})-1 &= \det(\hat{\mathbf{F}})\,(1+\hat{\vec{\nabla}}\cdot\Delta\vec{x})-1+\mathcal{O}(\Delta^2)
\end{aligned}$$

We introduce some abbreviations:

$$\begin{aligned}
&\mathbf{L}_{\Delta x} = (\hat{\vec{\nabla}}\Delta\vec{x})^c = (\hat{\mathbf{F}}^{-c}\cdot\vec{\nabla}_0\Delta\vec{x})^c = \Delta\mathbf{F}\cdot\hat{\mathbf{F}}^{-1} = \mathbf{D}_{\Delta x}+\boldsymbol{\Omega}_{\Delta x}\\
&\mathbf{D}_{\Delta x} = \frac{1}{2}(\mathbf{L}_{\Delta x}+\mathbf{L}_{\Delta x}{}^c)\ ;\ \mathbf{D}_{\Delta x} = \mathbf{D}_{\Delta x}{}^c\\
&\boldsymbol{\Omega}_{\Delta x} = \frac{1}{2}(\mathbf{L}_{\Delta x}-\mathbf{L}_{\Delta x}{}^c)\ ;\ \boldsymbol{\Omega}_{\Delta x} = -\boldsymbol{\Omega}_{\Delta x}{}^c\\
&\mathbf{L}_w = (\hat{\vec{\nabla}}\vec{w})^c
\end{aligned}$$

So:

$$(\vec{\nabla}\vec{w})^c : -p\mathbf{I} = \hat{p}\,(\hat{\vec{\nabla}}\cdot\vec{w})-\Delta p\,(\hat{\vec{\nabla}}\cdot\vec{w})+\hat{p}\,(\mathbf{L}_{\Delta x}{}^c\cdot\hat{\vec{\nabla}})\cdot\vec{w}+\mathcal{O}(\Delta^2)$$

$$(\vec{\nabla}\vec{w})^c : \boldsymbol{\tau} = \mathbf{L}_w : (\hat{\boldsymbol{\tau}} + 4c\mathbf{D}_{\Delta x} + \hat{\boldsymbol{\tau}} \cdot \mathbf{L}_{\Delta x}{}^c) + \mathcal{O}(\Delta^2) \quad \text{(A.8)}$$

$$\det(\mathbf{F}) - 1 = \det(\hat{\mathbf{F}})\,(1 + \hat{\vec{\nabla}} \cdot \Delta\vec{x}) - 1 + \mathcal{O}(\Delta^2) \quad \text{(A.9)}$$

Using the relation $(\vec{a}\vec{b}) : \mathbf{I} = \mathrm{tr}(\vec{a}\vec{b}) = \vec{a} \cdot \vec{b}$

$$\begin{aligned}(\vec{\nabla}\vec{w})^c : -p\,\mathbf{I} &= -\hat{p}\,(\hat{\vec{\nabla}} \cdot \vec{w}) - \Delta p\,(\hat{\vec{\nabla}} \cdot \vec{w}) + \hat{p}\,\mathbf{L}_{\Delta x}{}^c \cdot \hat{\vec{\nabla}} \cdot \vec{w} + \mathcal{O}(\Delta^2) \\ &= -\hat{p}\,(\hat{\vec{\nabla}}\vec{w}) : \mathbf{I} - \Delta p\,(\hat{\vec{\nabla}}\vec{w}) : \mathbf{I} + \hat{p}\,\mathbf{L}_{\Delta x}{}^c \cdot (\hat{\vec{\nabla}}\vec{w}) : \mathbf{I} + \mathcal{O}(\Delta^2) \\ &= -\hat{p}\,\mathbf{L}_w{}^c : \mathbf{I} - \Delta p\,\mathbf{L}_w{}^c : \mathbf{I} + \hat{p}\,\mathbf{L}_{\Delta x}{}^c \cdot \mathbf{L}_w{}^c : \mathbf{I} + \mathcal{O}(\Delta^2)\end{aligned}$$

Using $\mathbf{A} : \mathbf{B} = \mathbf{A}^c : \mathbf{B}^c$, $\mathbf{A} \cdot \mathbf{B} : \mathbf{C} = \mathbf{A} : \mathbf{B} \cdot \mathbf{C}$ and $\mathbf{A} : \mathbf{B} = \mathbf{B} : \mathbf{A}$

$$\begin{aligned}(\vec{\nabla}\vec{w})^c : -p\,\mathbf{I} &= -\hat{p}\,\mathbf{L}_w : \mathbf{I} - \Delta p\,\mathbf{L}_w : \mathbf{I} + \hat{p}\,\mathbf{L}_{\Delta x} : \mathbf{L}_w + \mathcal{O}(\Delta^2) \\ &= \mathbf{L}_w : [-\hat{p}\,\mathbf{I} - \Delta p\,\mathbf{I} + \hat{p}\,\mathbf{L}_{\Delta x}] + \mathcal{O}(\Delta^2) \quad \text{(A.10)}\end{aligned}$$

Substitution of equations (A.8) , (A.9) and (A.10) in the integrals (A.3) and (A.4) produces the linearized system:

$$\begin{aligned}&\int_\Omega \mathbf{L}_w : [-\hat{p}\,\mathbf{I} - \Delta p\,\mathbf{I} + \hat{p}\,\mathbf{L}_{\Delta x}]d\Omega \; + \\ &\int_\Omega \mathbf{L}_w : (\hat{\boldsymbol{\tau}} + 4c\,\mathbf{D}_{\Delta x} + \hat{\boldsymbol{\tau}} \cdot \mathbf{L}_{\Delta x}{}^c)d\Omega = \int_\Gamma \vec{w} \cdot \vec{b}\,d\Gamma\end{aligned}$$

$$\int_\Omega r\,[\det(\hat{\mathbf{F}})\,(1 + \hat{\vec{\nabla}} \cdot \Delta\vec{x}) - 1]d\Omega = 0$$

Or, after replacing weighting function r by $\frac{r}{det\hat{\mathbf{F}}}$ in order to derive a symmetric matrix, and rearranging the terms:

$$\begin{aligned}&\int_\Omega \mathbf{L}_w : [-\hat{p}\,\mathbf{I} - \Delta p\,\mathbf{I} + \hat{p}\,\mathbf{L}_{\Delta x}]d\Omega \; + \\ &\int_\Omega \mathbf{L}_w : (\hat{\boldsymbol{\tau}} + 4c\,\mathbf{D}_{\Delta x} + \hat{\boldsymbol{\tau}} \cdot \mathbf{L}_{\Delta x}{}^c)d\Omega = \int_\Gamma \vec{w} \cdot \vec{b}\,d\Gamma \quad \text{(A.11)}\end{aligned}$$

$$\int_\Omega r\,\hat{\vec{\nabla}} \cdot \Delta\vec{x}\,d\Omega = \int_\Omega r\,(\frac{1}{\det(\hat{\mathbf{F}})} - 1)d\Omega \quad \text{(A.12)}$$

A.2 Impenetrability constraint

The contribution of the impenetrability constraint has to be linearized also. This contribution is given by

$$-\int_{\Gamma_{cp}} \frac{1}{\epsilon_2}\,\vec{w} \cdot g^+\,\vec{n}\,d\Gamma \quad \text{(A.13)}$$

where:

$$
\begin{aligned}
g &= (\vec{x} - \vec{x}_c) \cdot \vec{n} + R_c \\
g^+ &= max(0, g) \\
\vec{n} &= \frac{(\vec{x}_c - \vec{x})}{|\vec{x}_c - \vec{x}|} \\
\vec{x}_c &= \frac{\vec{\beta}\vec{\beta}}{|\vec{\beta}|^2} \cdot \vec{x} + (\mathbf{I} - \frac{\vec{\beta}\vec{\beta}}{|\vec{\beta}|^2}) \cdot \vec{\alpha}
\end{aligned}
$$

Using $\vec{x} = \hat{\vec{x}} + \Delta\vec{x}$, linearization of vector $\vec{x}_c$ yields

$$
\begin{aligned}
\vec{x}_c &= \hat{\vec{x}}_c + \Delta\vec{x}_c \\
\hat{\vec{x}}_c &= \frac{\vec{\beta}\vec{\beta}}{|\vec{\beta}|^2} \cdot \hat{\vec{x}} + (\mathbf{I} - \frac{\vec{\beta}\vec{\beta}}{|\vec{\beta}|^2}) \cdot \vec{\alpha} \\
\Delta\vec{x}_c &= \frac{\vec{\beta}\vec{\beta}}{|\vec{\beta}|^2} \cdot \Delta\vec{x}
\end{aligned}
$$

For the linearization of the normal vector $\vec{n}$ a Taylor series is used:

$$
\begin{aligned}
\vec{n} &= \hat{\vec{n}} + \Delta\vec{n} \\
\hat{\vec{n}} &= \frac{(\hat{\vec{x}}_c - \hat{\vec{x}})}{|\hat{\vec{x}}_c - \hat{\vec{x}}|} \\
\Delta\vec{n} &= \frac{(\hat{\vec{x}}_c + \Delta\vec{x}_c - \hat{\vec{x}} - \Delta\vec{x})}{|\hat{\vec{x}}_c + \Delta\vec{x}_c - \hat{\vec{x}} - \Delta\vec{x}|} - \frac{(\hat{\vec{x}}_c - \hat{\vec{x}})}{|\hat{\vec{x}}_c - \hat{\vec{x}}|}
\end{aligned}
$$

Introduction of the shorter notations:

$$
\begin{aligned}
\hat{\vec{h}} &= \hat{\vec{x}}_c - \hat{\vec{x}} \\
\Delta\vec{h} &= \Delta\vec{x}_c - \Delta\vec{x}
\end{aligned}
$$

and of the tangential vector r, which is defined and linearized as

$$
\begin{aligned}
\vec{r} &= \frac{\vec{n} * \vec{\beta}}{|\vec{\beta}|} \\
\vec{r} &= \hat{\vec{r}} + \Delta\vec{r} \\
\hat{\vec{r}} &= \frac{\hat{\vec{n}} * \vec{\beta}}{|\vec{\beta}|} \\
\Delta\vec{r} &= \frac{\Delta\vec{n} * \vec{\beta}}{|\vec{\beta}|}
\end{aligned}
$$

yields

$$\begin{aligned}
\Delta\vec{n} &= \frac{(\hat{\vec{h}}+\Delta\vec{h})}{\sqrt{(\hat{\vec{h}}+\Delta\vec{h})\cdot(\hat{\vec{h}}+\Delta\vec{h})}} - \frac{\hat{\vec{h}}}{|\hat{\vec{h}}|} \\
&= \frac{\hat{\vec{h}}}{|\hat{\vec{h}}|} - \frac{\hat{\vec{h}}}{|\hat{\vec{h}}|} + \left[\frac{\mathbf{I}}{|\hat{\vec{h}}|} - \frac{\hat{\vec{h}}\hat{\vec{h}}}{|\hat{\vec{h}}|^3}\right]\cdot(\Delta\vec{h}) + \mathcal{O}(\Delta^2) \\
&= \left[\frac{\mathbf{I}}{|\hat{\vec{h}}|} - \frac{\hat{\vec{h}}\hat{\vec{h}}}{|\hat{\vec{h}}|^3}\right]\cdot(\Delta\vec{h}) + \mathcal{O}(\Delta^2) \\
&= \left[\frac{\mathbf{I}-\hat{\vec{n}}\hat{\vec{n}}}{|\hat{\vec{x}}_c-\hat{\vec{x}}|}\right]\cdot(\Delta\vec{x}_c-\Delta\vec{x}) + \mathcal{O}(\Delta^2) \\
&= \left[\frac{\mathbf{I}-\hat{\vec{n}}\hat{\vec{n}}}{|\hat{\vec{x}}_c-\hat{\vec{x}}|}\right]\cdot\left[\frac{\vec{\beta}\vec{\beta}}{|\vec{\beta}|^2}-\mathbf{I}\right]\cdot\Delta\vec{x} + \mathcal{O}(\Delta^2)
\end{aligned}$$

Since $\vec{n}\perp\vec{\beta}$ and $\mathbf{I}=\hat{\vec{n}}\hat{\vec{n}}+\hat{\vec{r}}\hat{\vec{r}}+\frac{\vec{\beta}\vec{\beta}}{|\vec{\beta}|^2}$:

$$\begin{aligned}
\Delta\vec{n} &= -\frac{\mathbf{I}-\frac{\vec{\beta}\vec{\beta}}{|\vec{\beta}|^2}-\hat{\vec{n}}\hat{\vec{n}}}{|\hat{\vec{x}}_c-\hat{\vec{x}}|}\cdot\Delta\vec{x} + \mathcal{O}(\Delta^2) \\
&= -\frac{\hat{\vec{r}}\hat{\vec{r}}}{|\hat{\vec{x}}_c-\hat{\vec{x}}|}\cdot\Delta\vec{x} + \mathcal{O}(\Delta^2)
\end{aligned}$$

Linearization of the functional $g=(\vec{x}-\vec{x}_c)\cdot\vec{n}+R_c$ yields

$$\begin{aligned}
g &= \hat{g}+\Delta g \\
&= (\hat{\vec{x}}+\Delta\vec{x}-\hat{\vec{x}}_c-\Delta\vec{x}_c)\cdot(\hat{\vec{n}}+\Delta\vec{n})+R_c \\
\hat{g} &= (\hat{\vec{x}}-\hat{\vec{x}}_c)\cdot\hat{\vec{n}}+R_c \\
\Delta g &= (\hat{\vec{x}}-\hat{\vec{x}}_c)\cdot\Delta\vec{n}+(\Delta\vec{x}-\Delta\vec{x}_c)\cdot\hat{\vec{n}}+\mathcal{O}(\Delta^2)
\end{aligned}$$

Substitution of one of the linearized equation for $\Delta\vec{n}$ gives

$$\begin{aligned}
\Delta g &= (\hat{\vec{x}}-\hat{\vec{x}}_c)\cdot\left[\frac{\mathbf{I}}{|\hat{\vec{x}}_c-\hat{\vec{x}}|}-\frac{(\hat{\vec{x}}_c-\hat{\vec{x}})(\hat{\vec{x}}_c-\hat{\vec{x}})}{|\hat{\vec{x}}_c-\hat{\vec{x}}|^3}\right]\cdot(\Delta\vec{x}_c-\Delta\vec{x}) \\
&\quad -(\Delta\vec{x}_c-\Delta\vec{x})\cdot\hat{\vec{n}}+\mathcal{O}(\Delta^2) \\
&= \left[\frac{(\hat{\vec{x}}-\hat{\vec{x}}_c)}{|\hat{\vec{x}}_c-\hat{\vec{x}}|}-\frac{|\hat{\vec{x}}_c-\hat{\vec{x}}|^2(\hat{\vec{x}}_c-\hat{\vec{x}})}{|\hat{\vec{x}}_c-\hat{\vec{x}}|^3}\right]\cdot(\Delta\vec{x}_c-\Delta\vec{x})
\end{aligned}$$

$$-(\Delta\vec{x}_c - \Delta\vec{x}) \cdot \hat{\vec{n}} + \mathcal{O}(\Delta^2)$$

$$= -(\Delta\vec{x}_c - \Delta\vec{x}) \cdot \hat{\vec{n}} + \mathcal{O}(\Delta^2)$$

Substitution of the equations for $\hat{\vec{n}}$, $\hat{\vec{x}}_c$ and $\Delta\vec{x}_c$ yields

$$\begin{aligned}
\Delta g &= -(\frac{\vec{\beta}\vec{\beta}}{|\vec{\beta}|^2} \cdot \Delta\vec{x} - \Delta\vec{x}) \cdot \frac{(\mathbf{I} - \frac{\vec{\beta}\vec{\beta}}{|\vec{\beta}|^2}) \cdot \vec{\alpha} + \frac{\vec{\beta}\vec{\beta}}{|\vec{\beta}|^2} \cdot \hat{\vec{x}} - \hat{\vec{x}}}{|\hat{\vec{x}}_c - \hat{\vec{x}}|} + \mathcal{O}(\Delta^2) \\
&= \Delta\vec{x} \cdot (\mathbf{I} - \frac{\vec{\beta}\vec{\beta}}{|\vec{\beta}|^2}) \cdot \frac{(\mathbf{I} - \frac{\vec{\beta}\vec{\beta}}{|\vec{\beta}|^2}) \cdot (\vec{\alpha} - \hat{\vec{x}})}{|\hat{\vec{x}}_c - \hat{\vec{x}}|} + \mathcal{O}(\Delta^2) \\
&= \Delta\vec{x} \cdot (\mathbf{I} - \frac{\vec{\beta}\vec{\beta}}{|\vec{\beta}|^2} - \frac{\vec{\beta}\vec{\beta}}{|\vec{\beta}|^2} + \frac{\vec{\beta}\vec{\beta}}{|\vec{\beta}|^2}) \cdot \frac{(\vec{\alpha} - \hat{\vec{x}})}{|\hat{\vec{x}}_c - \hat{\vec{x}}|} + \mathcal{O}(\Delta^2) \\
&= \Delta\vec{x} \cdot (\mathbf{I} - \frac{\vec{\beta}\vec{\beta}}{|\vec{\beta}|^2}) \cdot \frac{(\vec{\alpha} - \hat{\vec{x}})}{|\hat{\vec{x}}_c - \hat{\vec{x}}|} + \mathcal{O}(\Delta^2) \\
&= \Delta\vec{x} \cdot \frac{(\hat{\vec{x}}_c - \hat{\vec{x}})}{|\hat{\vec{x}}_c - \hat{\vec{x}}|} + \mathcal{O}(\Delta^2) \\
&= \Delta\vec{x} \cdot \hat{\vec{n}} + \mathcal{O}(\Delta^2)
\end{aligned}$$

With the linearization of functional g and vector $\vec{n}$, now the contribution of the impenetrability constraint (A.13) can be linearized.

$$-\int_{\Gamma_{cp}} \frac{1}{\epsilon_2} \vec{w} \cdot g^+ \vec{n}\, d\Gamma = -\int_{\Gamma_{cp}} \frac{1}{\epsilon_2} \vec{w} \cdot (\hat{g}^+ \hat{\vec{n}} + \Delta g^+ \hat{\vec{n}} + \hat{g}^+ \Delta\vec{n}) d\Gamma + \mathcal{O}(\Delta^2)$$

Substitution of the linearization for Δg and $\Delta\vec{n}$ gives the linearized form of the impenetrability constraint.

$$-\int_{\Gamma_{cp}} \frac{1}{\epsilon_2} \vec{w} \cdot g^+ \vec{n}\, d\Gamma = -\int_{\Gamma_{cp}} \frac{1}{\epsilon_2} \vec{w} \cdot (\hat{g}^+ \hat{\vec{n}} + (\hat{\vec{n}}\hat{\vec{n}})^+ \cdot \Delta\vec{x} - \hat{g}^+ \frac{\hat{\vec{r}}\hat{\vec{r}}}{|\hat{\vec{x}}_c - \hat{\vec{x}}|} \cdot \Delta\vec{x}) d\Gamma + \mathcal{O}(\Delta^2) \quad \text{(A.14)}$$

where

$$\begin{aligned}
\hat{\vec{n}} &= \frac{(\hat{\vec{x}}_c - \hat{\vec{x}})}{|\hat{\vec{x}}_c - \hat{\vec{x}}|} \\
\hat{g} &= (\hat{\vec{x}} - \hat{\vec{x}}_c) \cdot \hat{\vec{n}} + R_c \\
\hat{g}^+ &= max(0, g)
\end{aligned}$$

$$\hat{\vec{x}}_c = \frac{\vec{\beta}\vec{\beta}}{|\vec{\beta}|^2} \cdot \hat{\vec{x}} + (\mathbf{I} - \frac{\vec{\beta}\vec{\beta}}{|\vec{\beta}|^2}) \cdot \vec{\alpha}$$

$$\hat{\vec{r}} = \frac{\hat{\vec{n}} * \vec{\beta}}{|\vec{\beta}|}$$

$(\ )^+$ means that it is only taken into account if $\hat{g} > 0$

A.3 Coulomb friction (slip)

If slip occurs, the contribution of the Coulomb friction to the system of equations is given by

$$\int_{\Gamma_{cp}} \frac{\mu}{\epsilon_2} g^+ \vec{w} \cdot \frac{\vec{u}_c - \vec{u}}{|\vec{u}_c - \vec{u}|} d\Gamma \tag{A.15}$$

with

$$g = (\vec{x} - \vec{x}_c) \cdot \vec{n} + R_c$$

$$\vec{u}_c = \vec{s} + \bar{\omega}\, \Delta t\, R_c\, \vec{r}$$

$$\vec{r} = \frac{\vec{n} * \vec{\beta}}{|\vec{\beta}|}$$

$$\vec{u} = \vec{x}(t) - \vec{x}(t - \Delta t) \quad ; \quad \vec{x}(t - \Delta t) \text{ is the solution of the previous time step}$$

Before equation (A.15) can be linearized, all non-linear terms must be linearized separately. The displacement vector $\vec{u}$ is linearized first.

$$\vec{u} = \hat{\vec{u}} + \Delta\vec{u}$$

$$\hat{\vec{u}} = \hat{\vec{x}}(t) - \vec{x}(t - \Delta t)$$

$$\Delta\vec{u} = \Delta\vec{x}$$

Linearization of vector $\vec{r}$:

$$\vec{r} = \hat{\vec{r}} + \Delta\vec{r}$$

$$\hat{\vec{r}} = \frac{\hat{\vec{n}} * \vec{\beta}}{|\vec{\beta}|}$$

$$\Delta\vec{r} = \frac{\Delta\vec{n} * \vec{\beta}}{|\vec{\beta}|}$$

Substitution of the expression for $\Delta\vec{n}$, as it has been derived in the previous section, yields

$$\Delta\vec{r} = \left[\frac{\mathbf{I} - \hat{\vec{n}}\hat{\vec{n}}}{|\hat{\vec{x}}_c - \hat{\vec{x}}|} \cdot (\Delta\vec{x}_c - \Delta\vec{x})\right] * \frac{\vec{\beta}}{|\vec{\beta}|} + \mathcal{O}(\Delta^2)$$

$$= \left[\frac{\mathbf{I}-\hat{\vec{n}}\hat{\vec{n}}}{|\hat{\vec{x}}_c-\hat{\vec{x}}|}\cdot\left(\frac{\vec{\beta}\vec{\beta}}{|\vec{\beta}|^2}-\mathbf{I}\right)\cdot\Delta\vec{x}\right]*\frac{\vec{\beta}}{|\vec{\beta}|}+\mathcal{O}(\Delta^2)$$

Since $\hat{\vec{n}}$ is perpendicular to $\vec{\beta}$:

$$\Delta\vec{r}=\left[\frac{\frac{\vec{\beta}\vec{\beta}}{|\vec{\beta}|^2}-\mathbf{I}+\hat{\vec{n}}\hat{\vec{n}}}{|\hat{\vec{x}}_c-\hat{\vec{x}}|}\cdot\Delta\vec{x}\right]*\frac{\vec{\beta}}{|\vec{\beta}|}+\mathcal{O}(\Delta^2)$$

Since $\hat{\vec{n}}$, $\hat{\vec{r}}$ and $\frac{\vec{\beta}}{|\vec{\beta}|}$ are three orthonormal vectors, which form together a cartesian reference system, $\mathbf{I}=\hat{\vec{n}}\hat{\vec{n}}+\hat{\vec{r}}\hat{\vec{r}}+\frac{\vec{\beta}\vec{\beta}}{|\vec{\beta}|^2}$ can be used. This yields

$$\begin{aligned}\Delta\vec{r} &= \left(\frac{-\hat{\vec{r}}\hat{\vec{r}}}{|\hat{\vec{x}}_c-\hat{\vec{x}}|}\cdot\Delta\vec{x}\right)*\frac{\vec{\beta}}{|\vec{\beta}|}+\mathcal{O}(\Delta^2)\\ &= \frac{-(\hat{\vec{r}}\cdot\Delta\vec{x})}{|\hat{\vec{x}}_c-\hat{\vec{x}}|}\hat{\vec{r}}*\frac{\vec{\beta}}{|\vec{\beta}|}+\mathcal{O}(\Delta^2)\end{aligned}$$

Using $\hat{\vec{r}}*\frac{\vec{\beta}}{|\vec{\beta}|}=-\hat{\vec{n}}$:

$$\begin{aligned}\Delta\vec{r} &= \frac{-(\hat{\vec{r}}\cdot\Delta\vec{x})}{|\hat{\vec{x}}_c-\hat{\vec{x}}|}(-\hat{\vec{n}})+\mathcal{O}(\Delta^2)\\ &= \frac{\hat{\vec{n}}\hat{\vec{r}}}{|\hat{\vec{x}}_c-\hat{\vec{x}}|}\cdot\Delta\vec{x}+\mathcal{O}(\Delta^2)\end{aligned}$$

The linearization of $\vec{r}$ was necessary in order to be able to linearize vector $\vec{u}_c$:

$$\begin{aligned}\vec{u}_c &= \hat{\vec{u}}_c+\Delta\vec{u}_c\\ \hat{\vec{u}}_c &= \vec{s}+\bar{\omega}\,\Delta t\,R_c\,\hat{\vec{r}}\\ \Delta\vec{u}_c &= \bar{\omega}\,\Delta t\,R_c\Delta\vec{r}\end{aligned}$$

The functional g has already been linearized in the previous section. For the linearization of the direction of the relative displacement a Taylor series is applied.

$$\begin{aligned}\vec{d} &= \frac{\vec{u}_c-\vec{u}}{|\vec{u}_c-\vec{u}|}\\ \hat{\vec{d}} &= \frac{\hat{\vec{u}}_c-\hat{\vec{u}}}{|\hat{\vec{u}}_c-\hat{\vec{u}}|}\\ \Delta\vec{d} &= \frac{\hat{\vec{u}}_c+\Delta\vec{u}_c-\hat{\vec{u}}-\Delta\vec{u}}{|\hat{\vec{u}}_c+\Delta\vec{u}_c-\hat{\vec{u}}-\Delta\vec{u}|}-\frac{\hat{\vec{u}}_c-\hat{\vec{u}}}{|\hat{\vec{u}}_c-\hat{\vec{u}}|}\\ &= \left[\frac{\mathbf{I}}{|\hat{\vec{u}}_c-\hat{\vec{u}}|}-\frac{(\hat{\vec{u}}_c-\hat{\vec{u}})(\hat{\vec{u}}_c-\hat{\vec{u}})}{|\hat{\vec{u}}_c-\hat{\vec{u}}|^3}\right]\cdot(\Delta\vec{u}_c-\Delta\vec{u})+\mathcal{O}(\Delta^2)\end{aligned}$$

Linearization of the friction can be carried out with use of the linearizations of g and $\vec{d}$:

$$\begin{aligned}\int_{\Gamma_{cp}} \frac{\mu}{\epsilon_2} g^+ \vec{w}\cdot\vec{d}\,d\Gamma &= \int_{\Gamma_{cp}} \frac{\mu}{\epsilon_2} (\hat{g}+\Delta g)^+ \vec{w}\cdot(\hat{\vec{d}}+\Delta\vec{d})\,d\Gamma \\ &= \int_{\Gamma_{cp}} \frac{\mu}{\epsilon_2} (\hat{g}^+ \vec{w}\cdot\hat{\vec{d}}+\Delta g^+ \vec{w}\cdot\hat{\vec{d}}+\hat{g}^+ \vec{w}\cdot\Delta\vec{d})\,d\Gamma + \mathcal{O}(\Delta^2)\end{aligned}$$

Substitution of the expressions for $\hat{\vec{d}}$, Δg and $\Delta\vec{d}$ yields

$$\int_{\Gamma_{cp}} \frac{\mu}{\epsilon_2} \hat{g}^+ \vec{w}\cdot\hat{\vec{d}}\,d\Gamma = \int_{\Gamma_{cp}} \frac{\mu}{\epsilon_2} \hat{g}^+ \vec{w}\cdot\frac{\hat{\vec{u}}_c-\hat{\vec{u}}}{|\hat{\vec{u}}_c-\hat{\vec{u}}|}\,d\Gamma$$

$$\begin{aligned}\int_{\Gamma_{cp}} \frac{\mu}{\epsilon_2} (\Delta g^+ \vec{w}\cdot\hat{\vec{d}})\,d\Gamma &= \int_{\Gamma_{cp}} \frac{\mu}{\epsilon_2} \left[(\Delta\vec{x}\cdot\hat{\vec{n}})^+ \vec{w}\cdot\frac{\hat{\vec{u}}_c-\hat{\vec{u}}}{|\hat{\vec{u}}_c-\hat{\vec{u}}|}\right] d\Gamma + \mathcal{O}(\Delta^2) \\ &= \int_{\Gamma_{cp}} \frac{\mu}{\epsilon_2} \left[\vec{w}\cdot\frac{\hat{\vec{u}}_c-\hat{\vec{u}}}{|\hat{\vec{u}}_c-\hat{\vec{u}}|}(\hat{\vec{n}}\cdot\Delta\vec{x})\right]^+ d\Gamma + \mathcal{O}(\Delta^2) \\ &= \int_{\Gamma_{cp}} \frac{\mu}{\epsilon_2} \vec{w}\cdot\left[\frac{\hat{\vec{u}}_c-\hat{\vec{u}}}{|\hat{\vec{u}}_c-\hat{\vec{u}}|}\hat{\vec{n}}\right]^+ \cdot\Delta\vec{x}\,d\Gamma + \mathcal{O}(\Delta^2)\end{aligned}$$

$$\begin{aligned}&\int_{\Gamma_{cp}} \frac{\mu}{\epsilon_2} \hat{g}^+ \vec{w}\cdot\Delta\vec{d}\,d\Gamma \\ &= \int_{\Gamma_{cp}} \frac{\mu}{\epsilon_2} \hat{g}^+ \vec{w}\cdot\left[\frac{\mathbf{I}}{|\hat{\vec{u}}_c-\hat{\vec{u}}|}-\frac{(\hat{\vec{u}}_c-\hat{\vec{u}})(\hat{\vec{u}}_c-\hat{\vec{u}})}{|\hat{\vec{u}}_c-\hat{\vec{u}}|^3}\right]\cdot(\bar{\omega}\,\Delta t R_c\Delta\vec{r}-\Delta\vec{x})d\Gamma + \begin{matrix}\mathcal{O}(\Delta^2)\\ )d\Gamma + \mathcal{O}(\Delta\ )\end{matrix} \\ &= \int_{\Gamma_{cp}} \frac{\mu}{\epsilon_2} \hat{g}^+ \vec{w}\cdot\left[\frac{\mathbf{I}}{|\hat{\vec{u}}_c-\hat{\vec{u}}|}-\frac{(\hat{\vec{u}}_c-\hat{\vec{u}})(\hat{\vec{u}}_c-\hat{\vec{u}})}{|\hat{\vec{u}}_c-\hat{\vec{u}}|^3}\right]\cdot(\bar{\omega}\,\Delta t R_c\frac{\hat{\vec{n}}\hat{\vec{r}}}{|\hat{\vec{x}}_c-\hat{\vec{x}}|}\cdot\Delta\vec{x}-\Delta\vec{x})d\Gamma + \mathcal{O}(\Delta^2)\end{aligned}$$

Uniting the separate terms gives the linearized Coulomb friction

$$\begin{aligned}&\int_{\Gamma_{cp}} \frac{\mu}{\epsilon_2} \hat{g}^+ \vec{w}\cdot\frac{\hat{\vec{u}}_c-\hat{\vec{u}}}{|\hat{\vec{u}}_c-\hat{\vec{u}}|}\,d\Gamma + \int_{\Gamma_{cp}} \frac{\mu}{\epsilon_2} \vec{w}\cdot\left[\frac{(\hat{\vec{u}}_c-\hat{\vec{u}})}{|\hat{\vec{u}}_c-\hat{\vec{u}}|}\hat{\vec{n}}\right]^+ \cdot\Delta\vec{x}\,d\Gamma \\ +\ &\int_{\Gamma_{cp}} \frac{\mu}{\epsilon_2} \hat{g}^+ \vec{w}\cdot\left[\frac{\mathbf{I}}{|\hat{\vec{u}}_c-\hat{\vec{u}}|}-\frac{(\hat{\vec{u}}_c-\hat{\vec{u}})(\hat{\vec{u}}_c-\hat{\vec{u}})}{|\hat{\vec{u}}_c-\hat{\vec{u}}|^3}\right]\cdot(\bar{\omega}\Delta t R_c\frac{\hat{\vec{n}}\hat{\vec{r}}}{|\hat{\vec{x}}_c-\hat{\vec{x}}|}-\mathbf{I})\cdot\Delta\vec{x}\,d\Gamma + \mathcal{O}(\Delta^2)\end{aligned}$$

Or, in a shorter notation:

$$\begin{aligned}&\int_{\Gamma_{cp}} \frac{\mu}{\epsilon_2} g^+ \vec{w}\cdot\frac{(\vec{u}_c-\vec{u})}{|\vec{u}_c-\vec{u}|}\,d\Gamma = \\ &\int_{\Gamma_{cp}} \frac{\mu}{\epsilon_2} \hat{g}^+ \vec{w}\cdot\hat{\vec{d}}\,d\Gamma + \int_{\Gamma_{cp}} \frac{\mu}{\epsilon_2} \vec{w}\cdot((\hat{\vec{d}}\vec{n})^+ + \hat{g}^+ \mathbf{K}\cdot\mathbf{G})\cdot\Delta\vec{x}\,d\Gamma + \mathcal{O}(\Delta^2)\end{aligned} \quad \text{(A.16)}$$

where

$$
\begin{aligned}
\hat{g} &= (\hat{\vec{x}} - \hat{\vec{x}}_c) \cdot \hat{\vec{n}} + R_c \\
\hat{\vec{d}} &= \frac{\hat{\vec{u}}_c - \hat{\vec{u}}}{|\hat{\vec{u}}_c - \hat{\vec{u}}|} \\
\hat{\vec{r}} &= \frac{\hat{\vec{n}} * \vec{\beta}}{|\vec{\beta}|} \\
\mathbf{K} &= \frac{\mathbf{I}}{|\hat{\vec{u}}_c - \hat{\vec{u}}|} - \frac{(\hat{\vec{u}}_c - \hat{\vec{u}})(\hat{\vec{u}}_c - \hat{\vec{u}})}{|\hat{\vec{u}}_c - \hat{\vec{u}}|^3} = \frac{\mathbf{I} - \hat{\vec{d}}\hat{\vec{d}}}{|\hat{\vec{u}}_c - \hat{\vec{u}}|} \\
\mathbf{G} &= \bar{\omega}\, \Delta t\, R_c \frac{\hat{\vec{n}}\hat{\vec{r}}}{|\hat{\vec{x}}_c - \hat{\vec{x}}|} - \mathbf{I}
\end{aligned}
$$

A.4 Regularized Coulomb friction 1

The contribution of the approximated Coulomb friction to the system of equations is given by

$$\int_{\Gamma_{cp}} \frac{\mu}{\epsilon_2} g^+ \, \phi_1 \, \vec{w} \cdot \vec{d} \, d\Gamma \tag{A.17}$$

where

$$\phi_1 = \tanh\left(\frac{|\vec{u}_c - \vec{u}|}{\epsilon_3 \Delta t}\right)$$

In comparison with the unregularized stickless Coulomb friction, this relation contains one more nonlinear term, the function ϕ_1. Linearization of this function ϕ_1 yields

$$
\begin{aligned}
\phi_1 &= \hat{\phi}_1 + \Delta\phi_1 \\
\hat{\phi}_1 &= \tanh\left(\frac{|\hat{\vec{u}}_c - \hat{\vec{u}}|}{\epsilon_3 \Delta t}\right) \\
\Delta\phi_1 &= \frac{1}{\epsilon_3 \Delta t}\left[1 - \tanh^2\left(\frac{|\hat{\vec{u}}_c - \hat{\vec{u}}|}{\epsilon_3 \Delta t}\right)\right] \frac{\hat{\vec{u}}_c - \hat{\vec{u}}}{|\hat{\vec{u}}_c - \hat{\vec{u}}|} \cdot (\Delta\vec{u}_c - \Delta\vec{u}) + \mathcal{O}(\Delta^2)
\end{aligned}
$$

Using this, and the linearizations of the other quantities, as they have been derived in the previous section, term (A.17) can be linearized:

$$
\begin{aligned}
\int_{\Gamma_{cp}} \frac{\mu}{\epsilon_2} g^+ \, \phi_1 \, \vec{w} \cdot \vec{d} \, d\Gamma &= \int_{\Gamma_c} \frac{\mu}{\epsilon_2} (\hat{g} + \Delta g)^+ \, (\hat{\phi}_1 + \Delta\phi_1) \, \vec{w} \cdot (\hat{\vec{d}} + \Delta\vec{d}) \, d\Gamma \\
&= \int_{\Gamma_{cp}} \frac{\mu}{\epsilon_2} (\hat{g}^+ \, \hat{\phi}_1 \vec{w} \cdot \hat{\vec{d}} + \Delta g^+ \hat{\phi}_1 \vec{w} \cdot \hat{\vec{d}} + \hat{g}^+ \, \Delta\phi_1 \vec{w} \cdot \hat{\vec{d}} + \hat{g}^+ \, \hat{\phi}_1 \vec{w} \cdot \Delta\vec{d}) d\Gamma + \mathcal{O}(\Delta^2)
\end{aligned}
$$

Substitution of the relations for Δg, $\Delta\phi$ and $\Delta\vec{d}$ yields

$$\int_{\Gamma_{cp}} \frac{\mu}{\epsilon_2} \Delta g^+ \hat{\phi}_1 \vec{w} \cdot \hat{\vec{d}}\, d\Gamma = \int_{\Gamma_{cp}} \frac{\mu}{\epsilon_2} \hat{\phi}_1 \vec{w} \cdot (\hat{\vec{d}}\hat{\vec{n}})^+ \cdot \Delta\vec{x}\, d\Gamma + \mathcal{O}(\Delta^2)$$

$$\begin{aligned}
&\int_{\Gamma_{cp}} \frac{\mu}{\epsilon_2} \hat{g}^+ \Delta\phi_1 \vec{w} \cdot \hat{\vec{d}}\, d\Gamma \\
&= \int_{\Gamma_{cp}} \frac{\mu}{\epsilon_2} \frac{\hat{g}^+}{\epsilon_3 \Delta t} [1 - \tanh^2(\frac{|\hat{\vec{u}}_c - \hat{\vec{u}}|}{\epsilon_3 \Delta t})] \frac{(\hat{\vec{u}}_c - \hat{\vec{u}})}{|\hat{\vec{u}}_c - \hat{\vec{u}}|} \cdot (\bar{\omega}\, \Delta t\, R_c\, \Delta\vec{r} - \Delta\vec{x})\, (\vec{w} \cdot \hat{\vec{d}})\, d\Gamma + \mathcal{O}(\Delta^2) \\
&= \int_{\Gamma_{cp}} \frac{\mu}{\epsilon_2} \frac{\hat{g}^+}{\epsilon_3 \Delta t} [1 - \tanh^2(\frac{|\hat{\vec{u}}_c - \hat{\vec{u}}|}{\epsilon_3 \Delta t})] \vec{w} \cdot \hat{\vec{d}} \frac{(\hat{\vec{u}}_c - \hat{\vec{u}})}{|\hat{\vec{u}}_c - \hat{\vec{u}}|} \cdot (\bar{\omega} \Delta t R_c \frac{\hat{\vec{n}}\hat{\vec{r}}}{|\hat{\vec{x}}_c - \hat{\vec{x}}|} - \mathbf{I}) \cdot \Delta\vec{x} d\Gamma + \mathcal{O}(\Delta^2) \\
&= \int_{\Gamma_{cp}} \frac{\mu}{\epsilon_2} \frac{\hat{g}^+}{\epsilon_3 \Delta t} [1 - \tanh^2(\frac{|\hat{\vec{u}}_c - \hat{\vec{u}}|}{\epsilon_3 \Delta t})] \vec{w} \cdot \hat{\vec{d}}\hat{\vec{d}} \cdot \mathbf{G} \cdot \Delta\vec{x}\, d\Gamma + \mathcal{O}(\Delta^2)
\end{aligned}$$

$$\int_{\Gamma_{cp}} \frac{\mu}{\epsilon_2} \hat{g}^+ \hat{\phi}_1 \vec{w} \cdot \Delta\vec{d}\, d\Gamma = \int_{\Gamma_{cp}} \frac{\mu}{\epsilon_2} \hat{g}^+ \hat{\phi}_1 \vec{w} \cdot \mathbf{K} \cdot \mathbf{G} \cdot \Delta\vec{x}\, d\Gamma + \mathcal{O}(\Delta^2)$$

Combination of the separate terms gives the linearized contribution of the friction:

$$\begin{aligned}
&\int_{\Gamma_{cp}} \frac{\mu}{\epsilon_2} \hat{g}^+ \hat{\phi}_1 \vec{w} \cdot \hat{\vec{d}}\, d\Gamma + \int_{\Gamma_{cp}} \frac{\mu}{\epsilon_2} \hat{\phi}_1 \vec{w} \cdot (\hat{\vec{d}}\hat{\vec{n}})^+ \cdot \Delta\vec{x}\, d\Gamma \\
+ &\int_{\Gamma_{cp}} \frac{\mu}{\epsilon_2} \frac{\hat{g}^+}{\epsilon_3 \Delta t} [1 - \tanh^2(\frac{|\hat{\vec{u}}_c - \hat{\vec{u}}|}{\epsilon_3 \Delta t})] \vec{w} \cdot \hat{\vec{d}}\hat{\vec{d}} \cdot \mathbf{G} \cdot \Delta\vec{x}\, d\Gamma \\
+ &\int_{\Gamma_{cp}} \frac{\mu}{\epsilon_2} \hat{g}^+ \hat{\phi}_1 \vec{w} \cdot \mathbf{K} \cdot \mathbf{G} \cdot \Delta\vec{x}\, d\Gamma + \mathcal{O}(\Delta^2)
\end{aligned}$$

Or:

$$\begin{aligned}
&\int_{\Gamma_{cp}} \frac{\mu}{\epsilon_2} g^+ \phi_1 \vec{w} \cdot \vec{d}\, d\Gamma = \int_{\Gamma_{cp}} \frac{\mu}{\epsilon_2} \hat{g}^+ \hat{\phi}_1 \vec{w} \cdot \hat{\vec{d}}\, d\Gamma \\
+ &\int_{\Gamma_{cp}} \frac{\mu}{\epsilon_2} \vec{w} \cdot \left[\hat{\phi}_1 (\hat{\vec{d}}\hat{\vec{n}})^+ + \left(\frac{\hat{g}^+}{\epsilon_3 \Delta t} [1 - \tanh^2(\frac{|\hat{\vec{u}}_c - \hat{\vec{u}}|}{\epsilon_3 \Delta t})] \hat{\vec{d}}\hat{\vec{d}} + \hat{g}^+ \hat{\phi}_1 \mathbf{K} \right) \cdot \mathbf{G} \right] \cdot \Delta\vec{x}\, d\Gamma \\
&+ \mathcal{O}(\Delta^2)
\end{aligned} \tag{A.18}$$

A.5 Regularized Coulomb friction 2

As in the previous section, the contribution of the regularized Coulomb friction to the system of equations is given by

$$\int_{\Gamma_{cp}} \frac{\mu}{\epsilon_2} g^+ \phi_2 \vec{w} \cdot \vec{d} \, d\Gamma \tag{A.19}$$

However, the regularization function ϕ_2 is now given by

$$\phi_2 = \frac{2}{\pi} \arctan\left(\frac{|\hat{\vec{u}}_c - \hat{\vec{u}}|}{\epsilon_4 \Delta t}\right)$$

Linearization of this function ϕ_2 yields

$$\begin{aligned}
\phi_2 &= \hat{\phi}_2 + \Delta\phi_2 \\
\hat{\phi}_2 &= \frac{2}{\pi} \arctan\left(\frac{|\hat{\vec{u}}_c - \hat{\vec{u}}|}{\epsilon_4 \Delta t}\right) \\
\Delta\phi_2 &= \frac{2}{\pi} \frac{1}{\epsilon_4 \Delta t} \frac{1}{1 + \left(\frac{|\hat{\vec{u}}_c - \hat{\vec{u}}|}{\epsilon_4 \Delta t}\right)^2} \frac{\hat{\vec{u}}_c - \hat{\vec{u}}}{|\hat{\vec{u}}_c - \hat{\vec{u}}|} \cdot (\Delta\vec{u}_c - \Delta\vec{u}) + \mathcal{O}(\Delta^2) \\
&= \frac{2}{\pi} \frac{\epsilon_4 \Delta t}{(\epsilon_4 \Delta t)^2 + |\hat{\vec{u}}_c - \hat{\vec{u}}|^2} \frac{\hat{\vec{u}}_c - \hat{\vec{u}}}{|\hat{\vec{u}}_c - \hat{\vec{u}}|} \cdot (\Delta\vec{u}_c - \Delta\vec{u}) + \mathcal{O}(\Delta^2)
\end{aligned}$$

Using this, and the linearizations of the other quantities, as has been derived in the previous section, term (A.19) can be linearized as under.

$$\begin{aligned}
\int_{\Gamma_{cp}} \frac{\mu}{\epsilon_2} g^+ \phi_2 \vec{w} \cdot \vec{d} \, d\Gamma &= \int_{\Gamma_{cp}} \frac{\mu}{\epsilon_2} (\hat{g} + \Delta g)^+ (\hat{\phi}_2 + \Delta\phi_2) \vec{w} \cdot (\hat{\vec{d}} + \Delta\vec{d}) \, d\Gamma \\
&= \int_{\Gamma_{cp}} \frac{\mu}{\epsilon_2} (\hat{g}^+ \hat{\phi}_2 \vec{w} \cdot \hat{\vec{d}} + \Delta g^+ \hat{\phi}_2 \vec{w} \cdot \hat{\vec{d}} + \hat{g}^+ \Delta\phi_2 \vec{w} \cdot \hat{\vec{d}} + \hat{g}^+ \hat{\phi}_2 \vec{w} \cdot \Delta\vec{d}) \, d\Gamma + \mathcal{O}(\Delta^2)
\end{aligned}$$

In the previous section, all terms are linearized, except the term with $\Delta\phi_2$. This term is linearized, here. Substitution of the relation for $\Delta\phi_2$ yields

$$\begin{aligned}
&\int_{\Gamma_{cp}} \frac{\mu}{\epsilon_2} \hat{g}^+ \Delta\phi_2 \vec{w} \cdot \hat{\vec{d}} \, d\Gamma \\
&= \int_{\Gamma_{cp}} \frac{\mu}{\epsilon_2} \hat{g}^+ \frac{2\,\epsilon_4 \Delta t}{\pi((\epsilon_4 \Delta t)^2 + |\hat{\vec{u}}_c - \hat{\vec{u}}|^2)} \frac{\hat{\vec{u}}_c - \hat{\vec{u}}}{|\hat{\vec{u}}_c - \hat{\vec{u}}|} \cdot (\bar{\omega} \, \Delta t \, R_c \, \Delta\vec{r} - \Delta\vec{x}) \, (\vec{w} \cdot \hat{\vec{d}}) \, d\Gamma + \mathcal{O}(\Delta^2) \\
&= \int_{\Gamma_{cp}} \frac{\mu}{\epsilon_2} \hat{g}^+ \frac{2\,\epsilon_4 \Delta t}{\pi((\epsilon_4 \Delta t)^2 + |\hat{\vec{u}}_c - \hat{\vec{u}}|^2)} \vec{w} \cdot \hat{\vec{d}}\hat{\vec{d}} \cdot (\bar{\omega} \Delta t R_c \frac{\hat{\vec{n}}\hat{\vec{r}}}{|\hat{\vec{x}}_c - \hat{\vec{x}}|} - \mathbf{I}) \cdot \Delta\vec{x} \, d\Gamma + \mathcal{O}(\Delta^2) \\
&= \int_{\Gamma_{cp}} \frac{\mu}{\epsilon_2} \hat{g}^+ \frac{2\,\epsilon_4 \Delta t}{\pi((\epsilon_4 \Delta t)^2 + |\hat{\vec{u}}_c - \hat{\vec{u}}|^2)} \vec{w} \cdot \hat{\vec{d}}\hat{\vec{d}} \cdot \mathbf{G} \cdot \Delta\vec{x} \, d\Gamma + \mathcal{O}(\Delta^2)
\end{aligned}$$

The complete linearized contribution of the smoothed Coulomb friction is given by

$$\int_{\Gamma_{cp}} \frac{\mu}{\epsilon_2} g^+ \phi_2 \vec{w} \cdot \vec{d}\, d\Gamma = \int_{\Gamma_{cp}} \frac{\mu}{\epsilon_2} \hat{g}^+ \hat{\phi}_2 \vec{w} \cdot \hat{\vec{d}}\, d\Gamma$$
$$+ \int_{\Gamma_{cp}} \frac{\mu}{\epsilon_2} \vec{w} \cdot \left[\hat{\phi}_2 (\hat{\vec{d}}\vec{\hat{n}})^+ + \left(\frac{2\,\hat{g}^+ \epsilon_4\, \Delta t}{\pi((\epsilon_4 \Delta t)^2 + |\hat{\vec{u}}_c - \hat{\vec{u}}|^2)} \hat{\vec{d}}\hat{\vec{d}} + \hat{g}^+ \hat{\phi}_2 \mathbf{K} \right) \cdot \mathbf{G} \right] \cdot \Delta \vec{x}\, d\Gamma$$
$$+ \mathcal{O}(\Delta^2) \tag{A.20}$$

Appendix B

Discretization

In this appendix the linearized weighted residual equations will be discretized. These are the balance of momentum, the incompressibility constraint, the impenetrability constraint and the friction.

B.1 Balance of momentum and impressibility constraint

Starting-point for the discretization of the equations for the material behaviour is the following system of equations:

$$\begin{aligned} \int_\Omega \mathbf{L}_w : [-\hat{p}\mathbf{I} - \Delta p\mathbf{I} + \hat{p}\mathbf{L}_{\Delta x}]d\Omega \; + \\ + \int_\Omega \mathbf{L}_w : (\hat{\boldsymbol{\tau}} + 4c\mathbf{D}_{\Delta x} + \hat{\boldsymbol{\tau}} \cdot \mathbf{L}_{\Delta x}{}^c)d\Omega \;&=\; \int_\Gamma \vec{w} \cdot \vec{b}\, d\Gamma \end{aligned} \tag{B.1}$$

$$\int_\Omega r \hat{\vec{\nabla}} \cdot \Delta\vec{x}\, d\Omega \;=\; \int_\Omega r\,(\frac{1}{\det(\hat{\mathbf{F}})} - 1)d\Omega \tag{B.2}$$

Each term in these equations will be worked out separately. A three-dimensional Cartesian reference system will be used:

$$\underset{\sim}{\vec{e}}^{\,T} = \left[\begin{array}{ccc} \vec{e}_x & \vec{e}_y & \vec{e}_z \end{array}\right]$$

So:

$$\begin{aligned} \hat{\vec{\nabla}} &= \vec{e}_x \frac{\partial}{\partial x} + \vec{e}_y \frac{\partial}{\partial y} + \vec{e}_z \frac{\partial}{\partial z} \\ \vec{w} &= w^x \vec{e}_x + w^y \vec{e}_y + w^z \vec{e}_z \\ \Delta\vec{x} &= \Delta x\, \vec{e}_x + \Delta y\, \vec{e}_y + \Delta z\, \vec{e}_z \end{aligned}$$

The first term can be rewritten:

$$\begin{aligned}
\mathbf{L}_w : -\hat{p}\,\mathbf{I} &= (\hat{\vec{\nabla}}\vec{w})^c : -\hat{p}\,\mathbf{I} \\
&= (\hat{\vec{\nabla}}\vec{w}) : -\hat{p}\,\mathbf{I} \\
&= -\hat{p}\,\hat{\vec{\nabla}} \cdot \vec{w} \\
-\hat{p}\,\hat{\vec{\nabla}} \cdot \vec{w} &= -\hat{p}\begin{bmatrix} \frac{\partial}{\partial x} & \frac{\partial}{\partial y} & \frac{\partial}{\partial z} \end{bmatrix}\begin{bmatrix} w^x \\ w^y \\ w^z \end{bmatrix} = -\hat{p}\underset{\sim}{\nabla}^T\begin{bmatrix} w^x \\ w^y \\ w^z \end{bmatrix}
\end{aligned}$$

where

$$\underset{\sim}{\nabla}^T = \begin{bmatrix} \frac{\partial}{\partial x} & \frac{\partial}{\partial y} & \frac{\partial}{\partial z} \end{bmatrix}$$

Discretization of the components of $\vec{w}$ and of pressure p yields:

$$\begin{bmatrix} w^x \\ w^y \\ w^z \end{bmatrix} = \begin{bmatrix} \varphi_1 & 0 & 0 & ..... & \varphi_{nx} & 0 & 0 \\ 0 & \varphi_1 & 0 & & 0 & \varphi_{nx} & 0 \\ 0 & 0 & \varphi_1 & & 0 & 0 & \varphi_{nx} \end{bmatrix}\begin{bmatrix} {w_1}^x \\ {w_1}^y \\ {w_1}^z \\ . \\ . \\ {w_{nx}}^x \\ {w_{nx}}^y \\ {w_{nx}}^z \end{bmatrix} = \underline{\varphi}\,\underset{\sim}{w}$$

$$\hat{p} = \underset{\sim}{\psi}^T\underset{\sim}{\hat{p}} = (\underset{\sim}{\hat{p}})^T\underset{\sim}{\psi} = \begin{bmatrix} \hat{p}_1 & .... & \hat{p}_{np} \end{bmatrix}\begin{bmatrix} \psi_1 \\ . \\ . \\ \psi_{np} \end{bmatrix}$$

where nx denotes *the number of displacement nodes,*

$\underline{\varphi}$ is *the matrix with interpolation functions for the position,*

$\underset{\sim}{w}$ is *the column with weighting functions for the position at element nodes,*

np denotes *the number of pressure nodes,*

$\underset{\sim}{\psi}$ is *the column with interpolation functions for the pressure,*

$\underset{\sim}{\hat{p}}$ is *the column with estimations for the pressure at element nodes.*

The first term can be discretized as follows:

$$\mathbf{L}_w : -\hat{p}\,\mathbf{I} = -\hat{p}\,\hat{\vec{\nabla}} \cdot \vec{w}$$

$$
\begin{aligned}
&= -(\underset{\sim}{\hat{p}}\,)^T \underset{\sim}{\psi}\, \underset{\sim}{\nabla}^T \underline{\varphi}\, \underset{\sim}{w} \\
&= -(\underset{\sim}{\hat{p}}\,)^T \underset{\sim}{\psi}\, \underset{\sim}{a}^T \underset{\sim}{w} \\
&= -\underset{\sim}{w}^T \underset{\sim}{a}\, \underset{\sim}{\psi}^T \underset{\sim}{\hat{p}} \\
\mathbf{L}_w : -\hat{p}\mathbf{I} &= -\underset{\sim}{w}^T \underline{Q}\, \underset{\sim}{\hat{p}}
\end{aligned}
\tag{B.3}
$$

with:

$$
\begin{aligned}
\underset{\sim}{a}^T &= \underset{\sim}{\nabla}^T \underline{\varphi} \\
\underline{Q} &= \underset{\sim}{a}\, \underset{\sim}{\psi}^T
\end{aligned}
$$

The second term can be discretized in the same way:

$$
\mathbf{L}_w : -\Delta p\mathbf{I} = -\underset{\sim}{w}^T \underline{Q} \Delta \underset{\sim}{p} \tag{B.4}
$$

where $\Delta \underset{\sim}{p}$ *is the column with the variations of the pressures at element nodes.*

Now the third term of (B.1) will be worked out. For that purpose the matrix representation of tensor $\mathbf{L}_{\Delta x}$ will be determined with respect to the reference system $\{\vec{e}_x, \vec{e}_y, \vec{e}_z\}$:

$$
\underline{L}_{\Delta x} = \underline{D}_{\Delta x} + \underline{\Omega}_{\Delta x}
$$

Using its symmetry, the matrix representation of $\mathbf{D}_{\Delta x}$ with respect to $\{\vec{e}_x, \vec{e}_y, \vec{e}_z\}$ is denoted by

$$
\underline{D}_{\Delta x} = \underset{\sim}{\vec{e}} \cdot \mathbf{D}_{\Delta x} \cdot \underset{\sim}{\vec{e}}^T = \begin{bmatrix} d_{11}^{\Delta x} & d_{12}^{\Delta x} & d_{13}^{\Delta x} \\ d_{12}^{\Delta x} & d_{22}^{\Delta x} & d_{23}^{\Delta x} \\ d_{13}^{\Delta x} & d_{23}^{\Delta x} & d_{33}^{\Delta x} \end{bmatrix}
$$

while the matrix representation of $\mathbf{\Omega}_{\Delta x}$ with respect to $\{\vec{e}_x, \vec{e}_y, \vec{e}_z\}$ can be written as

$$
\underline{\Omega}_{\Delta x} = \underset{\sim}{\vec{e}} \cdot \mathbf{\Omega}_{\Delta x} \cdot \underset{\sim}{\vec{e}}^T = \begin{bmatrix} 0 & \omega_{12}^{\Delta x} & -\omega_{31}^{\Delta x} \\ -\omega_{12}^{\Delta x} & 0 & \omega_{23}^{\Delta x} \\ \omega_{31}^{\Delta x} & -\omega_{23}^{\Delta x} & 0 \end{bmatrix}
$$

So:

$$
\underline{L}_{\Delta x} = \begin{bmatrix} d_{11}^{\Delta x} & d_{12}^{\Delta x} + \omega_{12}^{\Delta x} & d_{13}^{\Delta x} - \omega_{31}^{\Delta x} \\ d_{12}^{\Delta x} - \omega_{12}^{\Delta x} & d_{22}^{\Delta x} & d_{23}^{\Delta x} + \omega_{23}^{\Delta x} \\ d_{13}^{\Delta x} + \omega_{31}^{\Delta x} & d_{23}^{\Delta x} - \omega_{23}^{\Delta x} & d_{33}^{\Delta x} \end{bmatrix}
$$

where

$$d_{ij}^{\Delta x} = \frac{1}{2}\left(\frac{\partial \Delta x^i}{\partial x^j} + \frac{\partial \Delta x^j}{\partial x^i}\right)$$
$$\omega_{ij}^{\Delta x} = \frac{1}{2}\left(\frac{\partial \Delta x^i}{\partial x^j} - \frac{\partial \Delta x^j}{\partial x^i}\right)$$

and $\Delta x^i = \Delta x$ for i=1
Δy for i=2
Δz for i=3

Similarly the tensors $\mathbf{D}_w$, $\mathbf{\Omega}_w$ and $\mathbf{L}_w$ can be represented in their matrix representations with respect to the Cartesian reference system:

$$\underline{D}_w = \begin{bmatrix} d_{11}^w & d_{12}^w & d_{13}^w \\ d_{12}^w & d_{22}^w & d_{23}^w \\ d_{13}^w & d_{23}^w & d_{33}^w \end{bmatrix}$$
$$\underline{\Omega}_w = \begin{bmatrix} 0 & \omega_{12}^w & -\omega_{31}^w \\ -\omega_{12}^w & 0 & \omega_{23}^w \\ \omega_{31}^w & -\omega_{23}^w & 0 \end{bmatrix}$$
$$\underline{L}_w = \begin{bmatrix} d_{11}^w & d_{12}^w + \omega_{12}^w & d_{13}^w - \omega_{31}^w \\ d_{12}^w - \omega_{12}^w & d_{22}^w & d_{23}^w + \omega_{23}^w \\ d_{13}^w + \omega_{31}^w & d_{23}^w - \omega_{23}^w & d_{33}^w \end{bmatrix}$$

The next step is the calculation of $\underline{L}_w : \underline{L}_{\Delta x} = \mathrm{tr}(\underline{L}_w \cdot \underline{L}_{\Delta x})$.

$$\begin{aligned} \underline{L}_w : \underline{L}_{\Delta x} &= d_{11}^w d_{11}^{\Delta x} + (d_{12}^w + \omega_{12}^w)(d_{12}^{\Delta x} - \omega_{12}^{\Delta x}) \\ &\quad + (d_{13}^w - \omega_{31}^w)(d_{13}^{\Delta x} + \omega_{31}^{\Delta x}) + (d_{12}^w - \omega_{12}^w)(d_{12}^{\Delta x} + \omega_{12}^{\Delta x}) \\ &\quad + d_{22}^w d_{22}^{\Delta x} + (d_{23}^w + \omega_{23}^w)(d_{23}^{\Delta x} - \omega_{23}^{\Delta x}) \\ &\quad + (d_{13}^w + \omega_{31}^w)(d_{13}^{\Delta x} - \omega_{31}^{\Delta x}) + (d_{23}^w - \omega_{23}^w)(d_{23}^{\Delta x} + \omega_{23}^{\Delta x}) \\ &\quad + d_{33}^w d_{33}^{\Delta x} \\ &= d_{11}^w d_{11}^{\Delta x} + 2d_{12}^w d_{12}^{\Delta x} + 2d_{13}^w d_{13}^{\Delta x} + d_{22}^w d_{22}^{\Delta x} + 2d_{23}^w d_{23}^{\Delta x} + d_{33}^w d_{33}^{\Delta x} \\ &\quad - 2\omega_{12}^w \omega_{12}^{\Delta x} - 2\omega_{31}^w \omega_{31}^{\Delta x} - 2\omega_{23}^w \omega_{23}^{\Delta x} \end{aligned}$$

Definition:

$$(\underset{\sim}{d}^w)^T = \left[\, d_{11}^w \;\; 2d_{12}^w \;\; d_{22}^w \;\; d_{33}^w \;\; 2d_{23}^w \;\; 2d_{13}^w \;\; 2\omega_{12}^w \;\; 2\omega_{23}^w \;\; -2\omega_{31}^w \,\right]$$
$$(\underset{\sim}{d}^{\Delta x})^T = \left[\, d_{11}^{\Delta x} \;\; 2d_{12}^{\Delta x} \;\; d_{22}^{\Delta x} \;\; d_{33}^{\Delta x} \;\; 2d_{23}^{\Delta x} \;\; 2d_{13}^{\Delta x} \;\; 2\omega_{12}^{\Delta x} \;\; 2\omega_{23}^{\Delta x} \;\; -2\omega_{31}^{\Delta x} \,\right]$$

With this definition, $\mathbf{L}_w : \mathbf{L}_{\Delta x}$ can be rewritten as

$$\mathbf{L}_w : \mathbf{L}_{\Delta x} = (\underset{\sim}{d}^{w})^T \underline{B}\, \underset{\sim}{d}^{\Delta x}$$

with:

$$\underline{B} = \begin{bmatrix} 1 & 0 & 0 & 0 & 0 & 0 & 0 & 0 & 0 \\ 0 & \frac{1}{2} & 0 & 0 & 0 & 0 & 0 & 0 & 0 \\ 0 & 0 & 1 & 0 & 0 & 0 & 0 & 0 & 0 \\ 0 & 0 & 0 & 1 & 0 & 0 & 0 & 0 & 0 \\ 0 & 0 & 0 & 0 & \frac{1}{2} & 0 & 0 & 0 & 0 \\ 0 & 0 & 0 & 0 & 0 & \frac{1}{2} & 0 & 0 & 0 \\ 0 & 0 & 0 & 0 & 0 & 0 & -\frac{1}{2} & 0 & 0 \\ 0 & 0 & 0 & 0 & 0 & 0 & 0 & -\frac{1}{2} & 0 \\ 0 & 0 & 0 & 0 & 0 & 0 & 0 & 0 & -\frac{1}{2} \end{bmatrix}$$

Now, the arrays $\underset{\sim}{d}^{w}$ and $\underset{\sim}{d}^{\Delta x}$ will be worked out. Both columns will be worked out similarly.

$$\underset{\sim}{d}^{w} = \begin{bmatrix} \frac{\partial}{\partial x}(w^x) \\ \frac{\partial}{\partial y}(w^x) + \frac{\partial}{\partial x}(w^y) \\ \frac{\partial}{\partial y}(w^y) \\ \frac{\partial}{\partial z}(w^z) \\ \frac{\partial}{\partial z}(w^y) + \frac{\partial}{\partial y}(w^z) \\ \frac{\partial}{\partial z}(w^x) + \frac{\partial}{\partial x}(w^z) \\ \frac{\partial}{\partial y}(w^x) - \frac{\partial}{\partial x}(w^y) \\ \frac{\partial}{\partial z}(w^y) - \frac{\partial}{\partial y}(w^z) \\ \frac{\partial}{\partial x}(w^z) - \frac{\partial}{\partial z}(w^x) \end{bmatrix} = \begin{bmatrix} \frac{\partial}{\partial x} & 0 & 0 \\ \frac{\partial}{\partial y} & \frac{\partial}{\partial x} & 0 \\ 0 & \frac{\partial}{\partial y} & 0 \\ 0 & 0 & \frac{\partial}{\partial z} \\ 0 & \frac{\partial}{\partial z} & \frac{\partial}{\partial y} \\ \frac{\partial}{\partial z} & 0 & \frac{\partial}{\partial x} \\ \frac{\partial}{\partial y} & -\frac{\partial}{\partial x} & 0 \\ 0 & \frac{\partial}{\partial z} & -\frac{\partial}{\partial y} \\ -\frac{\partial}{\partial z} & 0 & \frac{\partial}{\partial x} \end{bmatrix} \begin{bmatrix} w^x \\ w^y \\ w^z \end{bmatrix}$$

With the discretization of $\vec{w}$, $\underset{\sim}{d}^{w}$ can be discretized:

$$\underset{\sim}{d}^{w} = \begin{bmatrix} \frac{\partial}{\partial x} & 0 & 0 \\ \frac{\partial}{\partial y} & \frac{\partial}{\partial x} & 0 \\ 0 & \frac{\partial}{\partial y} & 0 \\ 0 & 0 & \frac{\partial}{\partial z} \\ 0 & \frac{\partial}{\partial z} & \frac{\partial}{\partial y} \\ \frac{\partial}{\partial z} & 0 & \frac{\partial}{\partial x} \\ \frac{\partial}{\partial y} & -\frac{\partial}{\partial x} & 0 \\ 0 & \frac{\partial}{\partial z} & -\frac{\partial}{\partial y} \\ -\frac{\partial}{\partial z} & 0 & \frac{\partial}{\partial x} \end{bmatrix} \begin{bmatrix} \varphi_1 & 0 & 0 & ..... & \varphi_{nx} & 0 & 0 \\ 0 & \varphi_1 & 0 & & 0 & \varphi_{nx} & 0 \\ 0 & 0 & \varphi_1 & & 0 & 0 & \varphi_{nx} \end{bmatrix} \begin{bmatrix} {w_1}^x \\ {w_1}^y \\ {w_1}^z \\ . \\ . \\ {w_{nx}}^x \\ {w_{nx}}^y \\ {w_{nx}}^z \end{bmatrix} = \underline{A}\, \underset{\sim}{w}$$

In the same way can be found for $\underset{\sim}{d}^{\Delta x}$:

$$\underset{\sim}{d}^{\Delta x} = \underline{A}\,\underset{\sim}{\Delta x}$$

with: $\underset{\sim}{\Delta x}$: *column with the position variations at element nodes,*

$$\underline{A} = \begin{bmatrix} \frac{\partial}{\partial x} & 0 & 0 \\ \frac{\partial}{\partial y} & \frac{\partial}{\partial x} & 0 \\ 0 & \frac{\partial}{\partial y} & 0 \\ 0 & 0 & \frac{\partial}{\partial z} \\ 0 & \frac{\partial}{\partial z} & \frac{\partial}{\partial y} \\ \frac{\partial}{\partial z} & 0 & \frac{\partial}{\partial x} \\ \frac{\partial}{\partial y} & -\frac{\partial}{\partial x} & 0 \\ 0 & \frac{\partial}{\partial z} & -\frac{\partial}{\partial y} \\ -\frac{\partial}{\partial z} & 0 & \frac{\partial}{\partial x} \end{bmatrix} \begin{bmatrix} \varphi_1 & 0 & 0 & ..... & \varphi_{nx} & 0 & 0 \\ 0 & \varphi_1 & 0 & & 0 & \varphi_{nx} & 0 \\ 0 & 0 & \varphi_1 & & 0 & 0 & \varphi_{nx} \end{bmatrix}$$

So, discretization of the third term of (B.1) gives

$$\begin{aligned} \mathbf{L}_w : \hat{p}\,\mathbf{L}_{\Delta x} &= (\underset{\sim}{d}^{w})^T \hat{p}\,\underline{B}\,\underset{\sim}{d}^{\Delta x} \\ &= (\underset{\sim}{d}^{w})^T \underset{\sim}{\psi}^T \underset{\sim}{\hat{p}}\,\underline{B}\,\underset{\sim}{d}^{\Delta x} \\ &= \underset{\sim}{w}^T \underline{A}^T \underset{\sim}{\psi}^T \underset{\sim}{\hat{p}}\;\underline{B}\,\underline{A}\,\underset{\sim}{\Delta x} \end{aligned} \tag{B.5}$$

The next term is $\mathbf{L}_w : \hat{\boldsymbol{\tau}}$. The matrix representation of $\mathbf{L}_w$ is already known. The matrix representation of the symmetric stress tensor $\hat{\boldsymbol{\tau}}$ is given by

$$\underline{\hat{\tau}} = \begin{bmatrix} \hat{\tau}_{xx} & \hat{\tau}_{xy} & \hat{\tau}_{xz} \\ \hat{\tau}_{xy} & \hat{\tau}_{yy} & \hat{\tau}_{yz} \\ \hat{\tau}_{xz} & \hat{\tau}_{yz} & \hat{\tau}_{zz} \end{bmatrix}$$

Calculation of $\underline{L}_w : \underline{\hat{\tau}} = \mathrm{tr}(\underline{L}_w \cdot \underline{\hat{\tau}})$ gives

$$\begin{aligned} \underline{L}_w : \underline{\hat{\tau}} &= d_{11}^w \hat{\tau}_{xx} + (d_{12}^w + \omega_{12}^w)\hat{\tau}_{xy} + (d_{13}^w + \omega_{31}^w)\hat{\tau}_{xz} \\ &\quad + (d_{12}^w - \omega_{12}^w)\hat{\tau}_{xy} + d_{22}^w \hat{\tau}_{yy} + (d_{23}^w + \omega_{23}^w)\hat{\tau}_{yz} \\ &\quad + (d_{13}^w - \omega_{31}^w)\hat{\tau}_{xz} + (d_{23}^w - \omega_{23}^w)\hat{\tau}_{yz} + d_{33}^w \hat{\tau}_{zz} \\ &= d_{11}^w \hat{\tau}_{xx} + 2d_{12}^w \hat{\tau}_{xy} + 2d_{13}^w \hat{\tau}_{xz} + d_{22}^w \hat{\tau}_{yy} + 2d_{23}^w \hat{\tau}_{yz} + d_{33}^w \hat{\tau}_{zz} \\ &= (\underset{\sim}{d}^{w})^T \underset{\sim}{\hat{\tau}} \end{aligned}$$

with

$$\underset{\sim}{\hat{\tau}}^T = \begin{bmatrix} \hat{\tau}_{xx} & \hat{\tau}_{xy} & \hat{\tau}_{yy} & \hat{\tau}_{zz} & \hat{\tau}_{yz} & \hat{\tau}_{xz} & 0 & 0 & 0 \end{bmatrix}$$

$\mathbf{L}_w : \hat{\boldsymbol{\tau}}$ can be discretized as follows:

$$\mathbf{L}_w : \hat{\boldsymbol{\tau}} = (\underset{\sim}{d}^w)^T \underset{\sim}{\hat{\tau}} = \underset{\sim}{w}^T \underline{A}^T \underset{\sim}{\hat{\tau}} \tag{B.6}$$

The last two terms to be discretized are $\mathbf{L}_w : 4c\mathbf{D}_{\Delta x}$ and $\mathbf{L}_w : \hat{\boldsymbol{\tau}} \cdot \mathbf{L}_{\Delta x}{}^c$. These terms can be rewritten:

$$\begin{aligned}
\mathbf{L}_w : [4c\mathbf{D}_{\Delta x} + \hat{\boldsymbol{\tau}} \cdot \mathbf{L}_{\Delta x}{}^c] &= (\mathbf{D}_w + \boldsymbol{\Omega}_w) : (4c\mathbf{D}_{\Delta x} + \hat{\boldsymbol{\tau}} \cdot (\mathbf{D}_{\Delta x} + \boldsymbol{\Omega}_{\Delta x})^c) \\
&= \mathbf{D}_w : 4c\mathbf{D}_{\Delta x} + \boldsymbol{\Omega}_w : 4c\mathbf{D}_{\Delta x} \\
&\quad + (\mathbf{D}_w + \boldsymbol{\Omega}_w) : (\hat{\boldsymbol{\tau}} \cdot (\mathbf{D}_{\Delta x} + \boldsymbol{\Omega}_{\Delta x})^c)
\end{aligned}$$

Using $\mathbf{A} : \mathbf{B} = \mathbf{0}$ when $\mathbf{A} = \mathbf{A}^c$ and $\mathbf{B} = -\mathbf{B}^c$ the following relation holds:

$$\begin{aligned}
\mathbf{L}_w : [4c\mathbf{D}_{\Delta x} + \hat{\boldsymbol{\tau}} \cdot \mathbf{L}_{\Delta x}{}^c] &= \mathrm{tr}[4c\mathbf{D}_w \cdot \mathbf{D}_{\Delta x}] \\
&\quad + \mathrm{tr}[(\mathbf{D}_w + \boldsymbol{\Omega}_w) \cdot \hat{\boldsymbol{\tau}} \cdot (\mathbf{D}_{\Delta x} + \boldsymbol{\Omega}_{\Delta x})^c]
\end{aligned}$$

Using the matrix representations for $\mathbf{D}_w$, $\mathbf{D}_{\Delta x}$, $\boldsymbol{\Omega}_w$, $\boldsymbol{\Omega}_{\Delta x}$ and $\hat{\boldsymbol{\tau}}$, the last two terms of the left hand side can be worked out, resulting in (see [6]):

$$\mathbf{L}_w : [4c\mathbf{D}_{\Delta x} + \hat{\boldsymbol{\tau}} \cdot \mathbf{L}_{\Delta x}] = 4c(\underset{\sim}{d}^w)^T \underline{D}\, \underset{\sim}{d}^{\Delta x} + (\underset{\sim}{d}^w)^T \underline{T}\, \underset{\sim}{d}^{\Delta x}$$

where

$$\underline{D} = \begin{bmatrix}
1 & 0 & 0 & 0 & 0 & 0 & 0 & 0 & 0 \\
0 & \frac{1}{2} & 0 & 0 & 0 & 0 & 0 & 0 & 0 \\
0 & 0 & 1 & 0 & 0 & 0 & 0 & 0 & 0 \\
0 & 0 & 0 & 1 & 0 & 0 & 0 & 0 & 0 \\
0 & 0 & 0 & 0 & \frac{1}{2} & 0 & 0 & 0 & 0 \\
0 & 0 & 0 & 0 & 0 & \frac{1}{2} & 0 & 0 & 0 \\
0 & 0 & 0 & 0 & 0 & 0 & 0 & 0 & 0 \\
0 & 0 & 0 & 0 & 0 & 0 & 0 & 0 & 0 \\
0 & 0 & 0 & 0 & 0 & 0 & 0 & 0 & 0
\end{bmatrix}$$

$$\underline{T} = \begin{bmatrix}
\hat{\tau}_{xx} & \frac{\hat{\tau}_{xy}}{2} & 0 & 0 & 0 & \frac{\hat{\tau}_{xz}}{2} & \frac{\hat{\tau}_{xy}}{2} & 0 & -\frac{\hat{\tau}_{xz}}{2} \\
 & \frac{\hat{\tau}_{xx}+\hat{\tau}_{yy}}{4} & \frac{\hat{\tau}_{xy}}{2} & 0 & \frac{\hat{\tau}_{xz}}{4} & \frac{\hat{\tau}_{yz}}{4} & \frac{\hat{\tau}_{yy}-\hat{\tau}_{xx}}{4} & \frac{\hat{\tau}_{xz}}{4} & -\frac{\hat{\tau}_{yz}}{4} \\
 & & \hat{\tau}_{yy} & 0 & \frac{\hat{\tau}_{yz}}{2} & 0 & -\frac{\hat{\tau}_{xy}}{2} & \frac{\hat{\tau}_{yz}}{2} & 0 \\
 & & & \hat{\tau}_{zz} & \frac{\hat{\tau}_{yz}}{2} & \frac{\hat{\tau}_{xz}}{2} & 0 & -\frac{\hat{\tau}_{yz}}{2} & \frac{\hat{\tau}_{xz}}{2} \\
 & & & & \frac{\hat{\tau}_{yy}+\hat{\tau}_{zz}}{4} & \frac{\hat{\tau}_{xy}}{4} & -\frac{\hat{\tau}_{xz}}{4} & \frac{\hat{\tau}_{zz}-\hat{\tau}_{yy}}{4} & \frac{\hat{\tau}_{xy}}{4} \\
 & & & & & \frac{\hat{\tau}_{xx}+\hat{\tau}_{zz}}{4} & \frac{\hat{\tau}_{yz}}{4} & -\frac{\hat{\tau}_{xy}}{4} & \frac{\hat{\tau}_{xx}-\hat{\tau}_{zz}}{4} \\
 & symm & & & & & \frac{\hat{\tau}_{xx}+\hat{\tau}_{yy}}{4} & -\frac{\hat{\tau}_{xz}}{4} & -\frac{\hat{\tau}_{yz}}{4} \\
 & & & & & & & \frac{\hat{\tau}_{yy}+\hat{\tau}_{zz}}{4} & -\frac{\hat{\tau}_{xy}}{4} \\
 & & & & & & & & \frac{\hat{\tau}_{xx}+\hat{\tau}_{zz}}{4}
\end{bmatrix}$$

Discretization of the last two terms of equation (B.1) gives

$$\begin{aligned} \mathbf{L}_w : [4c\,\mathbf{D}_{\Delta x} + \hat{\boldsymbol{\tau}} \cdot \mathbf{L}_{\Delta x}] &= (\underset{\sim}{d}^{w})^T (4c\,\underline{D} + \underline{T}) \underset{\sim}{d}^{\Delta x} \\ &= \underset{\sim}{w}^T \underline{A}^T (4c\,\underline{D} + \underline{T}) \underline{A} \underset{\sim}{\Delta x} \end{aligned} \tag{B.7}$$

Now, all terms of the left hand side of (B.1) are discretized. The right hand side $\vec{w} \cdot \vec{b}$ has to be discretized also.
The representation of $\vec{b}$ with respect to $\{\vec{e}_x, \vec{e}_y, \vec{e}_z\}$ is

$$\vec{b} = b^x \vec{e}_x + b^y \vec{e}_y + b^z \vec{e}_z$$

Vector $\vec{b}$ will be discretized in the same way as $\vec{w}$ and $\Delta\vec{x}$. So:

$$\begin{bmatrix} b^x \\ b^y \\ b^z \end{bmatrix} = \begin{bmatrix} \varphi_1 & 0 & 0 & \cdots & \varphi_{nx} & 0 & 0 \\ 0 & \varphi_1 & 0 & & 0 & \varphi_{nx} & 0 \\ 0 & 0 & \varphi_1 & & 0 & 0 & \varphi_{nx} \end{bmatrix} \begin{bmatrix} {b_1}^x \\ {b_1}^y \\ {b_1}^z \\ \cdot \\ \cdot \\ {b_{nx}}^x \\ {b_{nx}}^y \\ {b_{nx}}^z \end{bmatrix} = \underline{\varphi}\,\underset{\sim}{b}$$

With the use of this discretization, the right hand side can be discretized as follows:

$$\vec{w} \cdot \vec{b} = \underset{\sim}{w}^T \underline{\varphi}^T \underline{\varphi}\,\underset{\sim}{b} = \underset{\sim}{w}^T \underline{P}\,\underset{\sim}{b} \tag{B.8}$$

with

$$\underline{P} = \underline{\varphi}^T \underline{\varphi}$$

Substitution of the discretizations (B.3) to (B.8) in (B.1) yields

$$\begin{aligned} & \underset{\sim}{w}^T \int_\Omega (-\underline{Q}\,\underset{\sim}{\hat{p}} + \underline{A}^T \underset{\sim}{\hat{\tau}})\, d\Omega \\ + \; & \underset{\sim}{w}^T \int_\Omega [-\underline{Q}\,\underset{\sim}{\Delta p} + \underline{A}^T (\underset{\sim}{\psi}^T \underset{\sim}{\hat{p}}\,\underline{B} + 4c\,\underline{D} + \underline{T}) \underline{A} \underset{\sim}{\Delta x}]\, d\Omega \\ = \; & \underset{\sim}{w}^T \int_\Gamma \underline{P}\,\underset{\sim}{b}\, d\Gamma \end{aligned} \tag{B.9}$$

Equation (B.2) has to be discretized too. First the left hand side will be discretized. Discretization of this term is done similarly to the discretization of the first two terms of equation (B.1):

$$\begin{aligned} r &= \underset{\sim}{r}^T \underset{\sim}{\psi} \\ \hat{\vec{\nabla}} \cdot \Delta\vec{x} &= \underset{\sim}{a}^T \Delta\underset{\sim}{x} \end{aligned}$$

where $\underset{\sim}{r}$ *is the column with the weighting functions for the pressure at element nodes.* So:

$$r\hat{\vec{\nabla}} \cdot \Delta\vec{x} = \underset{\sim}{r}^T \underset{\sim}{\psi}\, \underset{\sim}{a}^T \Delta\underset{\sim}{x} = \underset{\sim}{r}^T \underline{Q}^T \Delta\underset{\sim}{x} \tag{B.10}$$

Discretization of the right hand side of (B.2) yields

$$r\hat{k} = \underset{\sim}{r}^T \underset{\sim}{\psi}\, \hat{k} \tag{B.11}$$

where

$$\hat{k} = \frac{1}{\det(\hat{\mathbf{F}})} - 1$$

So, the discretized formula for equation (B.2) is given by

$$\underset{\sim}{r}^T \int_\Omega \underline{Q}^T \Delta\underset{\sim}{x}\, d\Omega = \underset{\sim}{r}^T \int_\Omega \underset{\sim}{\psi}\, \hat{k}\, d\Omega \tag{B.12}$$

In a penalty function formulation, the weighted incompressibility constraint will look as follows:

$$\int_\Omega r\, \hat{\vec{\nabla}} \cdot \Delta\vec{x}\, d\Omega + \int_\Omega r\, \epsilon_1\, \Delta p d\Omega = \int_\Omega r\, \hat{k}\, d\Omega \tag{B.13}$$

The second term in the left hand side can be discretized by discretizing r and Δp according to

$$\begin{aligned} r &= \underset{\sim}{r}^T \underset{\sim}{\psi} \\ \Delta p &= \underset{\sim}{\psi}^T \Delta\underset{\sim}{p} \end{aligned}$$

So:

$$\begin{aligned} \int_\Omega r\, \epsilon_1\, \Delta p\, d\Omega &= \underset{\sim}{r}^T \int_\Omega \epsilon_1\, \underset{\sim}{\psi}\, \underset{\sim}{\psi}^T \Delta\underset{\sim}{p}\, d\Omega \\ &= \underset{\sim}{r}^T \int_\Omega \epsilon_1\, \underline{H}\, \Delta\underset{\sim}{p}\, d\Omega \end{aligned} \tag{B.14}$$

where

$$\underline{H} = \underset{\sim}{\psi}\,\underset{\sim}{\psi}^{T}$$

Substitution of (B.14) in the penalty function formulation (B.13) yields

$$\underset{\sim}{r}^{T} \int_{\Omega} \underline{Q}^{T} \Delta \underset{\sim}{x}\, d\Omega + \underset{\sim}{r}^{T} \int_{\Omega} \epsilon_1\, \underline{H}\, \Delta \underset{\sim}{p}\, d\Omega = \underset{\sim}{r}^{T} \int_{\Omega} \underset{\sim}{\psi}\, \hat{k}\, d\Omega \tag{B.15}$$

B.2 Impenetrability constraint

The contribution of the impenetrability constraint, that has to be discretized, is given by

$$-\int_{\Gamma_{cp}} \frac{1}{\epsilon_2} \vec{w} \cdot \left(\hat{g}^{+}\, \hat{\vec{n}} + \left[(\hat{\vec{n}}\hat{\vec{n}})^{+} - \hat{g}^{+}\, \frac{\hat{\vec{r}}\hat{\vec{r}}}{|\hat{\vec{x}}_c - \hat{\vec{x}}|} \right] \cdot \Delta\vec{x} \right) d\Gamma \tag{B.16}$$

The vectors $\vec{w}$, $\hat{\vec{n}}$, $\hat{\vec{r}}$, $\hat{\vec{x}}$, $\hat{\vec{x}}_c$ and $\Delta\vec{x}$ with respect to the Cartesian reference system are given by

$$\begin{aligned}
\vec{w} &= w^x \vec{e}_x + w^y \vec{e}_y + w^z \vec{e}_z \\
\hat{\vec{n}} &= \hat{n}^x \vec{e}_x + \hat{n}^y \vec{e}_y + \hat{n}^z \vec{e}_z \\
\hat{\vec{r}} &= \hat{r}^x \vec{e}_x + \hat{r}^y \vec{e}_y + \hat{r}^z \vec{e}_z \\
\hat{\vec{x}} &= \hat{x}\, \vec{e}_x + \hat{y}\, \vec{e}_y + \hat{z}\, \vec{e}_z \\
\hat{\vec{x}}_c &= \hat{x}_c \vec{e}_x + \hat{y}_c \vec{e}_y + \hat{z}_c \vec{e}_z \\
\Delta\vec{x} &= \Delta x\, \vec{e}_x + \Delta y\, \vec{e}_y + \Delta z\, \vec{e}_z
\end{aligned}$$

The first term of equation (B.16) can be rewritten as follows.

$$\frac{1}{\epsilon_2} \vec{w} \cdot \hat{g}^{+}\, \hat{\vec{n}} = \frac{1}{\epsilon_2}\, \hat{g}^{+} \begin{bmatrix} w^x & w^y & w^z \end{bmatrix} \begin{bmatrix} \hat{n}^x \\ \hat{n}^y \\ \hat{n}^z \end{bmatrix}$$

Discretization of the components of $\vec{w}$ yields

$$\begin{bmatrix} w^x \\ w^y \\ w^z \end{bmatrix} = \begin{bmatrix} \chi_1 & 0 & 0 & .... & \chi_{nb} & 0 & 0 \\ 0 & \chi_1 & 0 & & 0 & \chi_{nb} & 0 \\ 0 & 0 & \chi_1 & & 0 & 0 & \chi_{nb} \end{bmatrix} \begin{bmatrix} {w_1}^x \\ {w_1}^y \\ {w_1}^z \\ . \\ . \\ {w_{nb}}^x \\ {w_{nb}}^y \\ {w_{nb}}^z \end{bmatrix} = \underline{\chi}\, \underset{\sim}{w}$$

where nb is *the number of nodes in the boundary element,*

$\underline{\chi}$ is *the matrix with interpolation functions for the boundary element,*

$\underset{\sim}{w}$ is *the column with weighting functions.*

So:

$$\frac{1}{\epsilon_2}\vec{w}\cdot\hat{g}^+\hat{\vec{n}} = \frac{1}{\epsilon_2}\hat{g}^+\,\underset{\sim}{w}^T\underline{\chi}^T\underset{\sim}{\hat{n}} \tag{B.17}$$

where

$$\underset{\sim}{\hat{n}} = \begin{bmatrix} \hat{n}^x & \hat{n}^y & \hat{n}^z \end{bmatrix}$$

$\Delta\vec{x}$ is discretized in the same way as $\vec{w}$:

$$\begin{bmatrix} \Delta x \\ \Delta y \\ \Delta z \end{bmatrix} = \begin{bmatrix} \chi_1 & 0 & 0 & .... & \chi_{nb} & 0 & 0 \\ 0 & \chi_1 & 0 & & 0 & \chi_{nb} & 0 \\ 0 & 0 & \chi_1 & & 0 & 0 & \chi_{nb} \end{bmatrix} \begin{bmatrix} \Delta x_1 \\ \Delta y_1 \\ \Delta z_1 \\ . \\ . \\ \Delta x_{nb} \\ \Delta y_{nb} \\ \Delta z_{nb} \end{bmatrix} = \underline{\chi}\,\underset{\sim}{\Delta x}$$

Using the discretization of $\vec{w}$ and $\Delta\vec{x}$, the second term of the impenetrability constraint can be discretized:

$$\begin{aligned} \frac{1}{\epsilon_2}\vec{w}\cdot(\hat{\vec{n}}\hat{\vec{n}})^+\cdot\Delta\vec{x} &= \frac{1}{\epsilon_2}\begin{bmatrix} w^x & w^y & w^z \end{bmatrix}\left(\begin{bmatrix} \hat{n}^x \\ \hat{n}^y \\ \hat{n}^z \end{bmatrix}\begin{bmatrix} \hat{n}^x & \hat{n}^y & \hat{n}^z \end{bmatrix}\right)^+\begin{bmatrix} \Delta x \\ \Delta y \\ \Delta z \end{bmatrix} \\ &= \frac{1}{\epsilon_2}\underset{\sim}{w}^T\underline{\chi}^T\underline{N}^+\underline{\chi}\,\underset{\sim}{\Delta x} \end{aligned} \tag{B.18}$$

where: $\underset{\sim}{N} = \underset{\sim}{\hat{n}}\,\underset{\sim}{\hat{n}}^T$ *is the matrix with the components of the normal vector* $\hat{\vec{n}}$.

Similarly, the third term can be discretized, which yields

$$\begin{aligned}\frac{1}{\epsilon_2}\hat{g}^+\vec{w}\cdot\frac{\hat{\vec{r}}\hat{\vec{r}}}{|\hat{\vec{x}}_c-\hat{\vec{x}}|}\cdot\Delta\vec{x} &= \frac{1}{\epsilon_2}\frac{\hat{g}^+}{x_{dif}}\begin{bmatrix} w^x & w^y & w^z\end{bmatrix}\begin{bmatrix}\hat{r}^x\\ \hat{r}^y\\ \hat{r}^z\end{bmatrix}\begin{bmatrix}\hat{r}^x & \hat{r}^y & \hat{r}^z\end{bmatrix}\begin{bmatrix}\Delta x\\ \Delta y\\ \Delta z\end{bmatrix}\\ &= \frac{1}{\epsilon_2}\frac{\hat{g}^+}{x_{dif}}\underset{\sim}{w}^T\underline{\chi}^T\underline{R}\,\underline{\chi}\,\underset{\sim}{\Delta x} \qquad \text{(B.19)}\end{aligned}$$

where

$$\begin{aligned}\underline{R} &= \underset{\sim}{\hat{r}}\,\underset{\sim}{\hat{r}}^T\\ x_{dif} &= \sqrt{(\hat{x}_c-\hat{x})^2+(\hat{y}_c-\hat{y})^2+(\hat{z}_c-\hat{z})^2}\end{aligned}$$

Substitution of the discretizations (B.17), (B.18) and (B.19) in equation (B.16) gives the discretized contribution for the impenetrability constraint.

$$-\int_{\Gamma_{cp}}\frac{1}{\epsilon_2}\hat{g}^+\,\underset{\sim}{w}^T\underline{\chi}^T\underset{\sim}{\hat{n}}\,d\Gamma-\int_{\Gamma_{cp}}\frac{1}{\epsilon_2}\underset{\sim}{w}^T\underline{\chi}^T[\underline{N}^+-\frac{\hat{g}^+}{x_{dif}}\underline{R}]\,\underline{\chi}\,\underset{\sim}{\Delta x}\,d\Gamma \qquad \text{(B.20)}$$

B.3 Coulomb friction (slip)

The weighted residual formulation of the Coulomb friction is given in linearized form by

$$\int_{\Gamma_{cp}}\frac{\mu}{\epsilon_2}\hat{g}^+\vec{w}\cdot\hat{\vec{d}}\,d\Gamma+\int_{\Gamma_{cp}}\frac{\mu}{\epsilon_2}\vec{w}\cdot((\hat{\vec{d}}\hat{\vec{n}})^+\hat{g}^+\mathbf{K}\cdot\mathbf{G})\cdot\Delta\vec{x}\,d\Gamma \qquad \text{(B.21)}$$

with

$$\begin{aligned}\mathbf{K} &= \frac{\mathbf{I}-\hat{\vec{d}}\hat{\vec{d}}}{|\hat{\vec{u}}_c-\hat{\vec{u}}|}\\ \mathbf{G} &= \bar{\omega}\,\Delta t\,R_c\frac{\hat{\vec{n}}\hat{\vec{r}}}{|\hat{\vec{x}}_c-\hat{\vec{x}}|}-\mathbf{I}\end{aligned}$$

The components of vectors $\vec{w}$, $\hat{\vec{d}}$, $\hat{\vec{n}}$, $\hat{\vec{r}}$, $\hat{\vec{u}}$, $\hat{\vec{u}}_c$, $\hat{\vec{x}}$, $\hat{\vec{x}}_c$ and $\Delta\vec{x}$ with respect to the Cartesian reference system are given by

$$\vec{w} = w^x\vec{e}_x+w^y\vec{e}_y+w^z\vec{e}_z$$

$$
\begin{aligned}
\hat{\vec{d}} &= \hat{d}^x \vec{e}_x + \hat{d}^y \vec{e}_y + \hat{d}^z \vec{e}_z \\
\hat{\vec{n}} &= \hat{n}^x \vec{e}_x + \hat{n}^y \vec{e}_y + \hat{n}^z \vec{e}_z \\
\hat{\vec{r}} &= \hat{r}^x \vec{e}_x + \hat{r}^y \vec{e}_y + \hat{r}^z \vec{e}_z \\
\hat{\vec{u}} &= \hat{u}^x \vec{e}_x + \hat{u}^y \vec{e}_y + \hat{u}^z \vec{e}_z \\
\hat{\vec{u}}_c &= \hat{u}_c^x \vec{e}_x + \hat{u}_c^y \vec{e}_y + \hat{u}_c^z \vec{e}_z \\
\hat{\vec{x}} &= \hat{x} \vec{e}_x + \hat{y} \vec{e}_y + \hat{z} \vec{e}_z \\
\hat{\vec{x}}_c &= \hat{x}_c \vec{e}_x + \hat{y}_c \vec{e}_y + \hat{z}_c \vec{e}_z \\
\Delta\vec{x} &= \Delta x\, \vec{e}_x + \Delta y\, \vec{e}_y + \Delta z\, \vec{e}_z
\end{aligned}
$$

Discretization of the components of $\vec{w}$ and $\Delta\vec{x}$ yields

$$
\begin{bmatrix} w^x \\ w^y \\ w^z \end{bmatrix} = \begin{bmatrix} \chi_1 & 0 & 0 & .... & \chi_{nb} & 0 & 0 \\ 0 & \chi_1 & 0 & & 0 & \chi_{nb} & 0 \\ 0 & 0 & \chi_1 & & 0 & 0 & \chi_{nb} \end{bmatrix} \begin{bmatrix} {w_1}^x \\ {w_1}^y \\ {w_1}^z \\ . \\ . \\ w_{nb}^x \\ w_{nb}^y \\ w_{nb}^z \end{bmatrix} = \underset{\sim}{\chi}\, \underset{\sim}{w}
$$

$$
\begin{bmatrix} \Delta x \\ \Delta y \\ \Delta z \end{bmatrix} = \begin{bmatrix} \chi_1 & 0 & 0 & .... & \chi_{nb} & 0 & 0 \\ 0 & \chi_1 & 0 & & 0 & \chi_{nb} & 0 \\ 0 & 0 & \chi_1 & & 0 & 0 & \chi_{nb} \end{bmatrix} \begin{bmatrix} \Delta x_1 \\ \Delta y_1 \\ \Delta z_1 \\ . \\ . \\ \Delta x_{nb} \\ \Delta y_{nb} \\ \Delta z_{nb} \end{bmatrix} = \underset{\sim}{\chi}\, \underset{\sim}{\Delta x}
$$

Now, each term of equation (B.21) will be discretized separately. The first term is discretized as follows.

$$
\frac{\mu}{\epsilon_2}\, \hat{g}^+\, \vec{w} \cdot \hat{\vec{d}} = \frac{\mu}{\epsilon_2}\, \hat{g}^+ \begin{bmatrix} w^x & w^y & w^z \end{bmatrix} \begin{bmatrix} \hat{d}^x \\ \hat{d}^y \\ \hat{d}^z \end{bmatrix} = \frac{\mu}{\epsilon_2}\, \hat{g}^+\, \underset{\sim}{w}^T \underset{\sim}{\chi}^T \underset{\sim}{\hat{d}}
$$

The matrix representation of tensors $\mathbf{K}$ and $\mathbf{G}$ with respect to the Cartesian coordinate system is denoted by

$$\underset{\sim}{K} = \underset{\sim}{\vec{e}} \cdot \mathbf{K} \cdot \underset{\sim}{\vec{e}}^{\,T} = \underset{\sim}{\vec{e}} \cdot \frac{\mathbf{I} - \hat{\vec{d}}\hat{\vec{d}}}{|\hat{\vec{u}}_c - \hat{\vec{u}}|} \cdot \underset{\sim}{\vec{e}}^{\,T} = \frac{\underline{I} - \underset{\sim}{\hat{d}}\,\underset{\sim}{\hat{d}}^{\,T}}{u_{dif}}$$

$$\underline{G} = \underset{\sim}{\vec{e}} \cdot \mathbf{G} \cdot \underset{\sim}{\vec{e}}^{\,T} = \underset{\sim}{\vec{e}} \cdot (\bar{\omega}\Delta t R_c \frac{\hat{\vec{n}}\hat{\vec{r}}}{|\hat{\vec{x}}_c - \hat{\vec{x}}|} - \mathbf{I}) \cdot \underset{\sim}{\vec{e}}^{\,T} = \bar{\omega}\Delta t\, R_c \frac{\underset{\sim}{\hat{n}}\,\underset{\sim}{\hat{r}}^{\,T}}{x_{dif}} - \underline{I}$$

where

$$u_{dif} = \sqrt{(\hat{u}_c^x - \hat{u}^x)^2 + (\hat{u}_c^y - \hat{u}^y)^2 + (\hat{u}_c^z - \hat{u}^z)^2}$$
$$x_{dif} = \sqrt{(\hat{x}_c - \hat{x})^2 + (\hat{y}_c - \hat{y})^2 + (\hat{z}_c - \hat{z})^2}$$
$$\underset{\sim}{\hat{r}}^{\,T} = \begin{bmatrix} \hat{r}^x & \hat{r}^y & \hat{r}^z \end{bmatrix}$$

Using this matrix representation, the second term of the friction can be discretized as follows.

$$\frac{\mu}{\epsilon_2}\vec{w} \cdot ((\hat{\vec{d}}\hat{\vec{n}})^+ + \hat{g}^+ \mathbf{K} \cdot \mathbf{G}) \cdot \Delta\vec{x} = \frac{\mu}{\epsilon_2} \underset{\sim}{w}^{\,T} \underline{\chi}^T ((\underset{\sim}{\hat{d}}\,\underset{\sim}{\hat{n}}^{\,T})^+ + \hat{g}^+ \underline{K}\,\underline{G})\,\underline{\chi}\,\underset{\sim}{\Delta x}$$

Combining the discretized terms yields the discretized friction:

$$\int_{\Gamma_{cp}} \frac{\mu}{\epsilon_2} \hat{g}^+ \underset{\sim}{w}^{\,T} \underline{\chi}^T \underset{\sim}{\hat{d}}\, d\Gamma + \int_{\Gamma_{cp}} \frac{\mu}{\epsilon_2} \underset{\sim}{w}^{\,T} \underline{\chi}^T ((\underset{\sim}{\hat{d}}\,\underset{\sim}{\hat{n}}^{\,T})^+ + \hat{g}^+ \underline{K}\,\underline{G})\,\underline{\chi}\,\underset{\sim}{\Delta x}\, d\Gamma \qquad \text{(B.22)}$$

where

$$\underline{K} = \frac{\underline{I} - \underset{\sim}{\hat{d}}\,\underset{\sim}{\hat{d}}^{\,T}}{u_{dif}}$$

$$\underline{G} = \bar{\omega}\,\Delta t\, R_c \frac{\underset{\sim}{\hat{n}}\,\underset{\sim}{\hat{r}}^{\,T}}{x_{dif}} - \underline{I}$$

B.4 Regularized Coulomb friction 1

The first smoothed Coulomb friction is given by

$$\int_{\Gamma_{cp}} \frac{\mu}{\epsilon_2} \hat{g}^+ \hat{\phi}_1 \vec{w} \cdot \hat{\vec{d}}\, d\Gamma +$$
$$\int_{\Gamma_{cp}} \frac{\mu}{\epsilon_2}\vec{w} \cdot \left[\hat{\phi}_1(\hat{\vec{d}}\hat{\vec{n}})^+ + \left(\frac{\hat{g}^+}{\epsilon_3\Delta t}[1 - \tanh^2(\frac{|\hat{\vec{u}}_c - \hat{\vec{u}}|}{\epsilon_3\Delta t})]\hat{\vec{d}}\hat{\vec{d}} + \hat{g}^+\hat{\phi}_1\mathbf{K}\right) \cdot \mathbf{G}\right] \cdot \Delta\vec{x}\, d\Gamma \qquad \text{(B.23)}$$

In the previous sections all vectors and tensors in this relation are represented with respect to the Cartesian coordinate system. These representations will be applied again in the following discretization.

$$\frac{\mu}{\epsilon_2}\hat{g}^+\,\hat{\phi}_1\,\vec{w}\cdot\hat{\vec{d}} = \frac{\mu}{\epsilon_2}\hat{g}^+\,\hat{\phi}_1\,\underset{\sim}{w}^T\underline{\chi}^T\underset{\sim}{\hat{d}}$$

$$\frac{\mu}{\epsilon_2}\hat{\phi}_1\vec{w}\cdot(\hat{\vec{d}}\hat{\vec{n}})^+\cdot\Delta\vec{x} = \frac{\mu}{\epsilon_2}\hat{\phi}_1\,\underset{\sim}{w}^T(\underline{\chi}^T\underset{\sim}{\hat{d}}\,\underset{\sim}{\hat{n}}^T\underline{\chi})^+\Delta\underset{\sim}{x}$$

$$\frac{\mu}{\epsilon_2}\vec{w}\cdot\left[\frac{\hat{g}^+}{\epsilon_3\Delta t}[1-\tanh^2(\frac{|\hat{\vec{u}}_c-\hat{\vec{u}}|}{\epsilon_3\Delta t})]\hat{\vec{d}}\hat{\vec{d}}+\hat{g}^+\hat{\phi}_1\mathbf{K}\right]\cdot\mathbf{G}\cdot\Delta\vec{x}$$
$$=\frac{\mu}{\epsilon_2}\underset{\sim}{w}^T\underline{\chi}^T\left[\frac{\hat{g}^+}{\epsilon_3\Delta t}[1-\tanh^2(\frac{u_{dif}}{\epsilon_3\Delta t})]\underset{\sim}{\hat{d}}\,\underset{\sim}{\hat{d}}^T+\hat{g}^+\hat{\phi}_1\underline{K}\right]\underline{G}\underline{\chi}\Delta\underset{\sim}{x}$$

So, the discretized friction is given by

$$\int_{\Gamma_{cp}}\frac{\mu}{\epsilon_2}\hat{g}^+\,\hat{\phi}_1\,\underset{\sim}{w}^T\underline{\chi}^T\underset{\sim}{\hat{d}}\,d\Gamma +$$
$$\int_{\Gamma_{cp}}\frac{\mu}{\epsilon_2}\underset{\sim}{w}^T\underline{\chi}^T\left[\hat{\phi}_1(\underset{\sim}{\hat{d}}\,\underset{\sim}{\hat{n}}^T)^+ + \left(\frac{\hat{g}^+}{\epsilon_3\Delta t}[1-\tanh^2(\frac{u_{dif}}{\epsilon_3\Delta t})]\underset{\sim}{\hat{d}}\,\underset{\sim}{\hat{d}}^T+\hat{g}^+\hat{\phi}_1\underline{K}\right)\underline{G}\right]\underline{\chi}\Delta\underset{\sim}{x}\,d\Gamma \tag{B.24}$$

B.5 Regularized Coulomb friction 2

The relation of this friction model is given by

$$\int_{\Gamma_{cp}}\frac{\mu}{\epsilon_2}\hat{g}^+\hat{\phi}_2\vec{w}\cdot\hat{\vec{d}}\,d\Gamma +$$
$$\int_{\Gamma_{cp}}\frac{\mu}{\epsilon_2}\vec{w}\cdot\left[\hat{\phi}_2(\hat{\vec{d}}\hat{\vec{n}})^+ + \left(\frac{2\,\hat{g}^+\epsilon_4\Delta t}{\pi((\epsilon_4\Delta t)^2+|\hat{\vec{u}}_c-\hat{\vec{u}}|^2)}\hat{\vec{d}}\hat{\vec{d}}+\hat{g}^+\hat{\phi}_2\mathbf{K}\right)\cdot\mathbf{G}\right]\cdot\Delta\vec{x}\,d\Gamma \tag{B.25}$$

Analogous to all other discretizations, this relation is discretized, which yields

$$\int_{\Gamma_{cp}} \frac{\mu}{\epsilon_2}\,\hat{g}^{+}\,\hat{\phi}_2\,\underset{\sim}{w}^{T}\underline{\chi}^{T}\underset{\sim}{\hat{d}}\,d\Gamma +$$
$$\int_{\Gamma_{cp}} \frac{\mu}{\epsilon_2}\underset{\sim}{w}^{T}\underline{\chi}^{T}\left[\hat{\phi}_2(\underset{\sim}{\hat{d}}\,\underset{\sim}{\hat{n}}^{T})^{+} + \left(\frac{2\,\hat{g}^{+}\epsilon_4\Delta t}{\pi((\epsilon_4\Delta t)^2+(u_{dif})^2)}\underset{\sim}{\hat{d}}\,\underset{\sim}{\hat{d}}^{T} + \hat{g}^{+}\hat{\phi}_2\underline{K}\right)\underline{G}\right]\underline{\chi}\Delta\underset{\sim}{x}\,d\Gamma \tag{B.26}$$

Appendix C

Trilinear hexahedral element

In this appendix the shape functions of an arbitrary trilinear hexahedral element and the x-, y- and z-derivatives of these shape functions will be derived. For that purpose a parent domain in another space, the $\underset{\sim}{\xi}$-space, will be used. The $\underset{\sim}{\xi}$-space is an orthonormal space with ξ, η and ζ as independent coordinates. The parent domain, that will be used, is a bi-unit cube (see figure C.1). For this domain it is relatively simple to define shape functions.

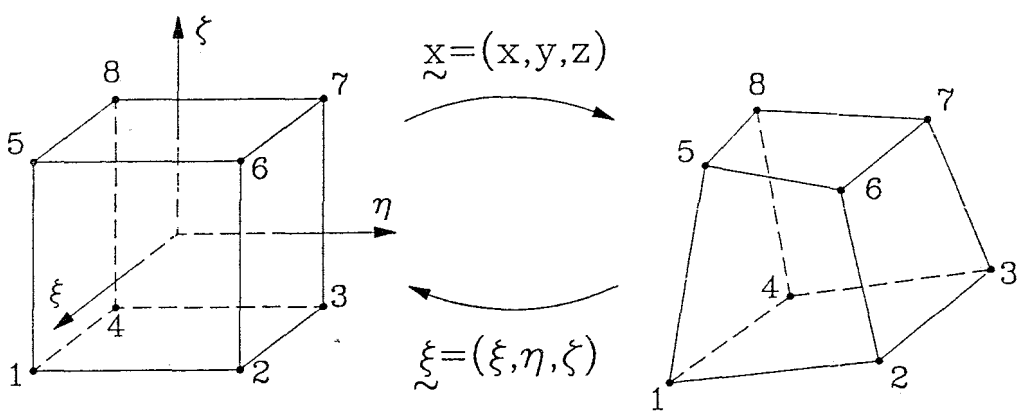

Figure C.1: *Parent domain*

The domain of an arbitrary trilinear hexahedral element in the $\{\vec{e}_x, \vec{e}_y, \vec{e}_z\}$-space is given by Ω^e. The domain Ω^e is the image of the parent domain in $\underset{\sim}{\xi}$-space under the trilinear mapping:

$$x(\underset{\sim}{\xi}) = \alpha_0 + \alpha_1\xi + \alpha_2\eta + \alpha_3\zeta + \alpha_4\xi\eta + \alpha_5\eta\zeta + \alpha_6\xi\zeta + \alpha_7\xi\eta\zeta \qquad \text{(C.1)}$$

i	ξ	η	ζ
1	1	-1	-1
2	1	1	-1
3	-1	1	-1
4	-1	-1	-1
5	1	-1	1
6	1	1	1
7	-1	1	1
8	-1	-1	1

Table C.1: *Coordinates of nodal points in* $\underset{\sim}{\xi}$ *-space*

with corresponding expressions for $y(\underset{\sim}{\xi})$ and $z(\underset{\sim}{\xi})$.
Of course, the nodes in both elements must correspond. So, the coefficients α_0,.....,α_7 have to be determined by the conditions

$$x(\underset{\sim}{\xi}_i) = x_i{}^e$$
$$y(\underset{\sim}{\xi}_i) = y_i{}^e$$
$$z(\underset{\sim}{\xi}_i) = z_i{}^e$$

where $x_i{}^e$ is *the x-coordinate of node i of the element,*
$y_i{}^e$ is *the y-coordinate of node i of the element,*
$z_i{}^e$ is *the z-coordinate of node i of the element.*

With the nodal points defined as in table C.1, this gives rise to a system of linear algebraic equations:

$$\begin{bmatrix} 1 & 1 & -1 & -1 & -1 & 1 & -1 & 1 \\ 1 & 1 & 1 & -1 & 1 & -1 & -1 & -1 \\ 1 & -1 & 1 & -1 & -1 & -1 & 1 & 1 \\ 1 & -1 & -1 & -1 & 1 & 1 & 1 & -1 \\ 1 & 1 & -1 & 1 & -1 & -1 & 1 & -1 \\ 1 & 1 & 1 & 1 & 1 & 1 & 1 & 1 \\ 1 & -1 & 1 & 1 & -1 & 1 & -1 & -1 \\ 1 & -1 & -1 & 1 & 1 & -1 & -1 & 1 \end{bmatrix} \begin{bmatrix} \alpha_0 \\ \alpha_1 \\ \alpha_2 \\ \alpha_3 \\ \alpha_4 \\ \alpha_5 \\ \alpha_6 \\ \alpha_7 \end{bmatrix} = \begin{bmatrix} x_1{}^e \\ x_2{}^e \\ x_3{}^e \\ x_4{}^e \\ x_5{}^e \\ x_6{}^e \\ x_7{}^e \\ x_8{}^e \end{bmatrix}$$

Solving the matrix equation for the α's and substitution of this solution in equation (C.1) gives

$$x(\underset{\sim}{\xi}) = \sum_{i=1}^{8} \varphi_i(\underset{\sim}{\xi}) x_i{}^e \tag{C.2}$$

where

$$\varphi_i(\xi, \eta, \zeta) = \frac{1}{8}(1 + \xi_i\xi)(1 + \eta_i\eta)(1 + \zeta_i\zeta) \tag{C.3}$$

See [4] for the derivation of the shape functions. For $y(\underset{\sim}{\xi})$ and $z(\underset{\sim}{\xi})$ similar equations as equation (C.2) are valid.

The shape functions (C.3) are a function of the coordinates in ξ-space. They have to be derivated to x, y and z. These derivatives will be deduced in the rest of this appendix.

The derivatives of the shape functions φ_i are given by

$$\begin{aligned}
\varphi_{i,x} &= \varphi_{i,\xi}\xi_{,x} + \varphi_{i,\eta}\eta_{,x} + \varphi_{i,\zeta}\zeta_{,x} \\
\varphi_{i,y} &= \varphi_{i,\xi}\xi_{,y} + \varphi_{i,\eta}\eta_{,y} + \varphi_{i,\zeta}\zeta_{,y} \\
\varphi_{i,z} &= \varphi_{i,\xi}\xi_{,z} + \varphi_{i,\eta}\eta_{,z} + \varphi_{i,\zeta}\zeta_{,z}
\end{aligned}$$

or, in matrix formulation:

$$\begin{bmatrix} \varphi_{i,x} \\ \varphi_{i,y} \\ \varphi_{i,z} \end{bmatrix} = \begin{bmatrix} \xi_{,x} & \eta_{,x} & \zeta_{,x} \\ \xi_{,y} & \eta_{,y} & \zeta_{,y} \\ \xi_{,z} & \eta_{,z} & \zeta_{,z} \end{bmatrix} \begin{bmatrix} \varphi_{i,\xi} \\ \varphi_{i,\eta} \\ \varphi_{i,\zeta} \end{bmatrix} \tag{C.4}$$

Here some difficulties are encountered: ξ, η and ζ are not known as a function of x, y and z. But the inverse relations exist:

$$\begin{aligned}
x(\underset{\sim}{\xi}) &= \sum_{i=1}^{8} \varphi_i(\underset{\sim}{\xi}) x_i{}^e \\
y(\underset{\sim}{\xi}) &= \sum_{i=1}^{8} \varphi_i(\underset{\sim}{\xi}) y_i{}^e \\
z(\underset{\sim}{\xi}) &= \sum_{i=1}^{8} \varphi_i(\underset{\sim}{\xi}) z_i{}^e
\end{aligned}$$

and the matrix $\underset{\sim}{x}_{,\underset{\sim}{\xi}}$, containing the ξ-, η- and ζ-derivatives of x, y and z can be determined:

$$\underset{\sim}{x}_{,\underset{\sim}{\xi}} = \begin{bmatrix} x_{,\xi} & x_{,\eta} & x_{,\zeta} \\ y_{,\xi} & y_{,\eta} & y_{,\zeta} \\ z_{,\xi} & z_{,\eta} & z_{,\zeta} \end{bmatrix}$$

with

$$
\begin{aligned}
x_{,\xi} &= \sum_{i=1}^{8} \varphi_{i,\xi} {x_i}^e \\
x_{,\eta} &= \sum_{i=1}^{8} \varphi_{i,\eta} {x_i}^e \\
x_{,\zeta} &= \sum_{i=1}^{8} \varphi_{i,\zeta} {x_i}^e
\end{aligned}
$$

Corresponding expressions for the derivatives of y and z are valid.
Now, the matrix $\underset{\sim}{\xi}_{,\underset{\sim}{x}}$,which is called the Jacobian matrix, can be computed by inverting matrix $\underset{\sim}{x}_{\underset{\sim}{\xi}}$:

$$
\underset{\sim}{\xi}_{,\underset{\sim}{x}} = \begin{bmatrix} \xi_{,x} & \xi_{,y} & \xi_{,z} \\ \eta_{,x} & \eta_{,y} & \eta_{,z} \\ \zeta_{,x} & \zeta_{,y} & \zeta_{,z} \end{bmatrix} = (\underset{\sim}{x}_{,\underset{\sim}{\xi}})^{-1} \tag{C.5}
$$

The array $\varphi_{i,\underset{\sim}{\xi}}$ in equation (C.4) can be obtained by differentiating the shape functions (C.3). This yields:

$$
\begin{aligned}
\varphi_{i,\xi} &= \frac{1}{8}\xi_i(1+\eta_i\eta)(1+\zeta_i\zeta) \\
\varphi_{i,\eta} &= \frac{1}{8}\eta_i(1+\xi_i\xi)(1+\zeta_i\zeta) \\
\varphi_{i,\zeta} &= \frac{1}{8}\zeta_i(1+\xi_i\xi)(1+\eta_i\eta)
\end{aligned}
$$

Substitution of (C.5) in (C.4) yields

$$
\varphi_{i,\underset{\sim}{x}} = (\underset{\sim}{x}_{,\underset{\sim}{\xi}})^{-T} \varphi_{i,\underset{\sim}{\xi}} \tag{C.6}
$$

Appendix D

Bilinear quadrilateral boundary element

In this appendix the shape functions of an arbitrary bilinear quadrilateral boundary element will be obtained. For that purpose, a change of coordinates is sought which maps the quadrilateral into a bi-unit square in a two-dimensional plane (see figure D.1). In this plane, there are two independent coordinates ξ and η. The bi-unit square is called the parent domain of the bilinear quadrilateral boundary element.

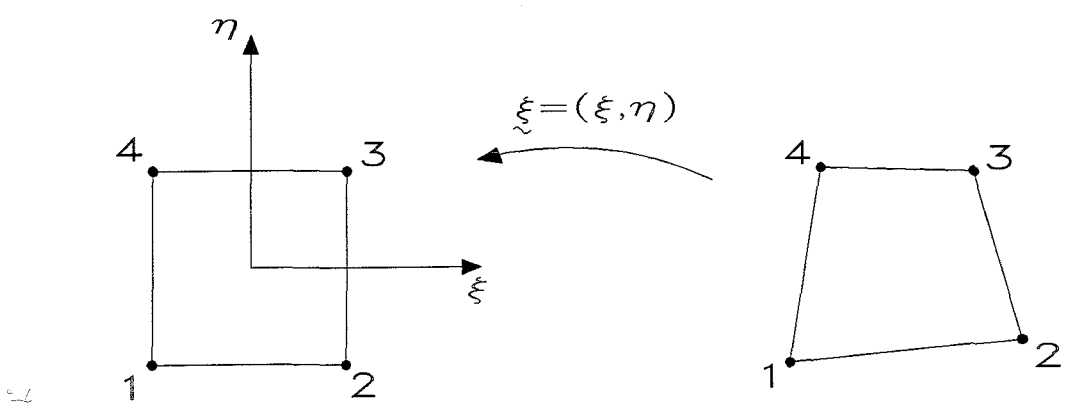

Figure D.1: *Quadrilateral element and its parent domain*

The coordinates ξ and η of a point in the bi-unit square are related to the coordinates x, y and z of a point in the quadrilateral boundary element. This mapping can be formulated by two different equations.

i	ξ_i	η_i
1	-1	-1
2	1	-1
3	1	1
4	-1	1

Table D.1: *Coordinates of nodal points in $\mathbb{R}^2$-space*

The first relation is of the form as given in the following equations.

$$x(\xi,\eta) = \sum_{i=1}^{4} \chi_i(\xi,\eta)\, x_i^e \tag{D.1}$$

$$y(\xi,\eta) = \sum_{i=1}^{4} \chi_i(\xi,\eta)\, y_i^e \tag{D.2}$$

$$z(\xi,\eta) = \sum_{i=1}^{4} \chi_i(\xi,\eta)\, z_i^e \tag{D.3}$$

where χ_i is *the shape function belonging to node i,*
x_i^e is *the x-coordinate of node i,*
y_i^e is *the y-coordinate of node i,*
z_i^e is *the z-coordinate of node i.*

The other relation between the coordinates x, y and z on the one hand and the natural coordinates ξ and η on the other is given by a bilinear mapping:

$$x(\xi,\eta) = \alpha_0 + \alpha_1\,\xi + \alpha_2\,\eta + \alpha_3\,\xi\eta \tag{D.4}$$

$$y(\xi,\eta) = \beta_0 + \beta_1\,\xi + \beta_2\,\eta + \beta_3\,\xi\eta \tag{D.5}$$

$$z(\xi,\eta) = \gamma_0 + \gamma_1\,\xi + \gamma_2\,\eta + \gamma_3\,\xi\eta \tag{D.6}$$

The parameters α's, β's and γ's can be determined by stipulating that equations (D.4), (D.5) and (D.6) must satisfy the conditions

$$x(\xi_i,\eta_i) = x_i^e \tag{D.7}$$

$$y(\xi_i,\eta_i) = y_i^e \tag{D.8}$$

$$z(\xi_i,\eta_i) = z_i^e \tag{D.9}$$

With the nodal points in the $\mathbb{R}^2$-plane defined as in table D.1, condition (D.7) gives rise to the following matrix equation for the x-coordinates of the nodal points

of the bilinear quadrilateral boundary element.

$$\begin{bmatrix} x_1^e \\ x_2^e \\ x_3^e \\ x_4^e \end{bmatrix} = \begin{bmatrix} 1 & -1 & -1 & 1 \\ 1 & 1 & -1 & -1 \\ 1 & 1 & 1 & 1 \\ 1 & 1 & 1 & -1 \end{bmatrix} \begin{bmatrix} \alpha_0 \\ \alpha_1 \\ \alpha_2 \\ \alpha_3 \end{bmatrix} \tag{D.10}$$

The second and third condition lead to corresponding expressions for the y- and z-coordinates of the nodes. In each case the coefficient matrix is the same.

Solving the matrix equation for the α's and substitution of the solution in equation (D.4) produces the shape function χ_i.

$$\chi_i(\xi, \eta) = \frac{1}{4}(1 + \xi_i \xi)(1 + \eta_i \eta) \tag{D.11}$$

Appendix E

Projection of vector $\vec{x}$ on the axis of the capstan

The axis of the capstan can be represented by

$$\vec{x}_a = \vec{\alpha} + \lambda \vec{\beta} \qquad (\lambda \in \mathbb{R}) \tag{E.1}$$

Or, in matrix formulation:

$$\begin{bmatrix} x_a \\ y_a \\ z_a \end{bmatrix} = \begin{bmatrix} \alpha_1 \\ \alpha_2 \\ \alpha_3 \end{bmatrix} + \lambda \begin{bmatrix} \beta_1 \\ \beta_2 \\ \beta_3 \end{bmatrix} \tag{E.2}$$

The support vector $\vec{\alpha}$ and the direction vector $\vec{\beta}$ are known.

To every vector $\vec{x}$ of the pinch roller coating belongs one projection vector $\vec{x}_c$ on the axis of the capstan. So, $\vec{x}_c$ can be written as a function of $\vec{x}$, which will be done in this appendix.

The end point of projection $\vec{x}_c$ is situated in the plane through the end point of vector $\vec{x}$ and perpendicular to the axis. This plane is defined by the following equation:

$$\beta_1 x_{plane} + \beta_2 y_{plane} + \beta_3 z_{plane} = \beta_1 x + \beta_2 y + \beta_3 z$$

where x_{plane} is *the x-coordinate of a point in the plane,*
y_{plane} is *the y-coordinate of a point in the plane,*
z_{plane} is *the z-coordinate of a point in the plane.*

Substitution of the x-, y- and z-coordinates of point $\vec{x}_c$, given by equation (E.2), yields

$$\beta_1 (\alpha_1 + \lambda \beta_1) + \beta_2 (\alpha_2 + \lambda \beta_2) + \beta_3 (\alpha_3 + \lambda \beta_3) = \beta_1 x + \beta_2 y + \beta_3 z$$

Solving this equation for λ yields

$$\begin{aligned} \lambda &= \frac{\beta_1 (x - \alpha_1) + \beta_2 (y - \alpha_2) + \beta_3 (z - \alpha_3)}{{\beta_1}^2 + {\beta_2}^2 + {\beta_3}^2} \\ &= \frac{\vec{\beta} \cdot (\vec{x} - \vec{\alpha})}{|\vec{\beta}|^2} \end{aligned} \tag{E.3}$$

Substitution of equation (E.3) in equation (E.1) gives $\vec{x}_c$ as a function of $\vec{x}$:

$$\vec{x}_c = \frac{\vec{\beta}\vec{\beta}}{|\vec{\beta}|^2} \cdot \vec{x} + (\mathbf{I} - \frac{\vec{\beta}\vec{\beta}}{|\vec{\beta}|^2}) \cdot \vec{\alpha} \tag{E.4}$$

Appendix F

Program structure

The system of equations that has to be solved, contains terms with estimates for the position $\vec{x}$, the pressure like quantity p and for quantities, dependent on $\vec{x}$ and p. The system of equations is solved iteratively. This iteration process is clearly shown in figures F.1 and F.2. Having solved the system, the estimates are updated. And after substitution of these updated estimates, the system is solved again and if the solution converges, a better solution is obtained. This is repeated as many times as necessary to get a solution, which satisfies the required accuracy demand.

Both the system matrix and the right hand side contain estimations. Consequently, both have to be changed every iteration.

If an accurate solution has been obtained, the program continues with the next time step. The solution of the previous time step will be used as first estimate for the new time step.

The assembly of the global stiffness matrix and of the global right hand side is done by the SEPRAN package. SEPRAN creates for every element the element stiffness matrix and the element right hand side and puts every component of the element stiffness matrix and the element right hand side on the right place in the global stiffness matrix and global right hand side. Difference is made between body elements and boundary elements.

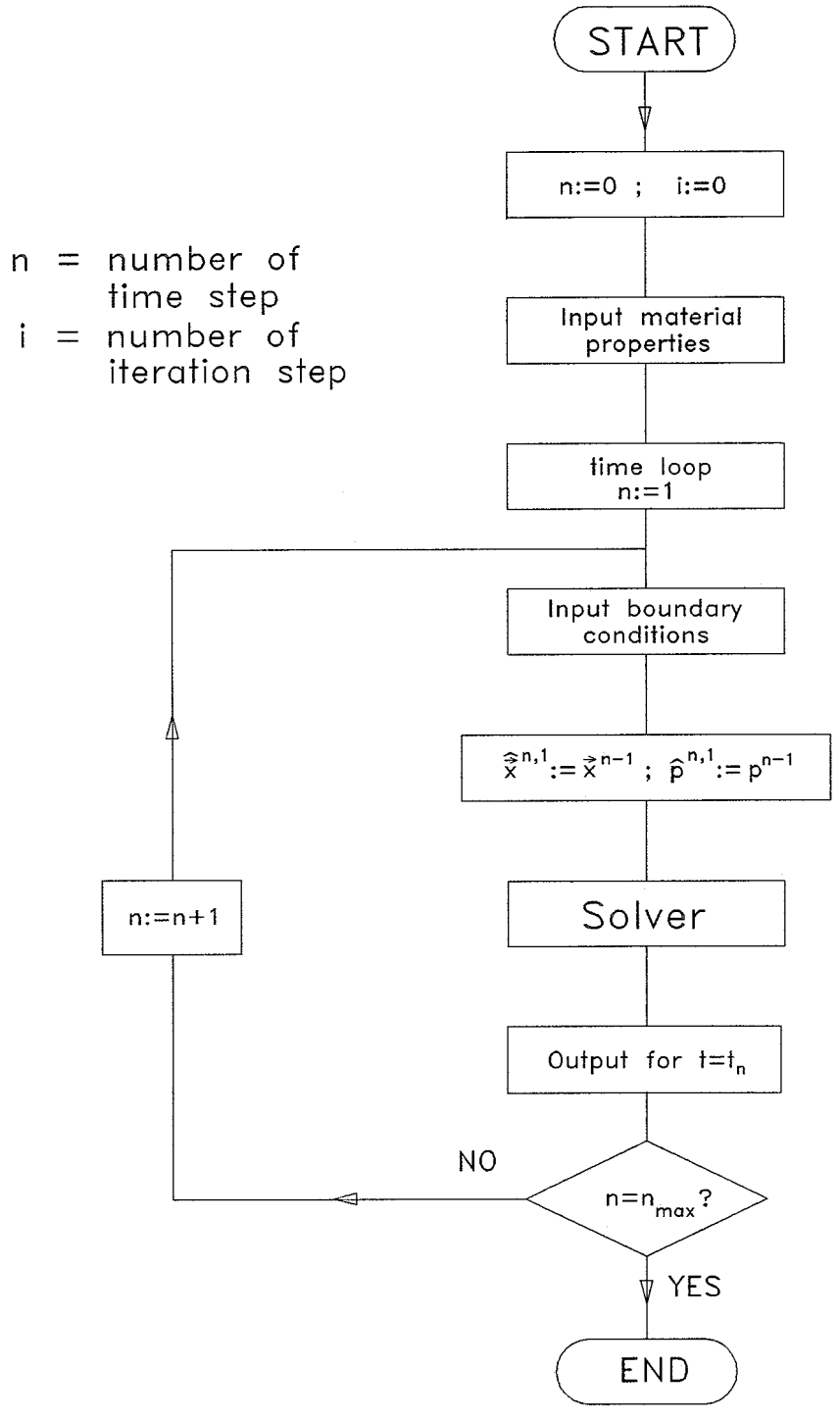

Figure F.1: *Program structure*

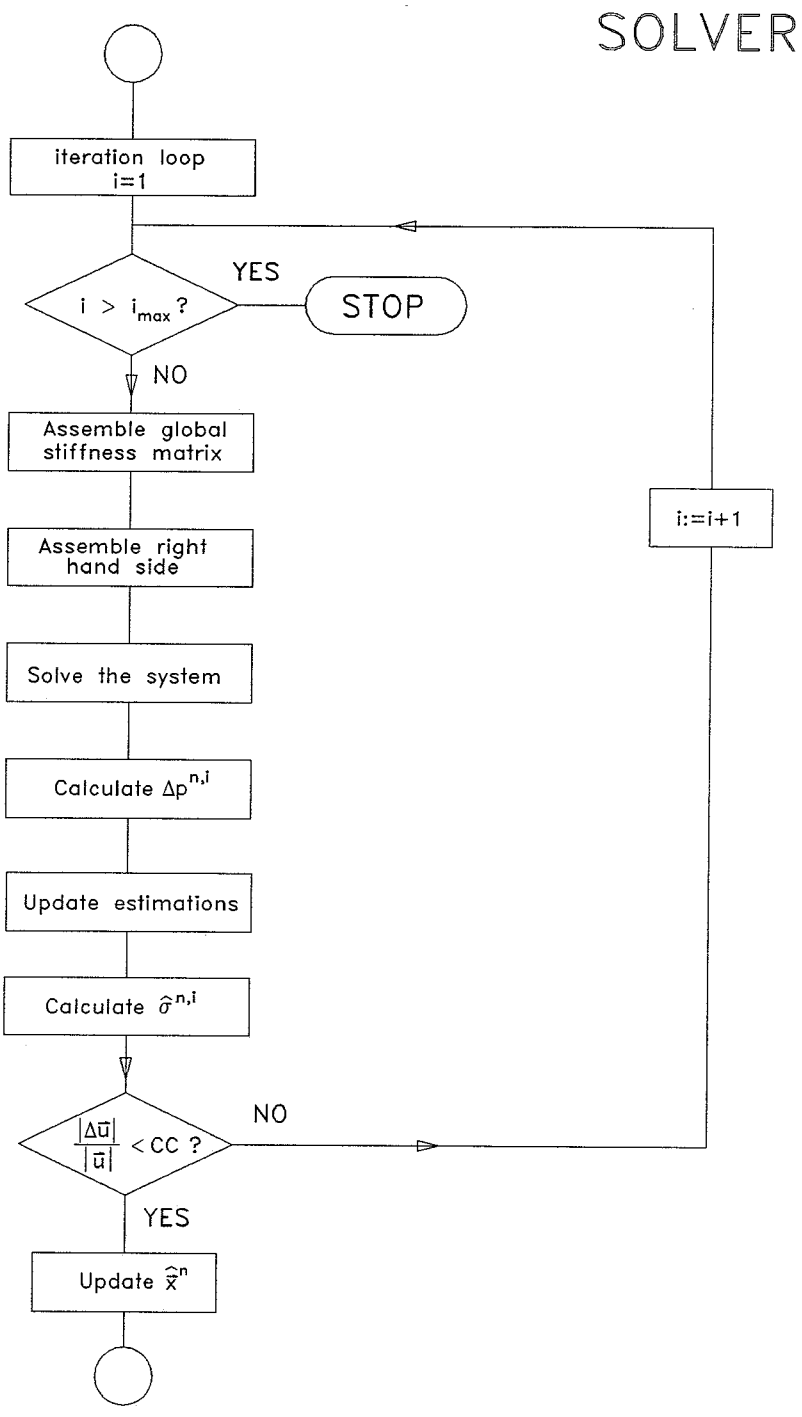

Figure F.2: *Iteration loop*

Appendix G

Test for frictionless contact

In this appendix the data and the results of the test for frictionless contact are given.

G.1 Test data

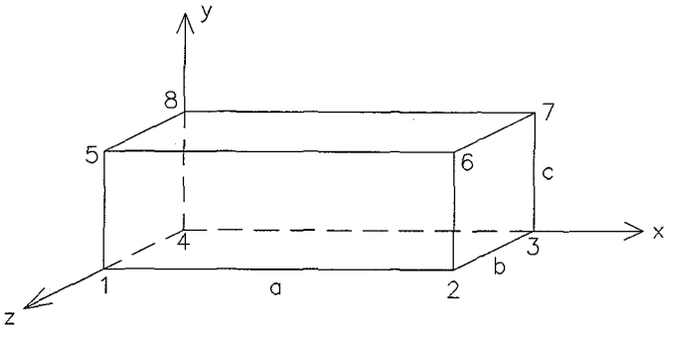

Figure G.1: *Undeformed geometry*

Geometry:

$a = 7.0$

$b = 4.0$

$c = 1.75$

Number of elements : 14 x 4 x 6 (see figure G.2)

Prescribed displacements:

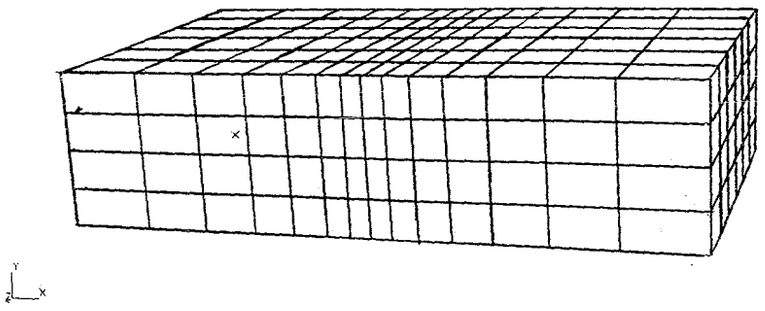

Figure G.2: *Element mesh*

Surface(1,2,3,4)	$u^x = 0 \quad u^y = 0 \quad u^z = 0$
Surface(5,6,7,8)	candidate contact surface

Capstan:

Radius:	2.0
Displacement per time step:	$dy = -0.1$
Number of time steps:	5

Material parameter: $c = 1$

Penalty parameters:

$$1E-15 < \epsilon_1 < 1E-1$$
$$1E-15 < \epsilon_2 < 1E-2$$

Axis of capstan in the different test cases:

1. $\begin{bmatrix} 3.5 \\ 3.75 \\ 0.0 \end{bmatrix} + \lambda \begin{bmatrix} 0.0 \\ 0.0 \\ 1.0 \end{bmatrix}$
2. $\begin{bmatrix} 3.5 \\ 3.75 \\ 0.5 \end{bmatrix} + \lambda \begin{bmatrix} 0.2 \\ 0.0 \\ 1.0 \end{bmatrix}$
3. $\begin{bmatrix} 3.5 \\ 3.75 \\ 4.0 \end{bmatrix} + \lambda \begin{bmatrix} 0.0 \\ -0.2 \\ 1.0 \end{bmatrix}$

G.2 Results

G.2.1 Test case 1

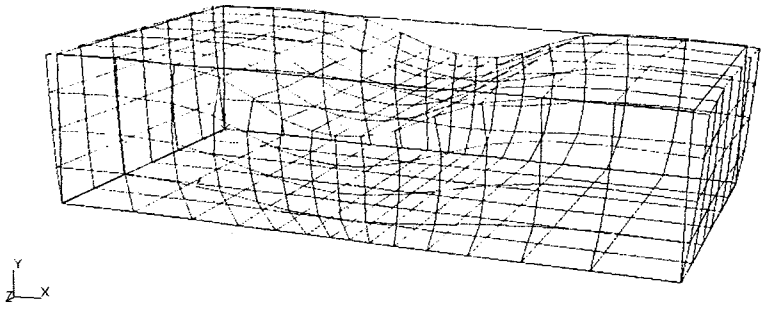

Figure G.3: *Deformed geometry calculated by SEPRAN*

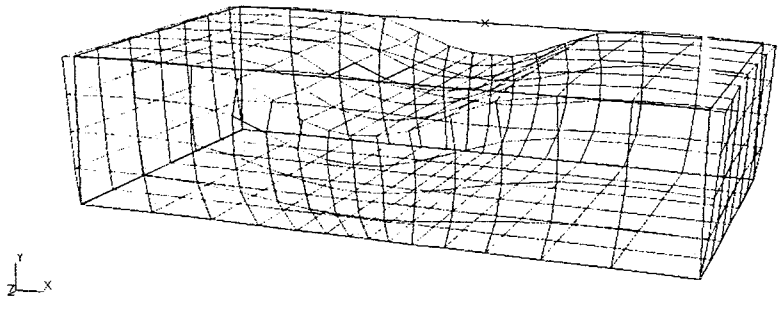

Figure G.4: *Deformed geometry calculated by MARC*

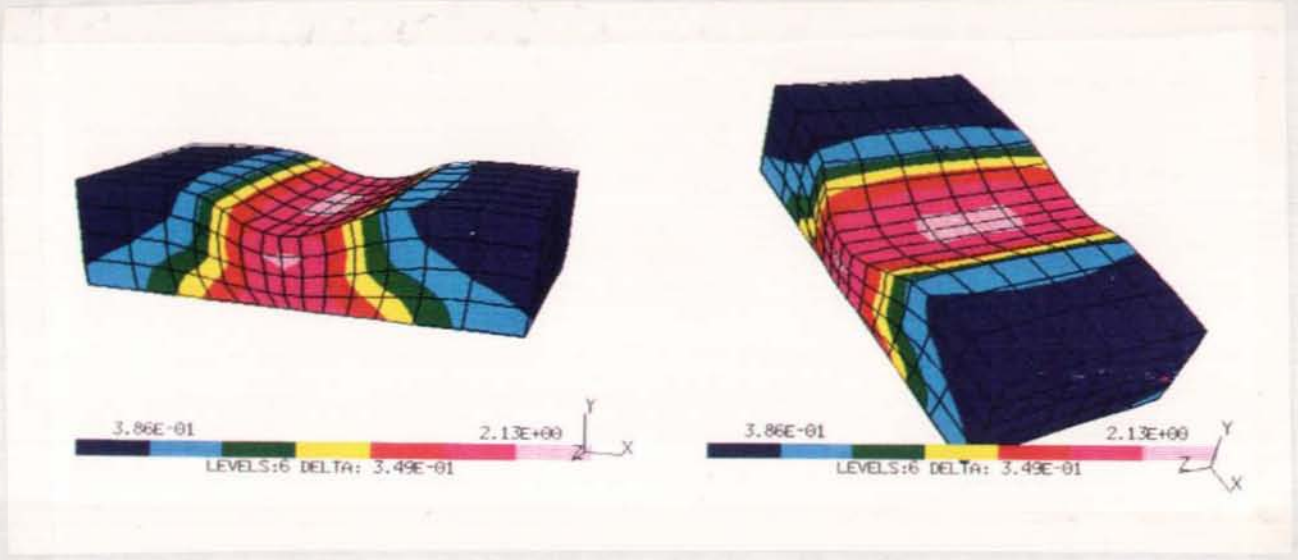

Figure G.5: *Von Mises stress calculated by SEPRAN*

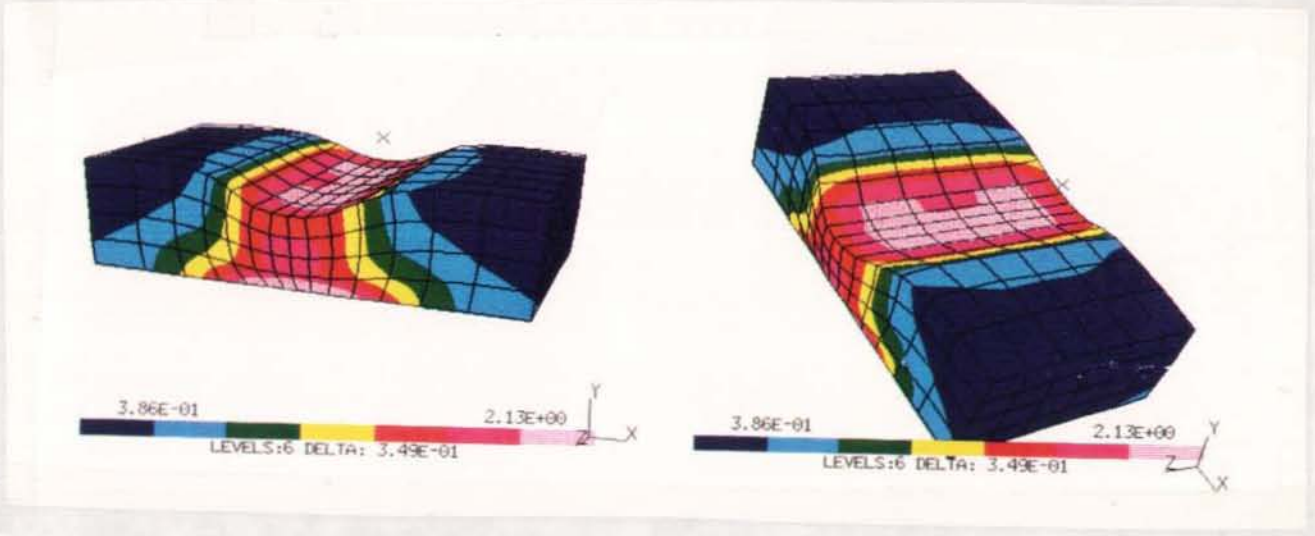

Figure G.6: *Von Mises stress calculated by MARC*

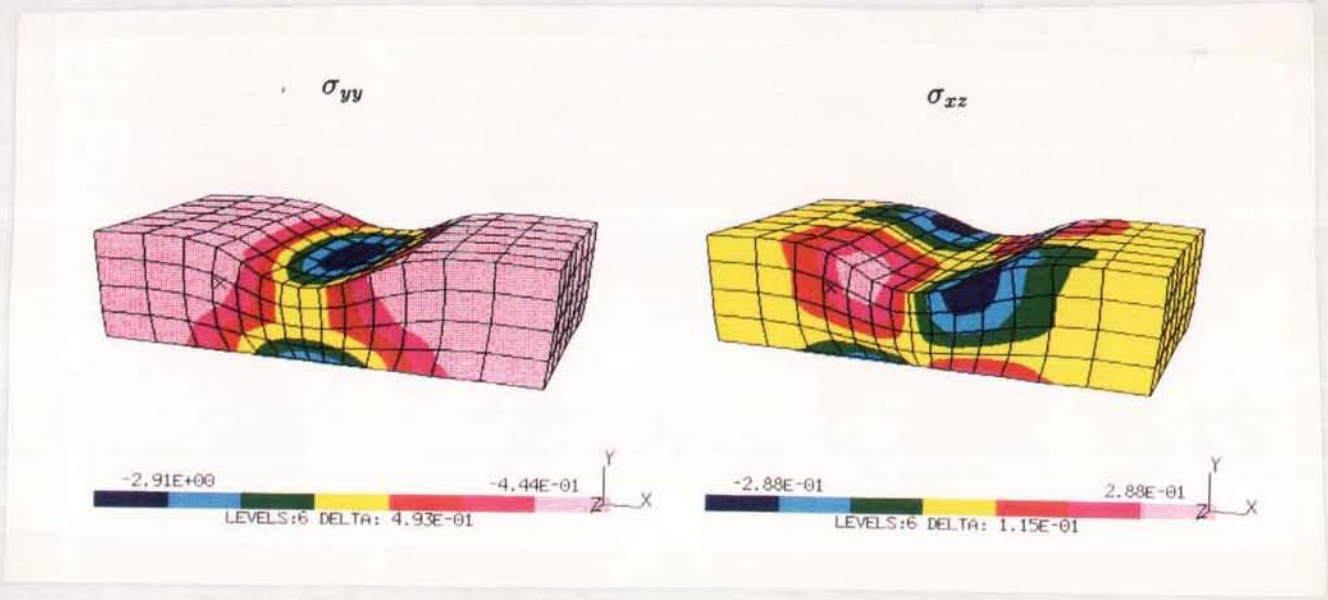

Figure G.7: *Stress component σ_{yy} and σ_{xz} calculated by SEPRAN*

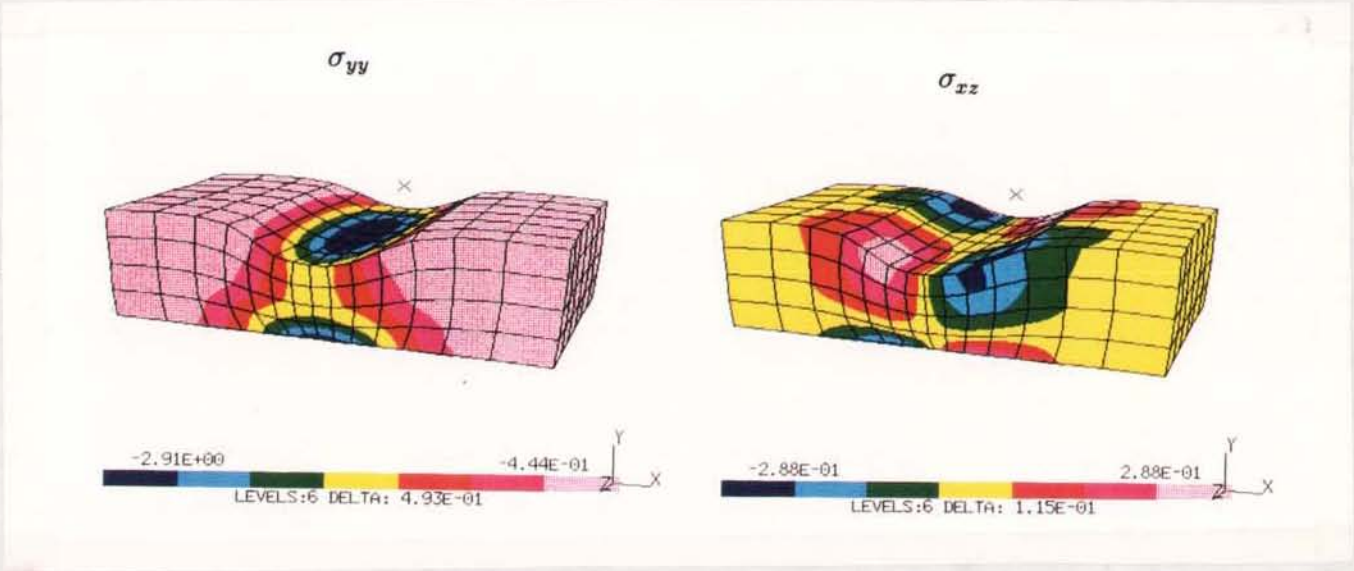

Figure G.8: *Stress component σ_{yy} and σ_{xz} calculated by MARC*

G.2.2 Test case 2

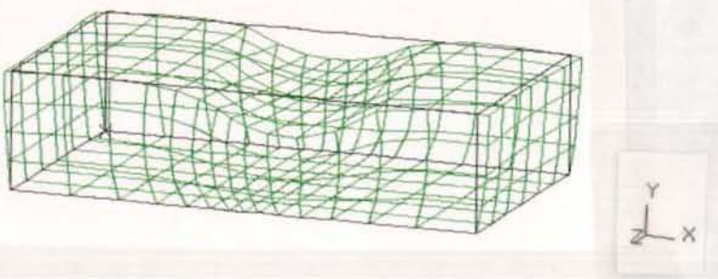

Figure G.9: *Deformed geometry*

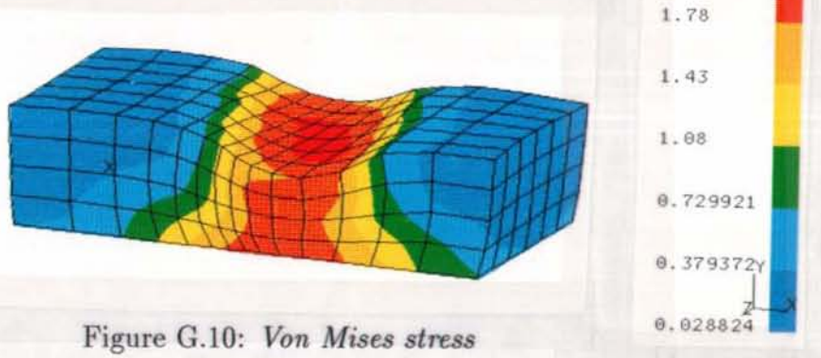

Figure G.10: *Von Mises stress*

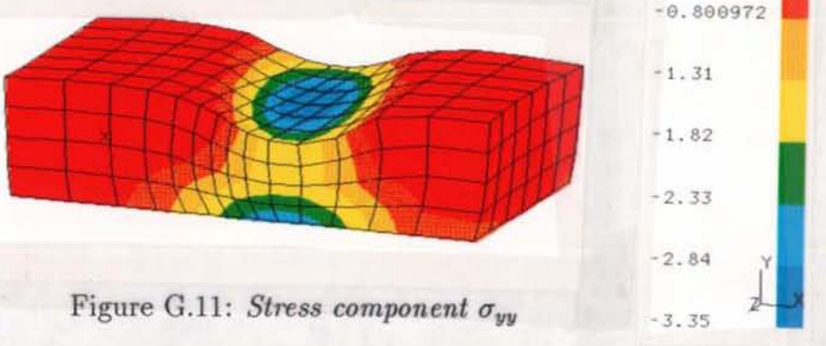

Figure G.11: *Stress component* σ_{yy}

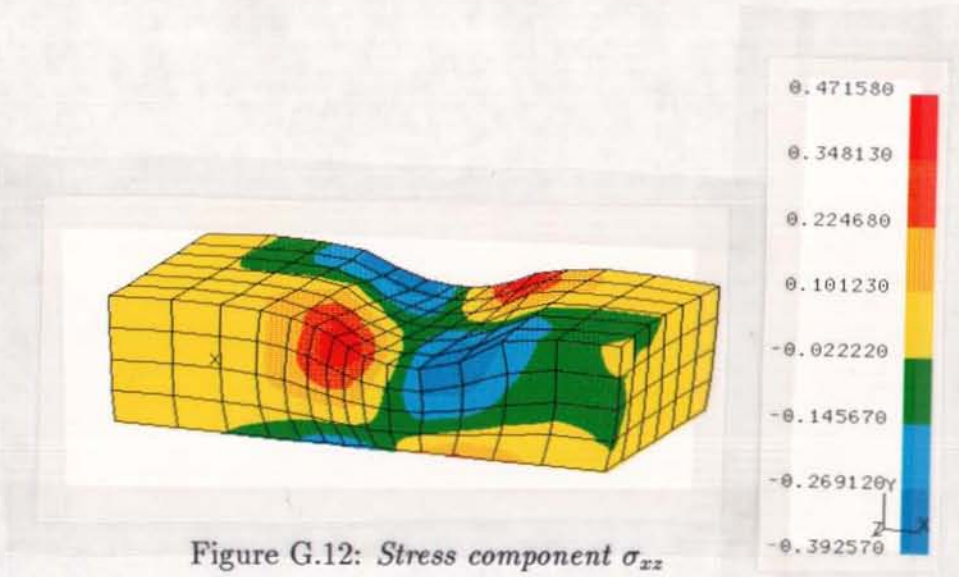

Figure G.12: *Stress component* σ_{xz}

G.2.3 Test case 3

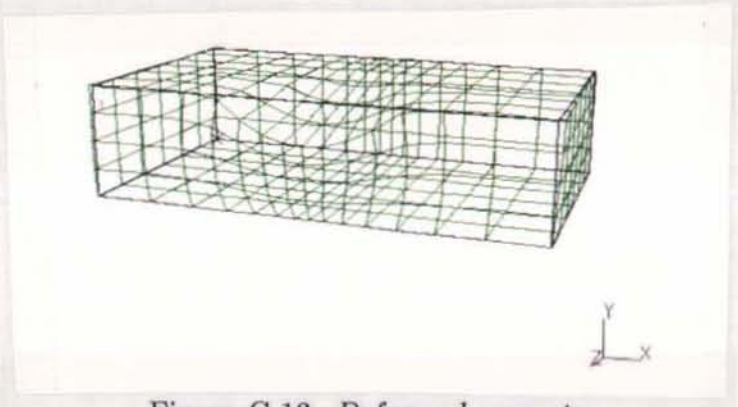

Figure G.13: *Deformed geometry*

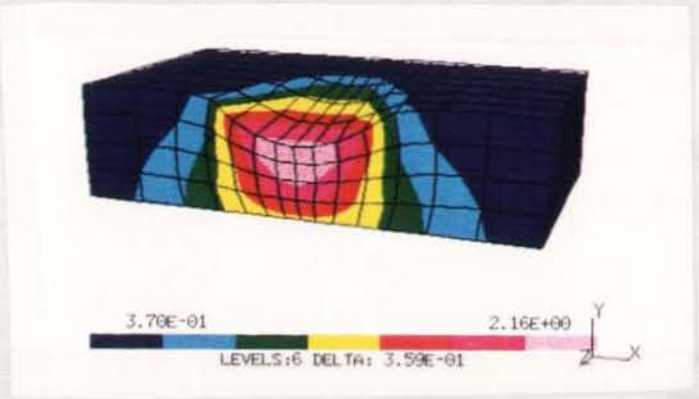

Figure G.14: *Von Mises stress*

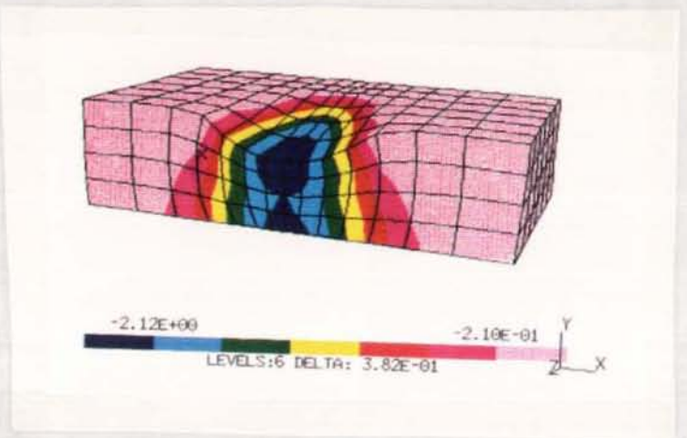

Figure G.15: *Stress component* σ_{yy}

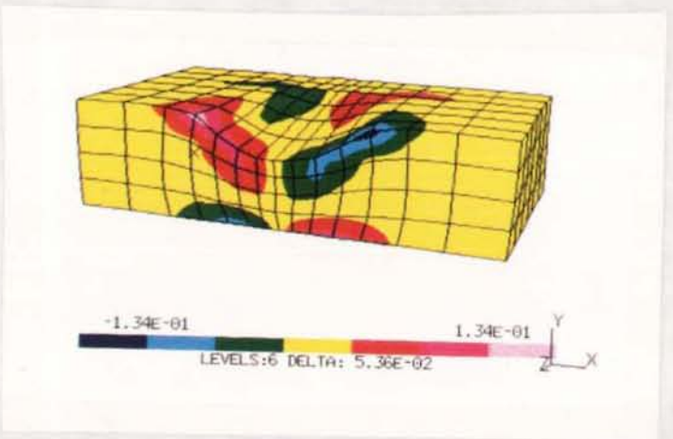

Figure G.16: *Stress component* σ_{xz}

Appendix H

Test for rolling contact

In this appendix the data and the results of the test for rolling contact are given.

H.1 Test data

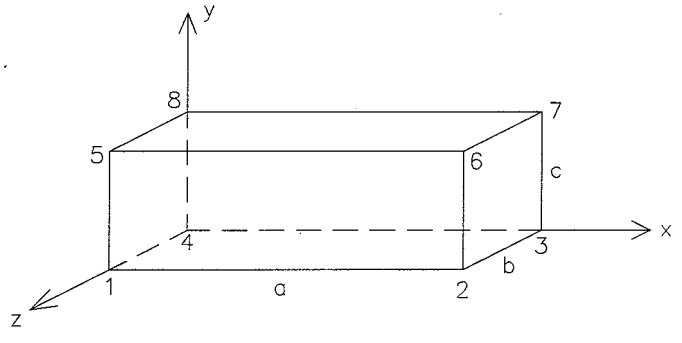

Figure H.1: *Undeformed geometry*

Geometry:

$a = 7.0$

$b = 1.0$

$c = 1.75$

Number of elements : 20 x 2 x 1 (see figure H.2)

Prescribed displacements:

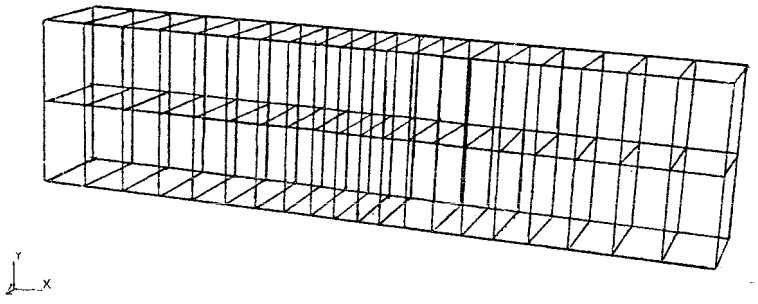

Figure H.2: *Element mesh*

Surface(1,2,3,4)	$u^x = 0 \quad u^y = 0 \quad u^z = 0$
Surface(5,6,7,8)	candidate contact surface

Capstan:

Axis:	$\begin{bmatrix} 3.5 \\ 3.575 \\ 0.0 \end{bmatrix} + \lambda \begin{bmatrix} 0.0 \\ 0.0 \\ 1.0 \end{bmatrix}$
Radius:	2.0
Rotation velocity:	12.5 rad/s

Material parameter: $c = 1$

Time:

Number of time steps:	4
Time step:	$dt = 0.02$

H.1.1 Test case 1

Prescribed boundary forces:

Surface(1,4,5,8)	$f^x = k\,(x - x_0) \quad ; \quad k = 1$
Surface(5,6,7,8)	regularized Coulomb friction 1

Friction coefficient: $\mu = 0.1$

Penalty parameters:

$$\begin{aligned} \epsilon_1 &= 1E-3 \\ \epsilon_2 &= 1E-3 \end{aligned}$$

Regularization parameter: $\epsilon_3 = 1E-3$

H.1.2 Test case 2

Prescribed boundary forces:

Surface(1,4,5,8)	$f^x = k\,(x - x_0) \quad ; \quad k = 1$
Surface(5,6,7,8)	regularized Coulomb friction 2

Regularization parameter: $\epsilon_4 = 1E-3$

Other test data: see test case 1.

H.1.3 Test case 3

Regularization parameter: $1E-15 \leq \epsilon_3 \leq 1E0$

Other test data: see test case 1.

H.1.4 Test case 4

Prescribed boundary forces:

Surface(1,4,5,8)	$f^x = k\,(x - x_0) \quad ; \quad k = 0.1$
Surface(5,6,7,8)	regularized Coulomb friction 1

Penalty parameter: $\epsilon_2 = 3E-2$

Other test data: see test case 1.

H.1.5 Test case 5

Friction coefficient: $\mu = 0.9$

Penalty parameter: $\epsilon_2 = 2E - 1$

Other test data: see test case 1.

H.2 Results

H.2.1 Test case 1, 2 and 3

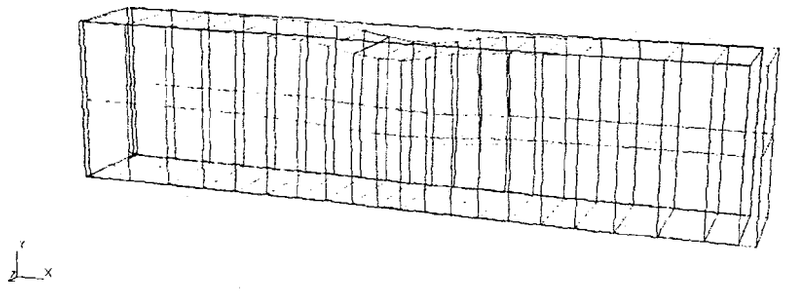

Figure H.3: *Deformed geometry calculated by SEPRAN*

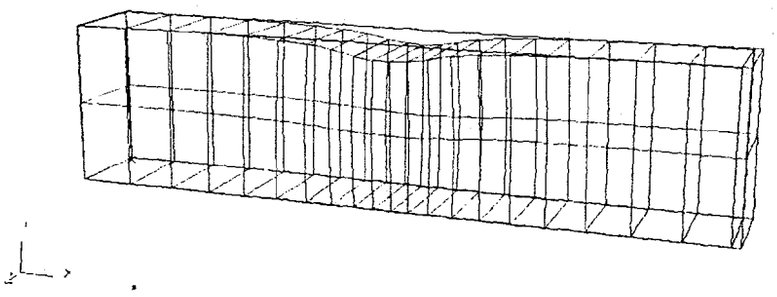

Figure H.4: *Deformed geometry calculated by MARC*

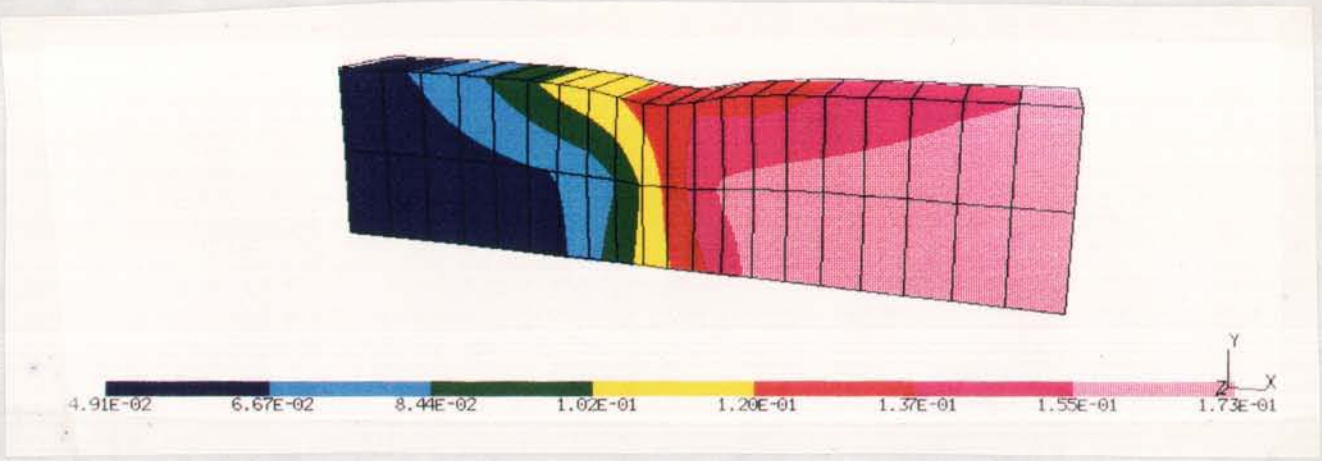

Figure H.5: *Displacement in x-direction calculated by SEPRAN*

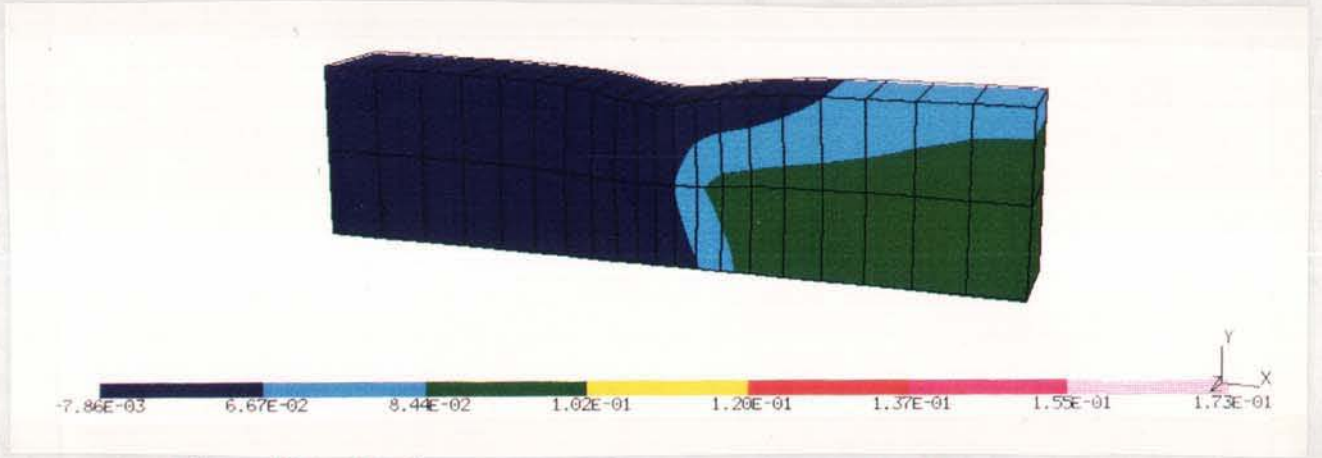

Figure H.6: *Displacement in x-direction calculated by MARC*

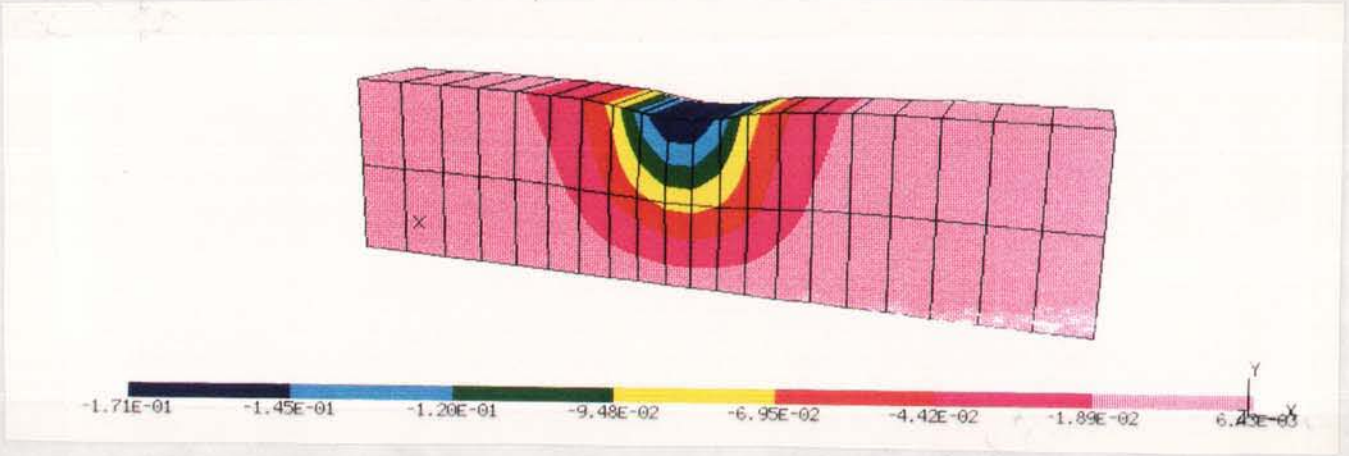

Figure H.7: *Displacement in y-direction calculated by SEPRAN*

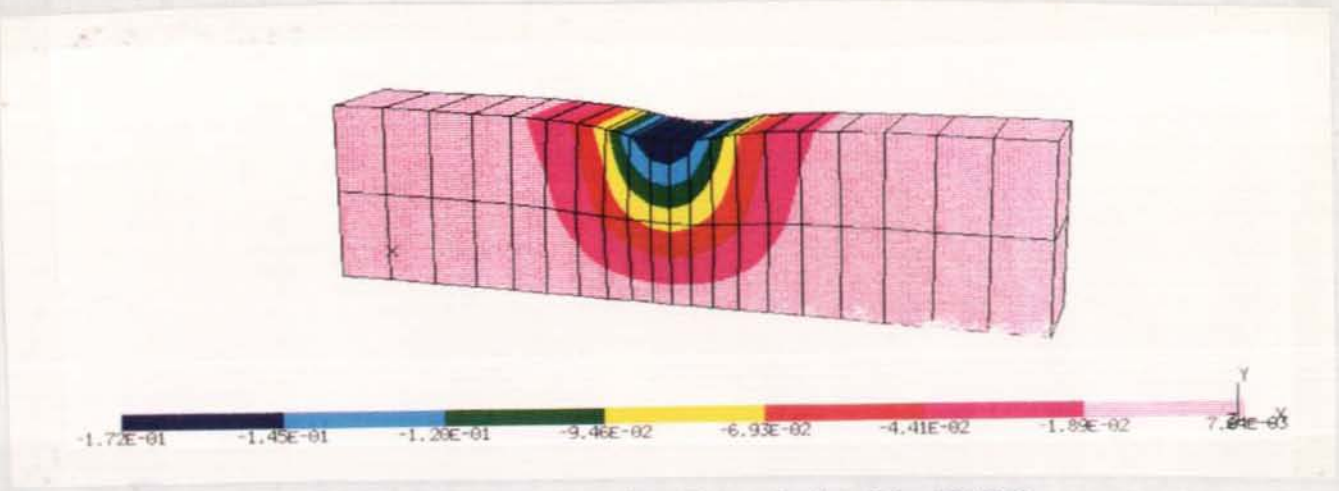

Figure H.8: *Displacement in y-direction calculated by MARC*

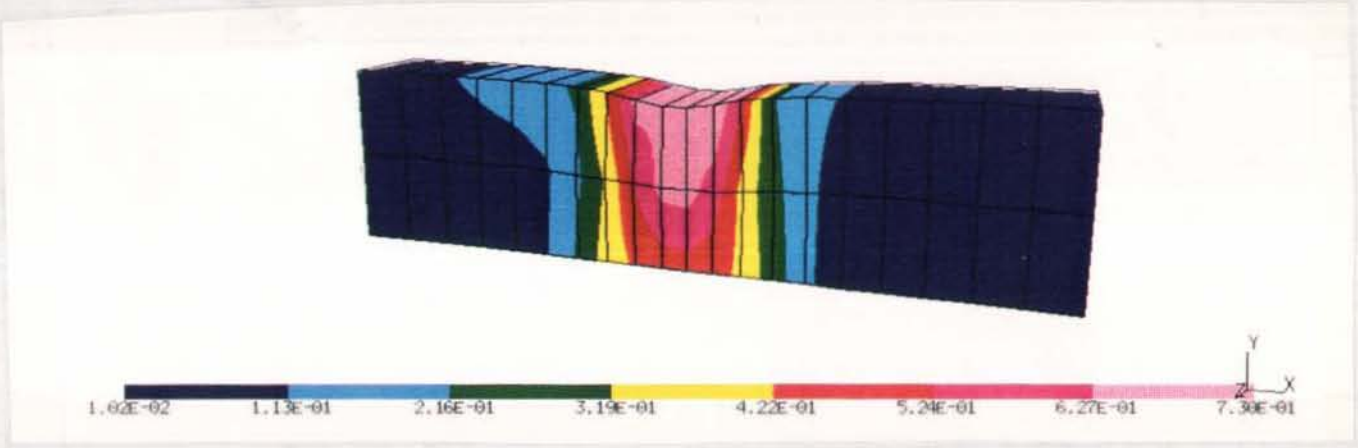

Figure H.9: *Von Mises stress calculated by SEPRAN*

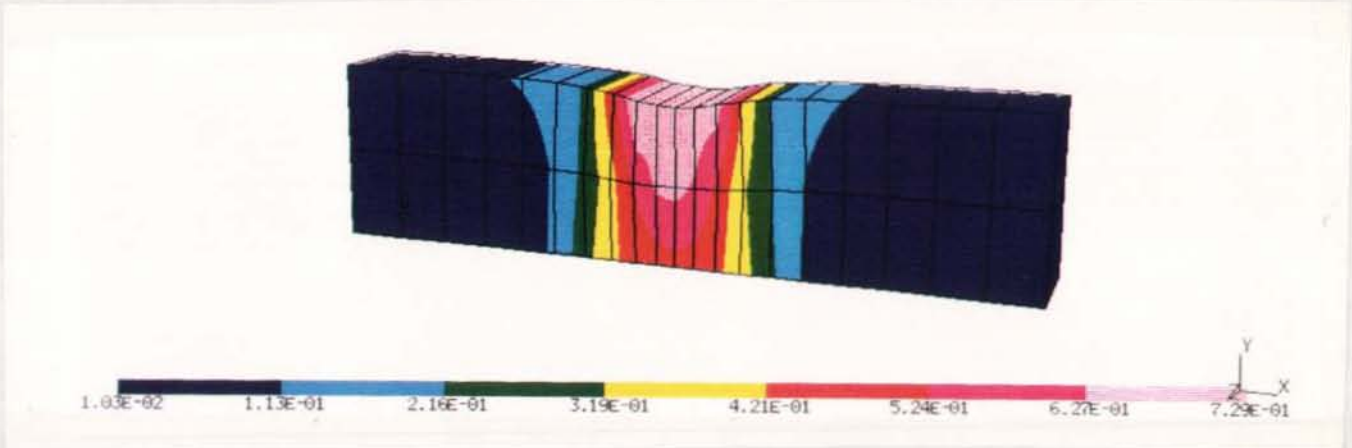

Figure H.10: *Von Mises stress calculated by MARC*

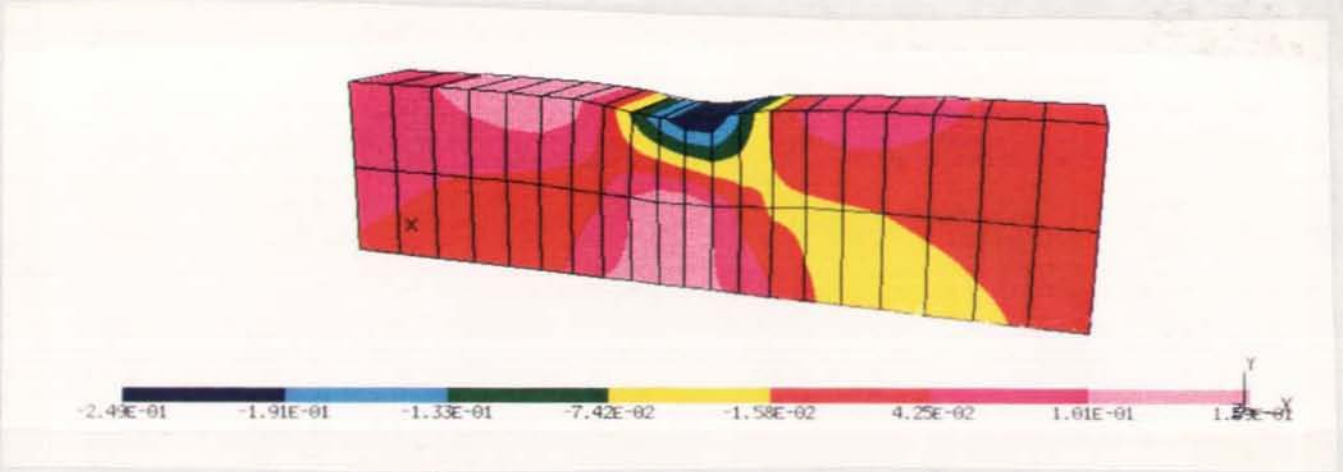

Figure H.11: *Stress component σ_{xx} calculated by SEPRAN*

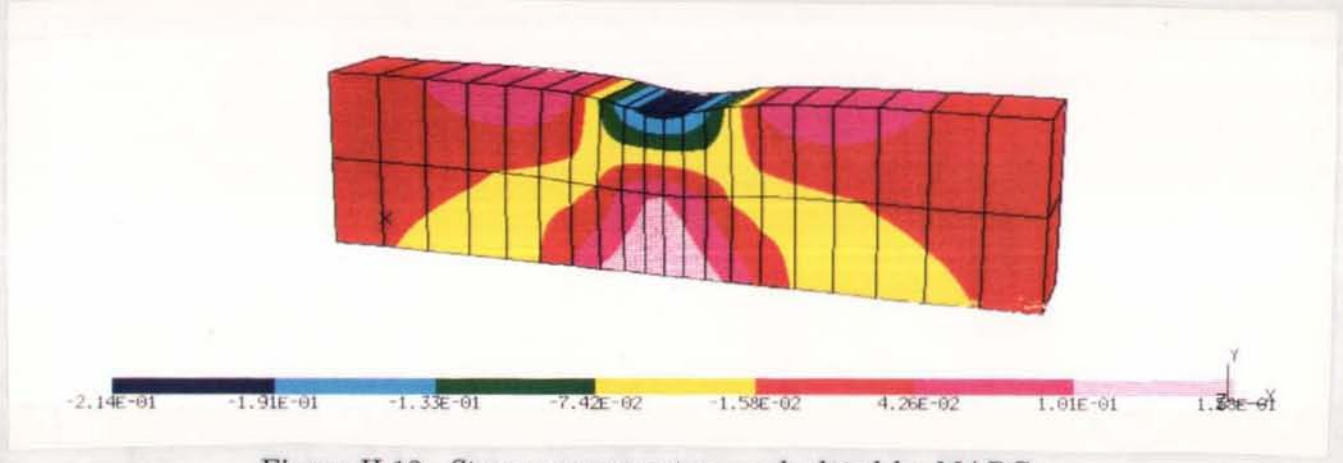

Figure H.12: *Stress component σ_{xx} calculated by MARC*

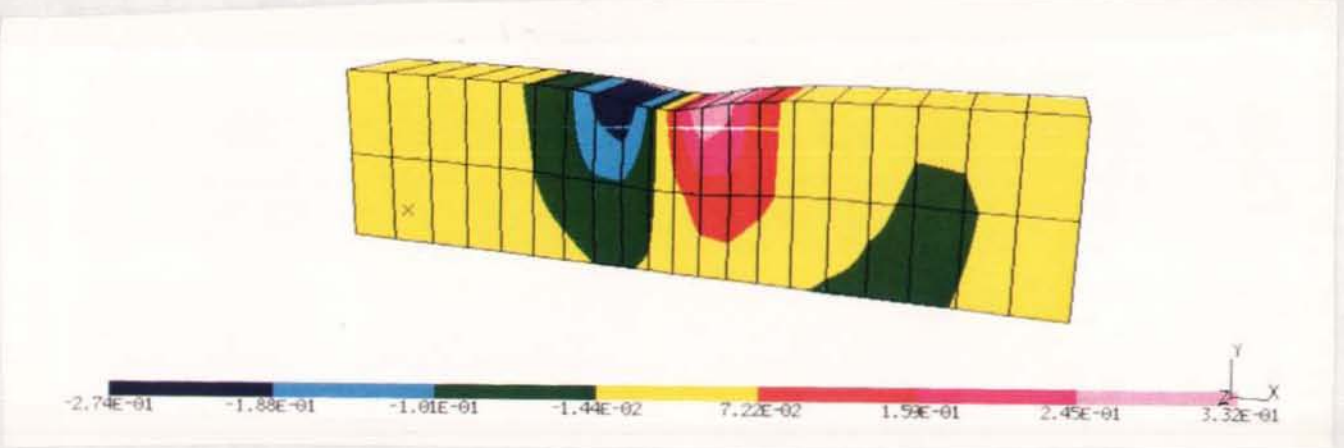

Figure H.13: *Stress component σ_{xy} calculated by SEPRAN*

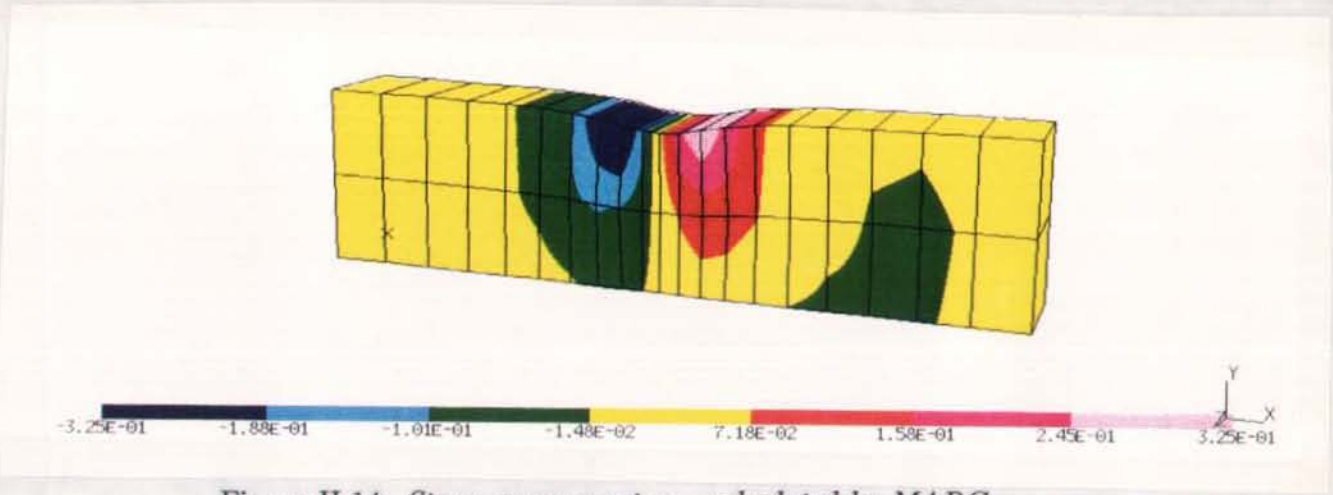

Figure H.14: *Stress component σ_{xy} calculated by MARC*

H.2.2 Test case 4

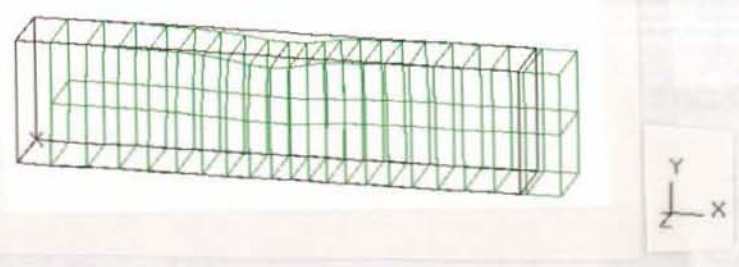

Figure H.15: *Deformed geometry*

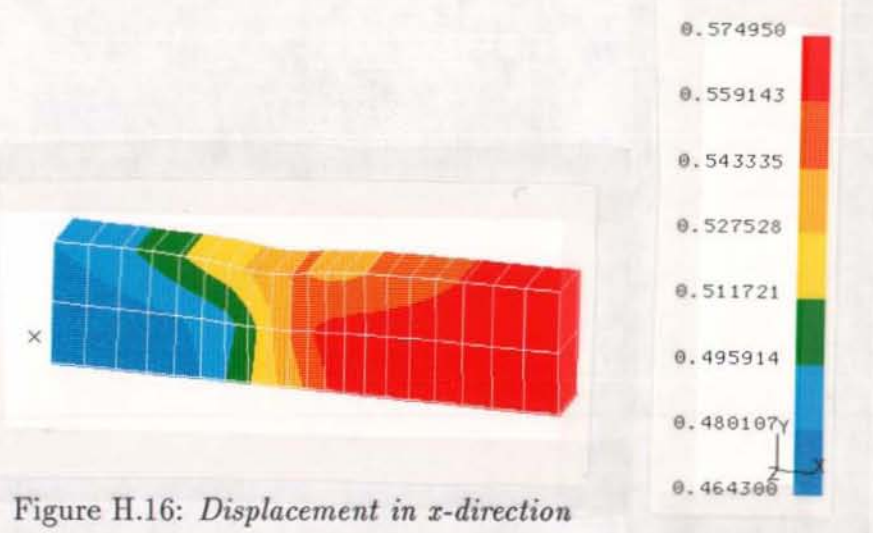

Figure H.16: *Displacement in x-direction*

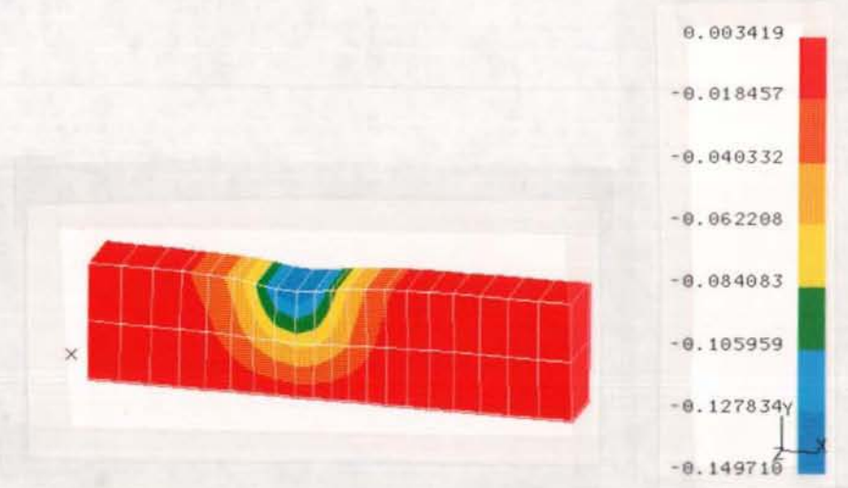

Figure H.17: *Displacement in y-direction*

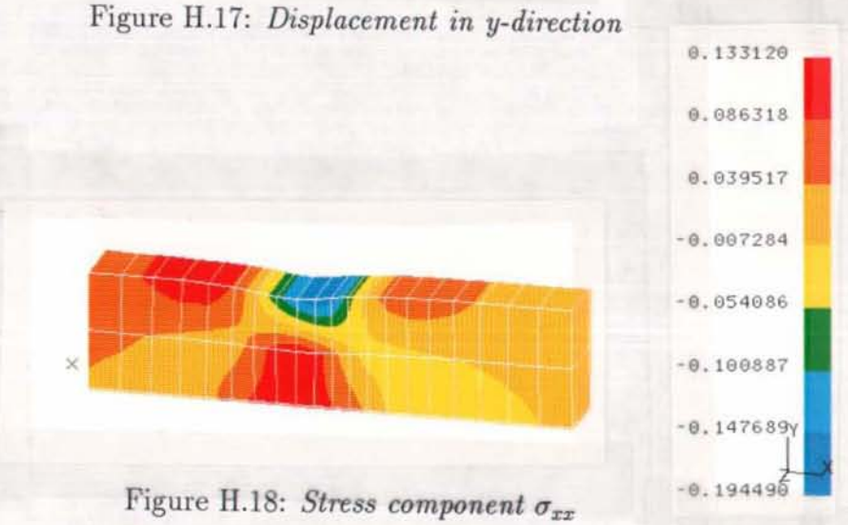

Figure H.18: *Stress component* σ_{xx}

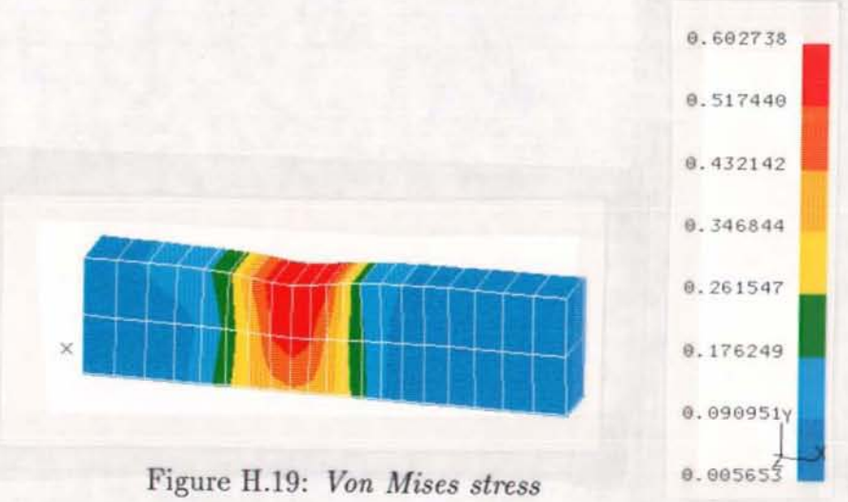

Figure H.19: *Von Mises stress*

H.2.3 Test case 5

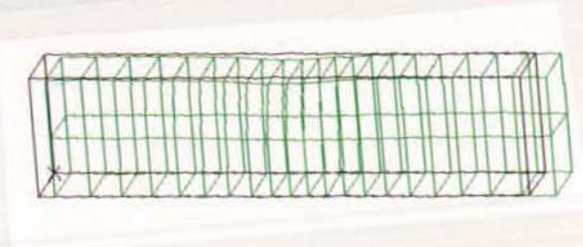

Figure H.20: *Deformed geometry*

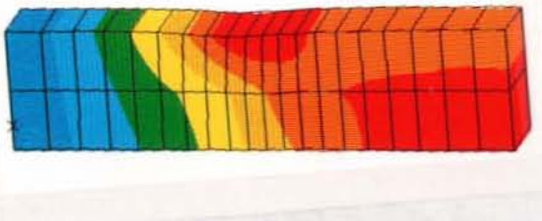

Figure H.21: *Displacement in x-direction*

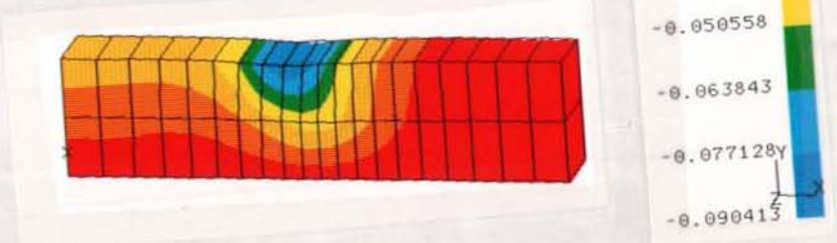

Figure H.22: *Displacement in y-direction*